10.35662/unine-thesis-2804

Faculty of Science, Institute of Biology

Plant Physiology Laboratory

Two atypical kinases of plastoglobules, ABC1K1/PGR6 and ABC1K3, maintain photosynthetic efficiency in *Arabidopsis* by acting on plastoquinone homeostasis.

A dissertation submitted to the

University of Neuchâtel

For the degree of

Doctor of Philosophy in Biological Sciences

Presented by

Thibaut Pralon

Thesis committee

Prof. Felix Kessler (Thesis Director) – University of Neuchâtel

Dr. Laurent Mène-Saffrané – University of Fribourg

Dr. Gaetan Glauser – University of Neuchâtel

Dr. Paolo Longoni – University of Neuchâtel

Supervisors

Dr. Shanmungabalaji Ventakasalam – University of Neuchâtel

January 2020

UNIVERSITÉ DE NEUCHÂTEL

Faculté des Sciences
Secrétariat-décanat de Faculté
Rue Emile-Argand 11
2000 Neuchâtel – Suisse
Tél : + 41 (0)32 718 21 00
E-mail : secretariat.sciences@unine.ch

IMPRIMATUR POUR THESE DE DOCTORAT

La Faculté des sciences de l'Université de Neuchâtel autorise l'impression de la présente thèse soutenue par

Monsieur Thibaut PRALON

Titre:

"Two atypical kinases of plastoglobules, ABC1K1/PGR6 and ABC1K3, maintain photosynthetic efficiency in *Arabidopsis* by acting on plastoquinone homeostasis"

sur le rapport des membres du jury composé comme suit:

- Prof. Felix Kessler, directeur de thèse, Université de Neuchâtel, Suisse
- Dr Paolo Longoni, Université de Neuchâtel, Suisse
- Dr Gaëtan Glauser, Université de Neuchâtel, Suisse
- Dr Laurent Mène-Saffrané, Université de Fribourg

Neuchâtel, le 5 novembre 2019

Le Doyen, Prof. P. Felber

P. Fel

Abstract

Life on Earth is mainly dependant on a single series of photochemical reactions: collectively known as photosynthesis. Indeed, these reactions provide chemical energy in the form of sugars for human nutrition and molecular oxygen that is necessary for human respiration. Photosynthesis is performed in photosynthetic organisms such as plants and algae inside green cellular organelles called chloroplasts. The light-dependent reactions of photosynthesis require a machinery consisting of multiple protein-pigment complexes embedded in the thylakoid membrane. While photosynthesis is a very robust process, its machinery is still fragile and may be damaged under environmental variations such as sudden changes in light intensity (*e.g.* during a sunny day with cloudy spells). Therefore, fine regulation and great photoprotection are necessary to maintain efficient photosynthesis. Small lipid droplets attached to thylakoid membrane, called plastoglobules (PG), contribute to photoprotection as they are filled with neutral lipid such as plastoquinone, phylloquinone (vitamin K_1), tocopherols (vitamin E) and carotenoids that are either essential molecules for photosynthetic electron transport and/or powerful membrane anti-oxidants. Proteins at the surface of PG, including atypical ABC1K kinases, contribute to the neutral lipid metabolic pathways. This suggests that PG play an important role in the photosynthesis regulation and protection.

My PhD thesis focuses on two of the atypical kinases, ABC1K1/PGR6 and ABC1K3, and their roles in photosynthesis regulation.

We have discovered a previously uncharacterized mechanism of photosynthesis regulation implicating the two atypical kinases ABC1K1/PGR6 and ABC1K3 in the regulation of the photoactive plastoquinone pool size. In a nutshell, the role of ABC1K1/PGR6 is to maintain a sufficient photoactive plastoquinone pool under high light conditions whereas ABC1K3 functions as a limiter to plastoquinone availability.

Thus, this PhD thesis provides new insight on the function of two atypical kinases in plastoglobules, ABC1K1/PGR6 and ABC1K3, in rapid adaptation of photosynthesis under high light.

The chapter 2, entitled "*Plastoglobules: Lipid droplets at the thylakoid membrane*" was published in the book "Chloroplasts: Current Research and Future Trends" (Kirchhoff H. Eds.) in 2016. The third chapter "Plastoquinone homoeostasis by Arabidopsis proton gradient regulation 6 is essential for photosynthetic efficiency" was published in the scientific journal "Communication Biology" in 2019.

Résumé

La vie sur Terre dépend principalement d'une suite de réactions photochimiques, appelée la photosynthèse. Ces réactions fournissent de l'énergie chimique sous forme de sucre pour notre alimentation et d'oxygène nécessaire à notre respiration. La photosynthèse s'effectue dans les organismes photosynthétiques tels que les plantes et les algues dans de petits organites nommés chloroplastes. Les réactions de la photosynthèse dépendantes de l'énergie lumineuse requièrent une machinerie composée de multiples complexes de pigments-protéines intégrés dans la membrane du thylakoïde. Alors que la photosynthèse est un mécanisme très robuste, sa machinerie reste fragile et peut être endommagée lors de conditions environnementales changeantes telle qu'une variation brusque d'intensité lumineuse (par ex. lors de passages nuageux par temps ensoleillé). Par conséquent, une régulation adaptée et une protection efficace sont nécessaires pour maintenir une photosynthèse optimale. Attachées aux thylakoïdes de petites gouttes lipidiques, nommées plastoglobules (PG), contribuent à la photoprotection par le fait qu'elles sont remplies de lipides neutres tels que la plastoquinone, la phylloquinone (vitamine K_1), les tocophérols (vitamine E) et les caroténoïdes, des molécules essentielles pour le transport des électrons et/ou agissantes comme de puissants antioxydants. Les protéines des PG, incluant des kinases atypiques ABC1K, participent aux voies métaboliques des lipides neutres. Cela suggère un rôle important des PG dans la régulation et la protection de la photosynthèse.

Ma thèse de doctorat porte sur deux kinases atypiques, ABC1K1/PGR6 et ABC1K3, et leurs implications dans la régulation de la photosynthèse.

Nous avons découvert un mécanisme de contrôle de la photosynthèse jusque-là non identifié, impliquant les deux kinases atypiques ABC1K1/PGR6 et ABC1K3 dans la régulation de la plastoquinone photoactive. En quelques mots, le rôle de ABC1K1/PGR6, sous une intensité lumineuse élevée, est de maintenir un pool de plastoquinone photoactive suffisant, alors que ABC1K3 fonctionnerai comme un limiteur de la mobilité de la plastoquinone.

Cette thèse de doctorat offre donc un nouveau regard sur la fonction de deux kinases atypiques des plastoglobules, ABC1K1/PGR6 et ABC1K3, dans l'adaptation rapide de la photosynthèse en condition de haute intensité lumineuse.

Le chapitre 2, intitulé "*Plastoglobules: Lipid droplets at the thylakoid membrane*" a été publié dans le livre "Chloroplasts: Current Research and Future Trends" (Kirchhoff H. Eds.) en 2016. Le troisième chapitre "*Plastoquinone homoeostasis by Arabidopsis proton gradient regulation 6 is essential for photosynthetic efficiency*" a été publié dans la revue scientifique "Communication Biology" en 2019.

Keywords: Chloroplasts, plastoglobules, photosynthesis, plastoquinone, PQ, plastoquinol, PQH_2, Activity of BC1 complex, Proton Gradient Regulation, ABC1K1, ABC1K3, PGR6, kinases, photoactive, phosphorylation, redox state, cytochrome *b6f*, electron transport, non-photochemical quenching, NPQ, light-harvesting complexes, LHC, state transitions.

Mots clés: Chloroplastes, plastoglobules, photosynthèse, plastoquinone, PQ, plastoquinol, PQH_2, Activity of BC1 complex, Proton Gradient Regulation, ABC1K1, ABC1K3, PGR6, kinases, photoactive, phosphorylation, état redox, cytochrome *b6f*, transport d'électrons, quenching non-photochimique, NPQ, antennes collectrices de lumière, LHC, transition d'état.

Contents

Abbreviations

ATP	adenosine triphosphate
ABC1K	activity of bc1 complex 1-like kinase
CBB	Calvin-Benson-Bassham
CO_2	carbon dioxide
Cyt	cytochrome
DGDG	digalactosyldiacylglycerol
DMPBQ	dimethylphytylbenzoquinone
ER	endoplasmic reticulum
ETC	electron transport chain
e^-	electron
FAPE	fatty acid phytyl
FAR	far-red
F_M	maximum fluorescence in dark-adapted state
F_0	minimum fluorescence in dark-adapted state
F_V	variable fluorescence in dark-adapted state
F_M'	maximum fluorescence in light
F_S	steady-state chlorophyll fluorescence in light
FNR	ferredoxin $NADP^+$ reductase
H_2O	water
HL	high light
HPLC	high-performance liquid chromatography
kDa	kilodaltons
LHC	light-harvesting complex
MGDG	monogalactosyldiacylglycerol
ML	moderate light
NADP(H)	nicotinamide adenine dinucleotide phosphate
NDH	NAD(P)H dehydrogenase
NPQ	non-photochemical quenching
O_2	molecular oxygen
PC-8	plastochromanol-8
PGR	proton gradient regulation

PQ	plastoquinone
PQH_2	plastoquinol
PSI	photosystem I
PSII	photosystem II
PTOX	plastid terminal oxidase / plastoquinone terminal oxidase
P_{680}	photosystem II special chlorophyll *a* pair
P_{700}	photosystem I special chlorophyll *a* pair
Q_A	plastoquinone strongly bounds to photosystem II reaction center
Q_B	plastoquinone exchange site at photosystem II reaction center
Q_I	quinone binding/exchange site of cytochrome *b6f* at the stromal side
Q_O	quinone binding/exchange site of cytochrome *b6f* at the lumenal side
qE	energy- or pH-dependent quenching
qI	photoinhibitory quenching
qZ	zeaxanthin-dependent quenching
ROS	reactive oxygen species
STN	state transition kinase
TAG	triacylglycerol
TMPBQ	trimethylphytylbenzoquinone
α-TQ	alpha-tocopherol quinone
V_I	variable fluorescence at 30 ms
V_J	variable fluorescence at 3 ms
WT	wild type
Φ_{MAX}	maximum photosystem II efficiency
Φ_{PSII}	photosystem II quantum yield
ΦET2o	quantum yield of the electron transport flux after Q_A
ΦPo	maximum quantum yield of primary photochemistry in photosystem II
ΦRE1o	quantum yield of electron transport to photosystem I electron acceptors

Chapter I

General introduction

Abstract

A large part of life on Earth is dependent on one major photochemical reaction, photosynthesis. Photosynthesis converts sunlight energy into chemical energy. It implies, thanks to light energy, the conversion of carbon dioxide (CO_2) and water (H_2O) into a primary organic compound (as glucose: $C_6H_{12}O_6$), which will be used for plant growth and metabolic activities, and molecular oxygen (O_2) as by-product. This reaction takes place in oxygenic photosynthetic organisms, such as in plants in small green specialized cellular organelles called chloroplasts. A sophisticated machinery, implying multiple protein-pigment complexes embedded in membrane, as well as various enzymes, lipid and small molecules, is required to perform photosynthesis. However, this photosynthetic machinery is fragile and sensitive to damage. Furthermore, environmental conditions, such as light intensity and quality, can suddenly change and compromise photosynthetic efficiency. Therefore, fine regulation and adaptation of the photosynthetic process is needed to ensure an optimal photosynthetic yield and to prevent possible impairment on the photosynthetic apparatus.

1.1 Chloroplast, a plastid designed for photosynthesis

Chloroplasts belong to a specialized organelle family called plastids. These have originated from a primary endosymbiotic event in which a heterotrophic eukaryote cell engulfed a cyanobacterium believed to have occurred approximately 1.5 billion years ago[1]. Since that time, the chloroplast evolved into several functionally different plastid types. The resulting organelles possess identical genetic material (chloroplast DNA called plastome) and machinery, and perform similar fundamental biochemical processes; however, they vary in shape, internal structure, size and are able to perform additional specific functions[2,3]. The term plastid reflects the strong plasticity of these organelles. In higher plants, the plastid family is very diverse. Proplastids are undifferentiated organelles found in meristematic tissues, and have a poorly developed internal membrane system[4]. Depending on developmental stages, tissue type as well as environmental conditions, proplastids can differentiate into leucoplasts, etioplasts, chloroplasts and chromoplasts. Leucoplasts are colorless plastids that can accumulate starch (amyloplasts), volatile compounds and lipids (oleoplasts). They are therefore considered storage organelles. Etioplasts are chloroplast precursor plastids and develop in the dark in

photosynthetic tissues. They possess internal structure, *i.e.* the prolamellar body, and accumulate proto-chlorophyllide, a precursor of chlorophyll[5,6]. Upon illumination, etioplasts differentiate into chloroplasts. Chloroplasts, the well-known green plastids, are the site of the photosynthesis and have a highly structured internal membrane that captures light energy and converts it into chemical energy. Chloroplast can differentiate into chromoplasts in ripening fruit[7,8] or gerontoplasts in senescent leaves[9]. Chromoplasts are orange-red plastids, synthetizing and accumulating large amounts of carotenoids. They possess crystal and globular structures that store carotenoids[7,8]. Gerontoplasts contain products, such as phytol esters and triacylglycerol, that are derived from the disassembly of thylakoid membrane during leaf senescence. These products accumulate in supersized plastoglobules[10]. The capacity to differentiate from one type to another lends plastids a strong capacity for adaptation[8,11,12].

Chloroplasts develop only in the presence of light. A mesophyll cell can contain up to 100 chloroplasts. They are quite large organelles, 5-10 µm diameter and 1-3 µm in thickness. As in all plastids, a dual membrane envelope, consisting of inner and outer membranes, bounds the chloroplast. The envelope plays a role as a physical barrier allowing a selective bidirectional passage of compounds and metabolites. The inner membrane delimits the chloroplast aqueous phase known as stroma. The stroma contains chloroplast DNA, ribosomes, enzymes and starch. In the stroma, CO_2 is fixed due to Rubisco activity in the Calvin-Benson-Bassham (CBB) cycle to form carbohydrates ($C_6H_{12}O_6$). In addition, chloroplasts possess a third highly structured internal membrane system surrounded by the stroma, the thylakoid membrane[13-16]. (Fig. 1.1)

Thylakoid membranes are mainly composed of integral membrane proteins, galactolipids (principally monogalactosyldiacylglycerol (MGDG) and digalactosyldiacylglycerol (DGDG)) and pigments (chlorophylls and carotenoids)[16,17]. The membrane lipids form a bilayer surrounding the interior aqueous phase, the lumen. Thylakoids resemble flattened discs and are arranged in stacks called grana that are connected by thylakoid stroma lamellae[18-20]. Attached to thylakoid membrane are small lipid droplets called plastoglobules[21,22] (Fig. 1.1). Plastoglobules are surrounded by a galactolipid monolayer coated by specific proteins[23-26]. They are filled of neutral lipid, as plastoquinone, phylloquinone, or tocopherols, which are essential for photosynthesis functioning and protection. The chapter 2 of this thesis reviews the state of the art of plastoglobules.

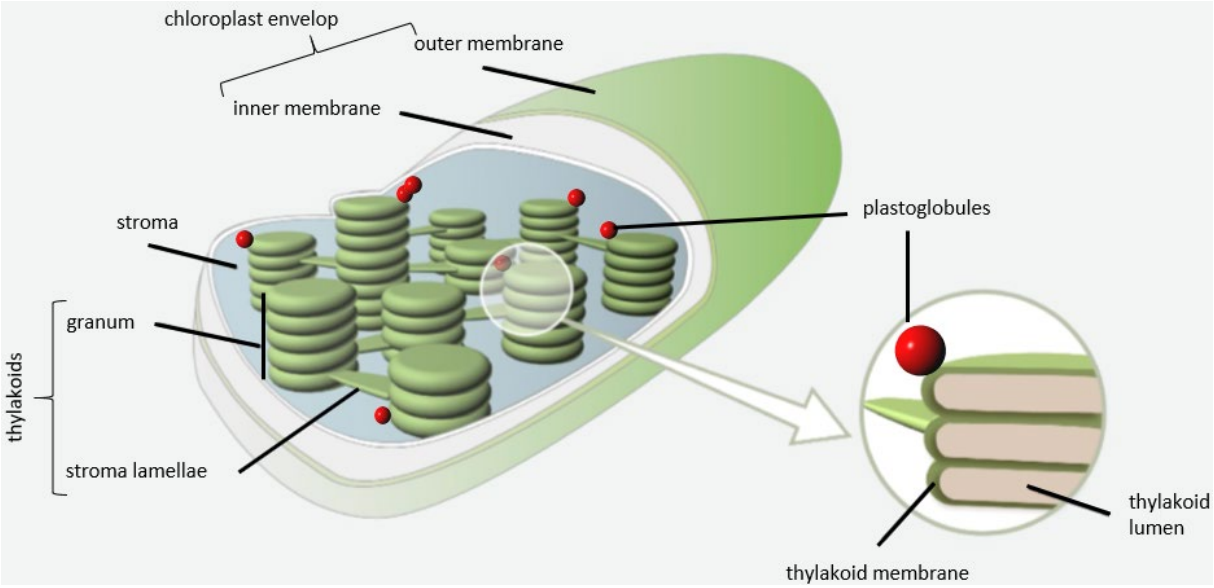

Figure 1.1. Scheme of chloroplast structure. Chloroplast is composed of an envelope, constituted by an outer and an inner membrane, which surrounds stroma and thylakoid membrane. Stacked thylakoid membranes are called grana (granum in the singular), while unstacked one that connect grana, are named stroma lamellae. Thylakoid membrane delimits thylakoid lumen from stroma. Attached to thylakoids are small spherical droplets, the plastoglobules (in red). Modified from Mirkovic *et al.* (2017)[27].

The photosynthetic machinery consists of multi-subunit protein (-pigment) complexes embedded in thylakoid membrane: photosystem II (PSII), photosystem I (PSI), light-harvesting complexes (LHC), cytochrome *b6f* and adenosine triphosphate (ATP) synthase that together drive the light-dependent photosynthesis reactions. (Fig. 1.2)

Around 30 subunits form the PSII complex. However, the PSII core is composed of two reaction center proteins, D1 (PsbA) and D2 (PsbD), and two core antenna, CP43 (PsbC) and CP47 (PsbB). At the lumen side, the PSII core associates with the oxygen-evolving complex, formed by three main subunits (PsbO, PsbP and PsbQ). The oxygen-evolving complex comprises a Mn-cluster, calcium and chloride essential for water-splitting activity[28]. Cytochrome *b559*, composed of two subunits, is located in reaction center. Cytochrome *b559* may be implicated in the assembly of PSII and may have a protective role[29]. In addition, PSII core is surrounded by peripheral antenna composed of major trimeric light-harvesting complexes (LHC) II proteins and minor monomeric LHCII proteins (CP24, CP26 and CP29) that together with the PSII core create a large supercomplex PSII-LHCII[30,31] (Fig. 1.2). Attached to the peripheral and core antenna are hundreds of chlorophyll molecules as well as dozens of carotenoid pigments. They absorb light energy and transfer it to PSII core reaction center. D1 and D2 proteins bind to chlorophyll *a*, pheophytin, beta-carotene, iron and plastoquinone molecules. They trap energy from antenna by a special chlorophyll *a* pair that gives an electron to the first electron acceptor thus initiating photosynthetic electron transport. The special pair of chlorophyll *a* in PSII, the primary electron donor

in PSII, is denoted P_{680} due to its maximal light absorption at 680 nm. The splitting of water molecules performed by the oxygen-evolving complex enables to refill electrons at the P_{680} reaction center. Additionally, LHCII are involved in photoprotection mechanisms by equally distributing light energy between the photosystems (state transitions) and by dissipating excess energy as heat (non-photochemical quenching). PsbS, a small protein, plays an essential role in non-photochemical quenching[32]. The roles of some of the remaining subunits of PSII remain yet undetermined.

PSI core is composed of 15 subunits. Two main proteins, PsaA and PsaB, which are associated with chlorophylls (a chlorophyll dimer, P_{700}, and monomer chlorophyll *a* (A0)), beta-carotene, two phylloquinone molecules (A1) and iron-sulphur clusters [4Fe-4S], form a central heterodimeric reaction center. PsaC subunit contains two iron-sulphur clusters (F_A and F_B). PSI core is encircled with asymmetrical peripheral antenna (LHCI) forming the PSI-LHCI supercomplex[30,33,34]. LHCI is composed of four subunits (Lhca1-4). Other small subunits are implicated in the association, stabilization, organisation between PSI core and antenna, in the binding of plastocyanin as well as other roles[34-36] (Fig. 1.2). The LHCI antenna capture light energy and allow energy transfer to the PSI reaction center. Here, the energy is used to transfer an electron from the special chlorophyll *a* pair, P_{700}, the primary electron donor in PSI, to reduce nicotinamide adenine dinucleotide phosphate ($NADP^+$) into NADPH via ferredoxin and ferredoxin $NADP^+$ reductase (FNR). Ferredoxin is a small iron-sulphur [2Fe-2S] protein located at the stromal side of PSI. FNR is the enzyme that catalyses the reduction of $NADP^+$ and also plays a role in cyclic electron flow.

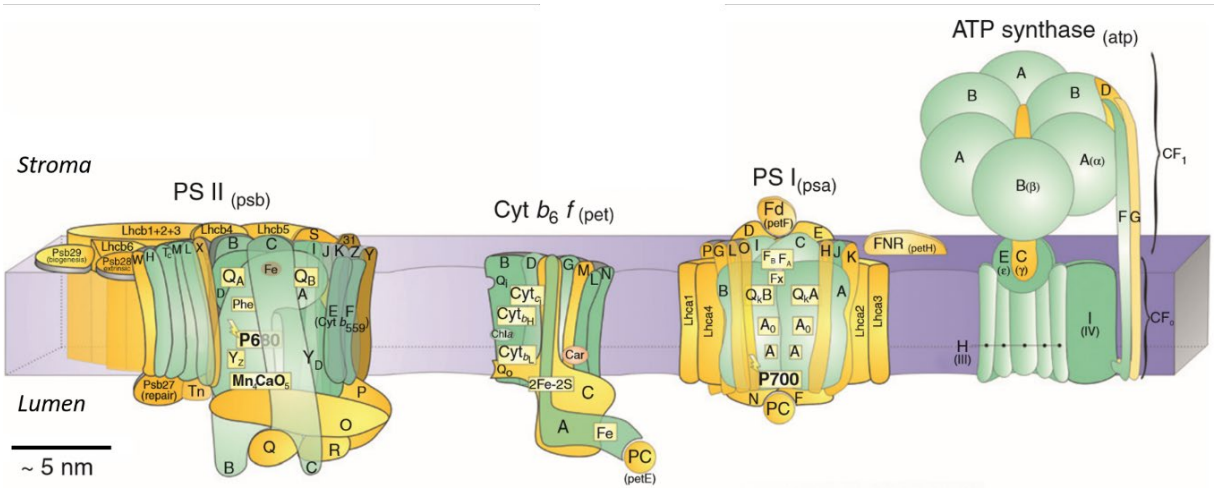

Figure 1.2. Schematic representation of photosynthetic apparatus on thylakoid membrane. The four main protein complexes of photosynthetic apparatus in *Arabidopsis thaliana* embedded in thylakoid membrane (violet): photosystem II (PSII), cytochrome *b6f* (Cyt *b6f*), photosystem I (PSI) and ATP synthase. They are constituted of multiple protein subunits. In yellow, subunits nucleus-encoded; in green plastid-encoded. Single letter (without prefix that indicates the corresponding complex) are used to named subunits that composed the complex. Complex prefix used for photosystem II is psb; for cytochrome *b6f* is pet; for photosystem I is psa; and for ATP synthase is atp. PC, plastocyanin; Fd, ferredoxin; FNR, ferredoxin-NADP reductase; Lhc, light-harvesting complex. Adapted from Allen *et al.* (2011)[37].

The cytochrome *b6f* complex (cyt *b6f*) resembles the mitochondrial cytochrome bc1. Cyt *b6f* is composed of a cytochrome *b6* (PetB), a cytochrome *f* (PetA), a subunit IV (PetD), the Rieske protein (PetC) with its iron-sulphur cluster [2Fe-2S], and other small subunits. It also contains chlorophyll *a*, beta-carotene and one c-type heme (heme *x*)[38]. Cytochrome *b6f* has two binding sites for plastoquinol (PQH_2) and plastoquinone (PQ): the Q_O-center (PQH_2 oxidase) located at the lumenal side near the iron-sulphur cluster, and the Q_I-center (PQ reductase) situated at the stromal side[39-41] (Fig. 1.2). Q_I and Q_O centers participate in an electron flow network called the Q-cycle[42]. Cytochrome *b6f* constitutes an electrochemical connection between PSII and PSI; therefore, it occupies a central position in the cyclic and linear electron transport chains. Cyt *b6f* operates as plastoquinol-plastocyanin oxidoreductase and contributes to the creation of the proton motive force across the thylakoid membrane[43] .

The chloroplast ATP synthase, like the ATP synthase of mitochondria, belongs to F1-type family. It is formed by two principal parts: CFo and CF1, connected by a stator. CFo, which is embedded in thylakoid membrane, is constituted by multiple subunits forming a rotary ring[44] (Fig. 1.2). Each CFo subunits allows the translocation of one proton from lumen to stroma using the electrochemical proton gradient established by photosynthesis. On the other side, CF1 is composed of 5 subunits among which some are copied three times (α3; β3; γ, δ and ε), and where α and β subunits are arranged in an alternate manner[45]. Transfer of protons from lumen to stroma releases energy that is used to provoke a conformation change of CF1. Conformational change of α and β subunits allows the creation of sites for the mechanochemical reaction between adenosine diphosphate (ADP) and inorganic phosphate to form ATP. A complete turn of CFo drives the hydrophilic head CF1 to produce three ATP molecules[46-48].

Photosynthetic protein complexes are differentially distributed in the thylakoid membrane. The grana contain mostly PSII-LHCII complexes, while PSI-LHCI complexes and ATP synthase are principally present in thylakoid stroma lamellae[18,49]. Cytochrome *b6f* is located in the entire thylakoid membrane and may accumulate at the margins between grana and stroma lamellae[18,50,51] (Fig. 1.3).

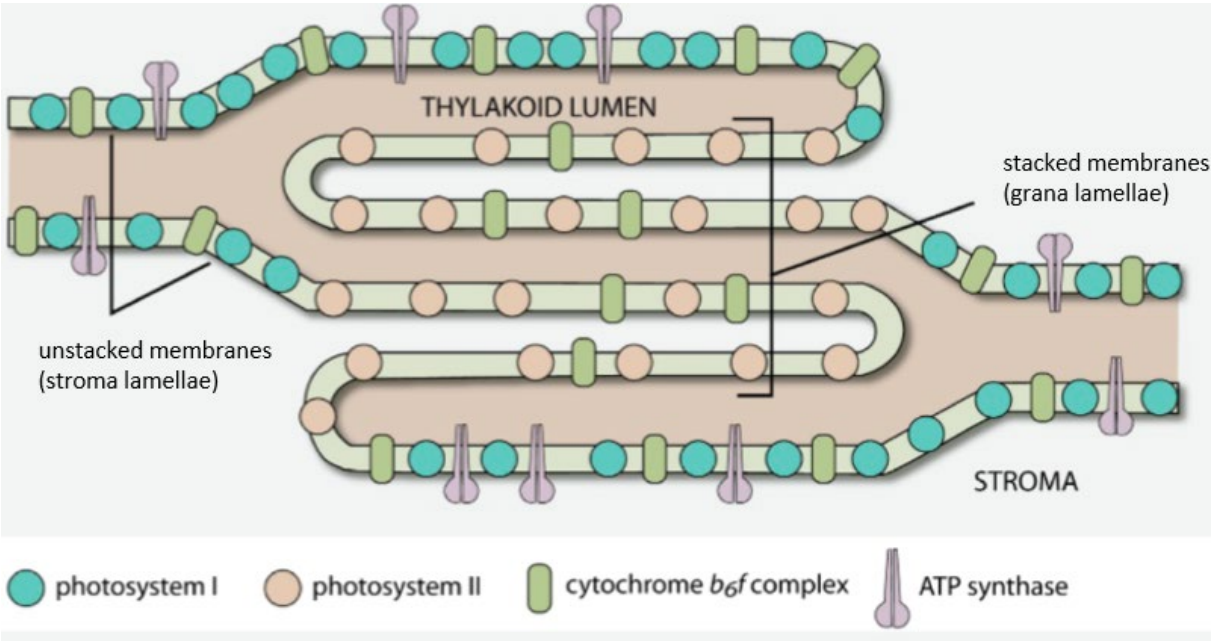

Figure 1.3. Local repartition of photosynthetic complexes in the thylakoid membrane. Photosystem II is mainly located in stacked regions, while photosystem I and ATP synthase are presents on stroma-exposed lamellae. Cytochrome *b6f* is founded everywhere on thylakoid membranes. Adapted from Mirkovic *et al.* (2017)[27].

The main function of the chloroplast is photosynthesis, but it is also involved in other metabolic activities such as the assimilation of nitrogen and sulphur and the synthesis of amino acids, fatty acids, and lipids.

1.2 Photosynthetic electron transport

The light-dependent photosynthetic reactions take place at the thylakoid membrane and convert light energy into chemical energy in the form of ATP and NADPH. These latter are used for carbon fixation in the Calvin-Benson-Bassham cycle, which does not directly require light energy to be active. However, synchronization of these two phases is necessary to perform efficient photosynthesis.

The light-dependent photosynthetic reactions start when light energy is absorbed by chlorophyll and carotenoids in LHCII antenna. As a consequence, the pigment molecule is converted from the ground state (lowest energy) to an excited state. Excited pigment molecules can return to the ground state by relaxation in the form of fluorescence, heat or resonance energy transfer to a nearby ground state chlorophyll molecule. Therefore, energy is funnelled to the PSII reaction center, where it excites the P_{680} chlorophyll dimer. The excited P_{680} transfers one electron to a final acceptor molecule of PSII, the quinone Q_B, via pheophytin and the quinone Q_A. A new electron coming from the water splitting reaction substitutes the one transferred by the P_{680} chlorophyll. Water splitting releases protons in

lumen, increasing their concentration, and oxygen as a by-product. A second electron is provided by P_{680} allowing the double reduction of the plastoquinone at the Q_B site, followed by its double protonation (protons from stroma) to form plastoquinol. PQH_2 is released in thylakoid membrane, and a new oxidized PQ molecule replaces it at the Q_B site. The reduced plastoquinol will then transfer the electrons within the thylakoid membrane to the cytochrome *b6f* complex. Once PQH_2 reaches the Q_O site of the cyt *b6f* complex, it is re-oxidized into PQ, releasing two electrons and two protons. Re-oxidation of PQH_2 at the cytochrome *b6f* is the rate-limiting step in photosynthetic electron transport chain. Release of protons in the lumen creates a trans-thylakoid proton motive force. In the Q-cycle, one electron goes to cytochrome *b*, where it will reduce a plastoquinone molecule at the Q_I site to the semiquinone form. After receiving a second electron and two protons, a new PQH_2 molecule is formed at Q_I site and can again bind to Q_O site and release protons into the lumen supporting trans-thylakoid proton gradient. The other electron is transferred by an iron-sulphur protein and cytochrome *f* to plastocyanin[43,52]. Plastocyanin is a water-soluble protein that can diffuse freely in the thylakoid lumen. At PSI, light energy is used to excite P_{700} chlorophyll that will then be able to transfer one electron, via chlorophyll, phylloquinone, iron-sulphur clusters and ferredoxin to the final acceptor $NADP^+$ to produce NADPH. The electron carried through thylakoid lumen to the PSI by plastocyanin will serve to reduce the power-oxidizing agent P_{700}^+. The transfer of electrons from water to $NADP^+$ by PSII and PSI is considered as the linear electron transport[53] (Fig. 1.4).

In contrast, cyclic electron flow around PSI recycles electrons from ferredoxin to plastoquinone[54-56]. Two pathways participate in cyclic electron transport: the main pathway depends on PGR5 (Proton gradient regulation 5) and PGRL1 (PGR5-like Photosynthetic phenotype 1) proteins[57-60], while the second cycle uses NADPH dehydrogenase-like (NDH-like) complex, a large multi-subunit complex[61-63]. (Fig. 1.4) Cyclic electron flows contribute to the trans-thylakoid proton motive force favouring the production of ATP without NADPH, thus allowing a balance in ATP/NADPH production ratio for the CBB cycle and protecting both photosystems[54,64]. Reallocation of LHCII between photosystems I and II, known as state transitions, may influence the switch between linear and cyclic electron flows. When LHCII is attached to PSII, linear electron transport is favoured, while when LHCII is bound to PSI, cyclic electron flow may be privileged[65].

Chlororespiration involves the NDH-like complex and the plastid terminal oxidase PTOX in the regulation of PQ pool redox state, preventing over-oxidation or over-reduction of this latter (Fig. 1.4). While NDH-like complex refills electrons from NADPH to PQ pool, PTOX transfers them from PQ to O_2 to form H_2O, playing a role as a safety valve and electron sink, thus preventing inhibition of photosynthesis. However, chlororespiration is a minor pathway compared to linear electron flow[66,67].

At the end of the light-dependent photosynthesis reactions, the final products, ATP and NADPH, will be used in CBB cycle to fix carbon into organic compound as well as in other fundamental metabolic reactions.

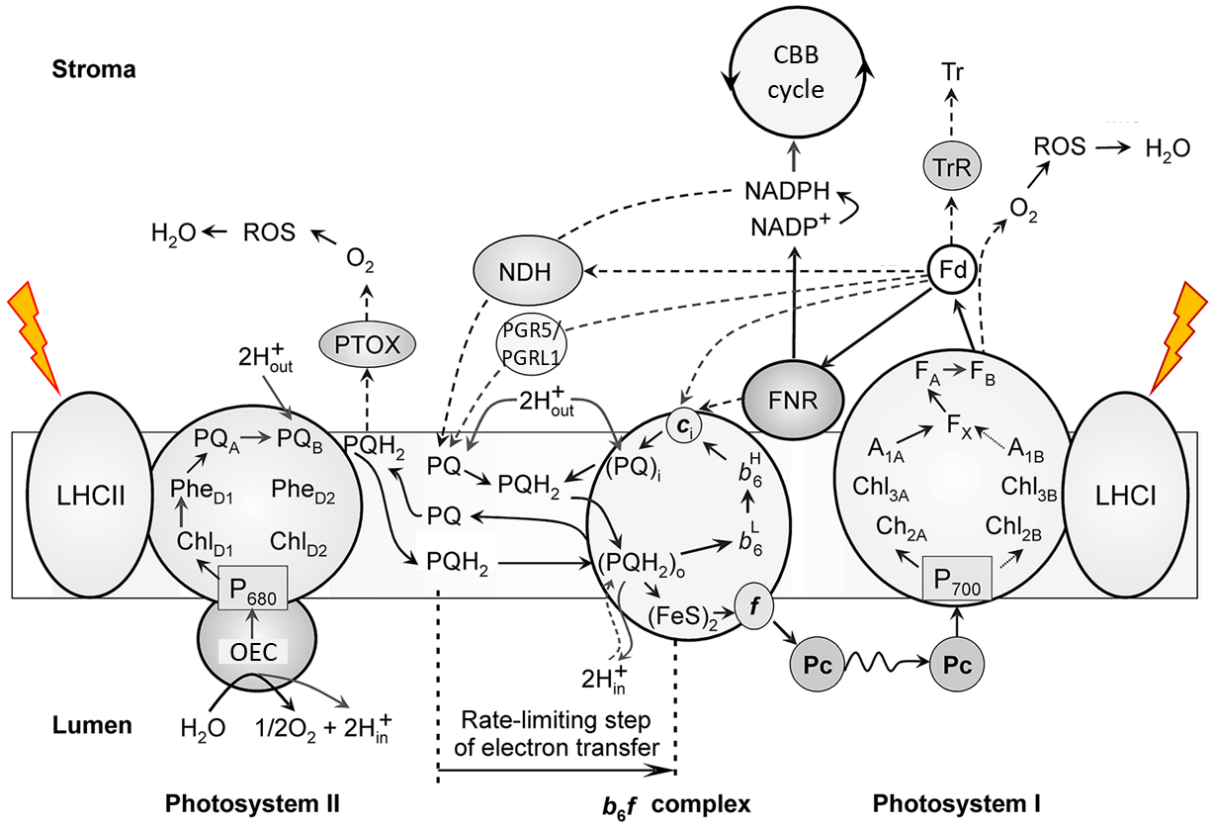

Figure 1.4. Schematic representation of photosynthetic electron transport routes through photosynthetic complexes: photosystem II, cytochrome *b6f* complex and photosystem I. Solid lines correspond to linear electron transport that starts, from PSII, continue via PQ/PQH_2 pool, through cytochrome *b6f* and due to plastocyanin (Pc), to ends at photosystem I by reducing $NADP^+$ into NADPH, which is used for CBB cycle, Dashed lines represent alternative electron transports as cyclic electron flows by NDH or PGR5/PGRL1 complexes, chlororespiration by PTOX and water-water cycle. A: phylloquinone; CBB cycle: Calvin-Benson-Bassham cycle; Chl: chlorophyll; OEC: oxygen evolving complex; Fd: ferredoxin; F(a,b,x): iron-sulphur cluster in PSI; FNR: ferredoxin-NADP-oxidoreductase; LHC: light-harvesting complex; $NADP^+$: Nicotinamide adenine dinucleotide phosphate; NADPH: $NADP^+$ reduced; NDH: chloroplast NAD(P)H-dehydrogenase complex; Pc: plastocyanin; PGR5: Proton gradient regulation 5; PGRL1: PGR5-like Photosynthetic phenotype 1; Phe: pheophytin; PQ/PQH_2: plastoquinone/ol; PTOX: plastid terminal oxidase; P_{680}: electron donor of photosystem II; P_{700}: electron donor of photosystem I; ROS: reactive oxygen species; Tr: thioredoxin; TrR: thioredoxin reductase. Modified from Tikhonov (2016)[68].

In photosynthetic electron transport (linear and cyclic electron flows), one key molecule is plastoquinone. PQ is composed of a hydrophilic quinone head attached to a hydrophobic nonaprenyl isoprenoid side chain[69,70]. PQ that participates in electron transport in the thylakoid membrane is considered the photoactive PQ pool, whereas the non-photoactive PQ pool represents the remaining PQ found in the chloroplast envelope or stored in plastoglobules[70-72]. A lipid exchange between thylakoid membrane and plastoglobules may be performed in order to provide electron carriers molecules for photosynthesis when conditions demand. This may point out a substantial role of

plastoglobules in photosynthesis regulation. In principle, PQ can move freely in the thylakoid membrane. In addition to shuttling electrons between photosynthetic complexes, PQ is involved in several other processes. The redox state of PQ is used as a sensor for state transitions[73] as well as nuclear and chloroplast gene expression[74-78]. PQ has antioxidant properties and is able to quench reactive oxygen species[72,79-81]. PQ is also the precursor of another antioxidant molecule, plastochromanol-8[82]. Furthermore, PQ, by transferring protons from the stroma to the thylakoid lumen, is indirectly involved in ATP production and in photoprotection by non-photochemical quenching.

1.3 Photoprotection

Plants are exposed to changes in environmental conditions such as a sudden increase in light intensity. Excess light generates reactive oxygen species (ROS) that may degrade the photosynthetic apparatus leading to a decrease of photosynthesis efficiency (photoinhibition). Under normal conditions, light energy converts chlorophyll into singlet-excited chlorophyll (^{1}Chl*) that transfers energy to the reaction center to perform charge separation. However, when the absorbed light energy surpasses the capacity of photosynthetic electron transport chain (*e.g.* over-reduction of electron transport chain), triplet chlorophyll excited state (^{3}Chl*) is formed and may react with molecular oxygen (O_2) resulting in singlet oxygen ($^1O_2$) mostly in the PSII reaction center and in LHCs[83-86]. In addition, reduced forms of oxygen as superoxide ($O_2^{\cdot -}$), hydrogen peroxide (H_2O_2) and hydroxyl radical ($^{\cdot}OH$)[87,88] may be produced. Singlet oxygen and superoxide are two powerful ROS that can provoke lipid peroxidation and proteins degradation leading to photoinhibition[88,89]. However, plants have developed photoprotective mechanisms to prevent ROS production and associated damage. Indeed, light energy can be equilibrated between the two photosystems by reallocating LHCII (state transitions) and excess energy can be released rapidly as heat (non-photochemical quenching) reducing ROS formation. Furthermore, antioxidant production and the PSII repair cycle can prevent photoinhibition by inhibiting ROS formation and by repairing ROS-induced damage.

1.3.1 State transitions

PSII and PSI have to co-operate and be coordinate in order to perform efficient linear electron transport. For that reason, excitation levels of the two photosystems have to be well equilibrated. However, environmental conditions often vary as can be seen in rapid changes of light intensity and quality. PSII and PSI absorb slightly different light spectra, and therefore changes in light quality may excited principally one photosystem over the other leading to an excitation energy imbalance. To

prevent over-excitation of one photosystem, the photosynthetic apparatus can be reorganised by reallocating mobile LHCII antenna, and thus equilibrating the excitation between photosystems[90-92]. When light favours the excitation of one photosystem, LHCII antenna migrate to the other photosystem. This process is called state transitions and allows the balance of light energy between both photosystems to be reestablished. When PSII is overexcited compared to PSI (*e.g.* under red illumination only), the photoactive PQ pool becomes overly reduced favouring the binding of PQH_2 to Qo site of cytochrome *b6f*. This activates the thylakoid protein kinase STN7 that phosphorylates LHCII[73,93-98]. As consequence, a mobile part of phosphorylated LHCII migrates from PSII to bind to PSI increasing PSI antenna cross-section. This allows excitation equilibration and thus reduces the excitation pressure on PSII. This state is called state 2 (Fig. 1.5). This phenomenon is reversible. Under light favouring PSI excitation (*e.g.* far-red illumination), the photoactive PQ pool becomes overly oxidized. Consequently, STN7 kinase becomes less active and LHCII is dephosphorylated by PPH1/TAP38 phosphatase[99,100]. Dephosphorylated LHCII reassociates with PSII. This state is called state 1 (Fig. 1.5). State transitions occur within a few minutes, rapidly reducing excitation pressure on photosystems. Movement of LHCII may be due to a stronger affinity of phosphorylated LHCII with PSI, while unphosphorylated LHCII preferentially binds to PSII[101]. State transitions may also be due to structural changes of the thylakoid membrane allowing the movement of LHCII[102]. However, under excess light, state transitions is inhibited[103] and other photoprotective mechanisms as non-photochemical quenching take over.

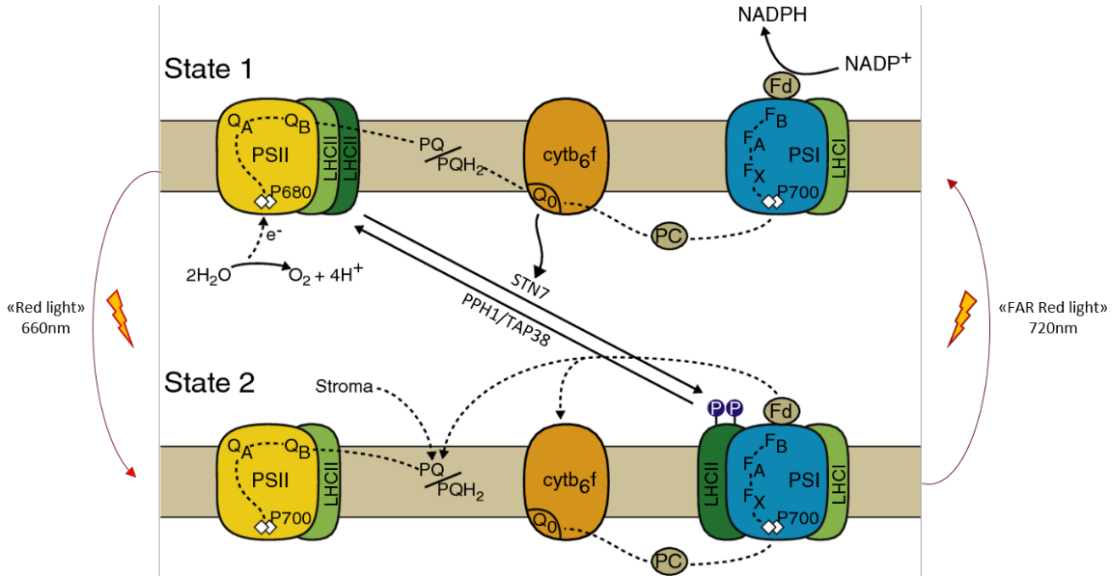

Figure 1.5. Model of state transitions process that allows the equilibrium of light energy between both photosystems. Red light preferentially excites photosystem II (PSII) compared to photosystem I (PSI) leading to reduction of plastoquinone pool (PQ/PQH_2). This activates the kinase STN7 that phosphorylates light-harvesting complexes II (LHCII). These latter migrate from PSII to PSI. This called state 2. In another hand, when light illumination (far-red light) promotes PSI activity compared to PSII, plastoquinone pool becomes overoxidized leading to inactivation of STN7 kinase and dephosphorylation of LHCII by PPH1/TAP38 phosphatase. Dephosphorylated LHCII move from PSI back to PSII. This called state 1. Modified from Rochaix (2011)[53].

1.3.2 Non-photochemical quenching (NPQ)

Non-photochemical quenching (NPQ) is a photoprotective process in which excess light is dissipated as heat. NPQ is mainly composed of three components that act in different timescales of induction and relaxation: qE (energy- or pH-dependent quenching), qZ (zeaxanthin-dependent quenching), and qI (photoinhibitory quenching)[104]. 85% of light energy absorbed by a chloroplast may be used for photosynthesis under ideal conditions, while the rest is released as fluorescence or dissipated as heat. At room temperature, chlorophyll fluorescence is mainly emitted by PSII. Therefore, measurement of chlorophyll fluorescence after a strong light pulse provides indications about photochemical quenching (in dark adapted: $F_V/F_M = (F_M-F_O)/F_M$) and non-photochemical quenching ($NPQ = F_M-F_M'/F_M'$)[104-108], where F_O is the basal fluorescence, F_M is the maximal fluorescence in dark, F_M' is the maximal fluorescence in light, and F_V is the variable fluorescence. (Fig. 1.6a). Chlorophyll fluorescence can also be used to monitor state transitions.

High light leads to an acidification of the thylakoid lumen that will immediately induce the protonation of the photosystem II protein subunit S (PsbS), a LHC-like protein required as a sensor initiating the qE process[32,105,109-111]. Simultaneously, the violaxanthin de-epoxidase (VDE) enzyme is activated and begins to convert violaxanthin to antheraxanthin and zeaxanthin[112,113]. Together, these two factors lead to a conformational rearrangement of LHCII-PSII supercomplexes (Fig. 1.6b) inducing a quenched state for a full qE response in which de-excitation of $^1Chl^*$ happens[109,111,114]. The quenched state of LHCII antenna provides an environment that facilitates the dissipation of excess energy as heat[110,115-117]. When light energy pressure diminishes, the thylakoid lumen becomes less protonated inducing a rapid deprotonation of PsbS[109,118] and the reconversion of zeaxanthin into violaxanthin by zeaxanthin epoxidase (ZEP)[119], thus leading to a fast reduction of NPQ. Conversion of violaxanthin into zeaxanthin and vice versa is known as the xanthophyll cycle. In addition, zeaxanthin can also participate in a slower quenching, termed qZ. The latter is independent from delta-pH and PsbS protein but is due to an accumulation of zeaxanthin in LHC minor antenna[114-116]. Despite these mechanisms to dissipate excess energy and minimize risks, PSII can be damaged. However, a repair mechanism exists allowing an efficient turnover of PSII.

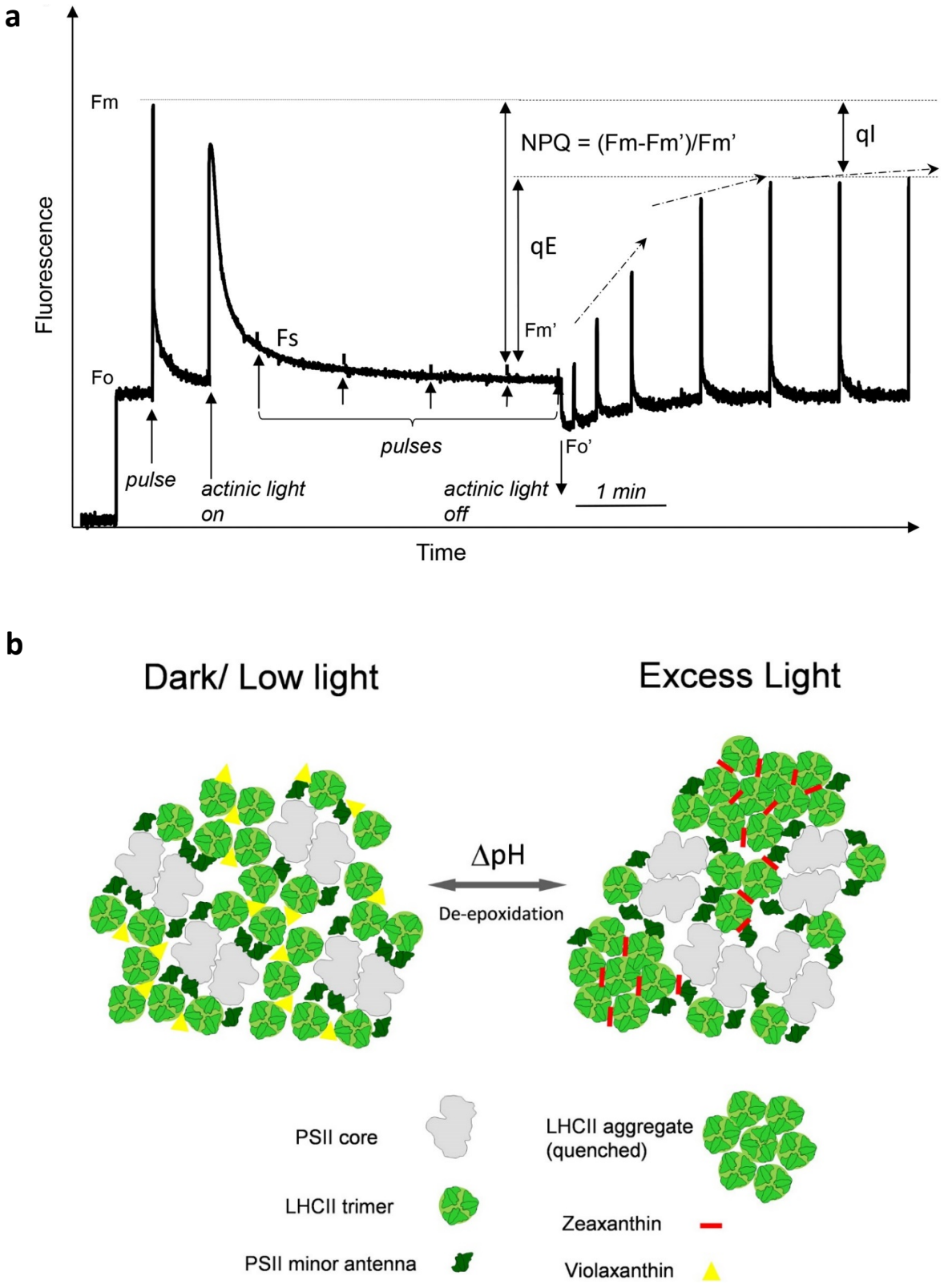

Figure 1.6. (a) Chlorophyll fluorescence kinetic traces of an *Arabidopsis* leaf. Fo: minimum fluorescence of dark-adapted; Fm: maximal fluorescence of dark-adapted leaf after strong light pulse; Fs: steady-state fluorescence; Fm': maximal fluorescence during actinic light exposure. NPQ: non-photochemical quenching; qE: energy-dependent quenching, the NPQ component rapidly activated and desactivated; qI: NPQ component related to photoinhibition, which is slowly induced and relaxed. From Ruban (2016)[104]. **(b)** Schematic representation of the (re)arrangement of PSII-LHCII supercomplexes under dark/low light and under excess light. Reorganization of PSII-LHCII allows dissipating excess light by heat in order to protect PSII under excess light. From Ruban *et al.* (2012)[120].

1.3.3 PSII repair cycle

During light-dependent photosynthetic reactions, mostly under excess light, PSII activity produces ROS, principally singlet oxygen, which may react with the D1 protein of the reaction center inducing its degradation and consequently decreasing photosynthetic efficiency[121,122]. The damaged PSII complex is subject to a multistep repair mechanism. Under high light, damaged PSII core proteins are strongly phosphorylated by the thylakoid protein kinase STN8 initiating the cycle repair[123,124]. Phosphorylation favors PSII complexes disassembly and migration to the stroma lamellae. There, PSII core is disassembled and D1 protein is degraded by FtsH and Deg proteases. Finally, PSII is reassembled with *de novo* synthesized D1 protein and returns to the grana[125-128] (Fig. 1.7). However, under very strong high light, PSII core damage can surpass the rate of D1 cycle repair leading to inhibition of PSII activity, known as photoinhibition (qI)[121,129,130]. Furthermore, ROS can also damage PSI leading to its photoinhibition; and unlike PSII, its recovery is slow[88,131,132]. In order to avoid photoinhibition due to ROS accumulation, chloroplasts can produce strong antioxidant molecules able to inhibit ROS formation and limit damages.

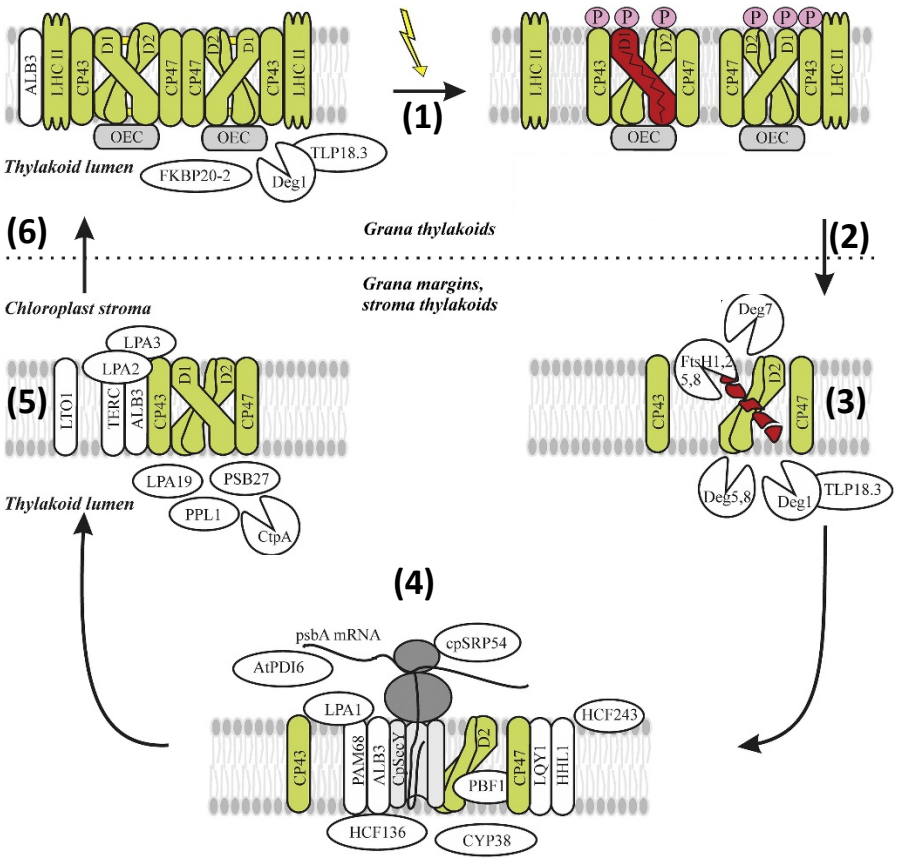

Figure 1.7. Schematic diagram of PSII cycle repair. (1) High light may damage D1 (PsbA) protein, and triggers PSII core phosphorylation by STN8 kinase. **(2)** Disassembly of PSII supercomplex and migration of damaged PSII core from grana stacks to stroma lamellae, followed by dephosphorylation of PSII core by PBCP phosphatase **(3)** Degradation of damaged D1 (PsbA) protein by Deg and FtsH proteases. **(4)** *De novo* synthesis of D1 protein performed by multiple co-factors. **(5)** (Re)assembly of PSII core. **(6)** Migration of PSIII core into grana and final (re)assembly of functional PSII-LHCII supercomplex. Adapted from Järvi *et al.* (2015)[125].

1.3.4 Antioxidants

Under excess light, chloroplasts accumulate lipid-soluble antioxidant molecules in the thylakoid membrane, such as carotenoids and prenylquinones, in order to prevent thylakoid lipid peroxidation and degradation of photosynthetic proteins due to reactive oxygen species[69,80,81,89,133-136]. These antioxidant molecules can act as physical or chemical quenchers to detoxify ROS. A physical quencher deactivates ROS using energy transfer and then dissipates excess energy by heat. This method allows the re-use of the same antioxidant molecule many times for ROS inactivation. During chemical quenching (or scavenging), the quencher is consumed by oxidization, requiring a recycling process or the *de novo* synthesis of antioxidant molecules[137]. Plastoglobules, lipidic spherical microdomain associated with thylakoid membrane and considered as lipid storage, are filled with lipid-soluble antioxidants. During stresses, such as oxidative stress, they increase in size and number, accumulating antioxidant molecules. In addition, some steps of biosynthesis as well as recycling of these lipid are performed in plastoglobules[82,138,139]. The close connection between thylakoid membrane and plastoglobules may allow a bidirectional lipid exchange between these two compartments. Therefore, plastoglobules may play an essential role in photoprotection allowing synthesis, recycling, accumulation and storage of lipid-soluble antioxidant molecules. In another hand, other water-soluble antioxidant systems exist including ascorbate (vitamin C), glutathione as well as enzymatic antioxidants such as superoxide dismutase and ascorbate peroxidase that also play major roles in chloroplast photoprotection[140,141].

Carotenoids are composed of eight isoprene units (tetraterpene). They are either pure hydrocarbons (carotenes) or may also contain oxygen (xanthophylls). They can exist freely in the thylakoid membrane or bound to protein-pigment complexes of the photosynthetic apparatus[142,143]. Carotenoids are involved in photosynthesis, considered accessory pigments, by absorbing a range of light spectra (where chlorophyll is weakly efficient), and then transferring the energy to chlorophyll. They may have a role in LHC stabilization[143]. What is more, carotenoids also play a major role in photoprotection[66]. They act as antioxidants by quenching excited chlorophyll or by scavenging ROS[86]. Xanthophylls (oxygenated carotenoids) such as violaxanthin, zeaxanthin and lutein, are principally found in LHCs. Violaxanthin and zeaxanthin play a role in the xanthophyll cycle by de-exciting singlet chlorophyll thus allowing qE and qZ of NPQ[112]. In addition, zeaxanthin has an antioxidant function as ROS scavenger independently of its role in NPQ[142-144]. Lutein, the most abundant xanthophyll, notably quenches chlorophyll triplet and scavenges ROS[145,146]. On the other hand, beta-carotene is mainly attached to PSI and PSII cores. Its antioxidant role would appear to be scavenging of singlet oxygen produced in reaction centers rather than quenching of triplet chlorophyll[147,148].

Prenylquinones as tocopherols, plastoquinols and plastochromanol are free in the thylakoid membrane. Tocopherols belong to the tocochromanol group. They consist of a polar chromanol head and a hydrophobic phytyl tail. Alpha-tocopherol, the most abundant form of tocopherols present in photosynthetic tissues, can prevent lipid peroxidation propagation in thylakoid membrane by scavenging lipid peroxyl radicals. This leads to the formation of a tocopheryl radical. Alpha-tocopherol may also chemically or physically quench ROS (singlet oxygen in particular) and then either release the excitation energy as heat or form tocopherol quinone by chromanol ring opening[86,149-153]. Notably, the tocopheryl radical, by means of ascorbate and glutathione, as well as tocopherol quinone, by enzymatic activity, can be recycled into tocopherol[137,139,154].

Plastoquinone/ol, in addition to its role in electron transport role, also has antioxidant proprieties evident in its ability to scavenge ROS (singlet oxygen) efficiently[79,80,155,156]. Under high light, a decrease of plastoquinone/ol is observed concomitantly with an increase of (tri)hydroxy-plastoquinone. This implies the oxidation of plastoquinone/ol[72,155,157]. PQH_2 seems to be less effective in chemical quenching of singlet oxygen than tocopherols but has a higher mobility, meaning that PQH_2 may have antioxidant activity comparable to that of tocopherols[158,159].

Plastochromanol-8 (PC-8), synthetized from the VTE1-dependent cyclization of PQH_2 in plastoglobules[82], consists in a tocochromanol head group and long solanesyl-derived side chain[70,160]. PC-8 presents antioxidant function, and due to its long unsaturated side chain may be able to quench singlet oxygen. Under high light, levels of hydroxy-plastochromanol are increased, suggesting oxidation by quenching of ROS [133,157,161,162]. Antioxidant functions of PC-8, associated with tocopherol, are essential to maintain longevity and quality of seeds[163]. Additionally, plastoquinone/ol and plastochromanol, as tocopherol, are also probably involved in the inhibition of lipid peroxidation formation[161,163,164].

The involvement of a diversity of antioxidant molecules therefore allows a powerful photoprotection of the photosynthetic apparatus even in very harmful case as excess light energy.

Together, photoprotective mechanisms effectively preserve the photosynthetic machinery by acting according to the type, the site and the level of damages. Finally, plants have developed various strategies of regulation and protection against environmental stress such as changes in light intensities to maintain an efficient photosynthesis.

Moreover, spherical microdomains of the thylakoid membrane, called plastoglobules, metabolize, accumulate and store essential small lipid molecules, such as plastoquinone/ol, phylloquinone, tocopherols and plastochromanol-8[22]. Plastoglobules were discovered about 60 years ago thanks to arrival of electronic microscopy techniques[82,165-173]. Initially, considered only as lipid storage particles[82,139,166,168-173], plastoglobules were revealed to have their own proteome[23-26,174,175] and gradually their implication in biosynthesis and metabolism of various neutral lipids, mostly in response to (a)biotic stresses, became clear. However, other novel roles of plastoglobules certainly remain to be discovered. The next chapter, entitled "*Plastoglobules: Lipid droplets at the thylakoid membrane*" and published in the book "Chloroplasts: Current Research and Future Trends" (Kirchhoff H. Eds.), describes in greater detail the state of the art in 2016 of these small lipid particles. An addendum was added at the end of the chapter II to describe the newly characterized PG proteins as well as some explanatory remarks on atypical kinases.

References

1 Marechal, E. Primary endosymbiosis: Emergence of the primary chloroplast and the chromatophore, two independent events. *Methods Mol Biol* **1829**, 3-16 (2018).

2 Reyes-Prieto, A., Weber, A. P. & Bhattacharya, D. The origin and establishment of the plastid in algae and plants. *Annu Rev Genet* **41**, 147-168 (2007).

3 Timmis, J. N., Ayliffe, M. A., Huang, C. Y. & Martin, W. Endosymbiotic gene transfer: organelle genomes forge eukaryotic chromosomes. *Nat Rev Genet* **5**, 123-135 (2004).

4 Thomson, W. W. & Whatley, J. M. Development of nongreen plastids. *Annu Rev Plant Physiol* **31**, 375-394 (1980).

5 J., R. & G., R. W. Chloroplast development: Fine structure and chlorophyll synthesis. *The Q Rev Biol* **47**, 160-191 (1972).

6 Selstam, E. & Sandelius, A. S. A Comparison between prolamellar bodies and prothylakoid membranes of etioplasts of dark-grown wheat concerning lipid and polypeptide composition. *Plant Physiol* **76**, 1036-1040 (1984).

7 Li, L. & Yuan, H. Chromoplast biogenesis and carotenoid accumulation. *Arch Biochem Biophys* **539**, 102-109 (2013).

8 Sadali, N. M., Sowden, R. G., Ling, Q. & Jarvis, R. P. Differentiation of chromoplasts and other plastids in plants. *Plant Cell Rep* **38**, 803-818 (2019).

9 Biswal, U. C., Biswal, B. & Raval, M. K. Transformation of chloroplast to gerontoplast. In: Chloroplast biogenesis: From proplastid to gerontoplast. *(Biswal, U. C. & Raval, M. K. Eds.)* Springer Netherlands. 155-242 (2003).

10 Golczyk, H., Greiner, S., Wanner, G., Weihe, A., Bock, R., Börner, T. & Herrmann, R. G. Chloroplast DNA in mature and senescing leaves: A reappraisal. *Plant Cell* **26**, 847-854 (2014).

11 Rolland, N., Bouchnak, I., Moyet, L., Salvi, D. & Kuntz, M. The main functions of plastids. *Methods Mol Biol* **1829**, 73-85 (2018).

12 Vothknecht, U. C. & Westhoff, P. Biogenesis and origin of thylakoid membranes. *Biochim Biophys Acta* **1541**, 91-101 (2001).

13 Arvidsson, P. & Sundby, C. A model for the topology of the chloroplast thylakoid membrane. *Funct Plant Biol* **26**, 687-694 (1999).

14 Kirchhoff, H. Architectural switches in plant thylakoid membranes. *Photosynth Res* **116**, 481-487 (2013).

15 Kirchhoff, H. Chloroplast ultrastructure in plants. *New Phytol* **223**, 565-574 (2019).

16 Pribil, M., Labs, M. & Leister, D. Structure and dynamics of thylakoids in land plants. *J Exp Bot* **65**, 1955-1972 (2014).

17 Kobayashi, K. Role of membrane glycerolipids in photosynthesis, thylakoid biogenesis and chloroplast development. *J Plant Res* **129**, 565-580 (2016).

18 Dekker, J. P. & Boekema, E. J. Supramolecular organization of thylakoid membrane proteins in green plants. *Biochim Biophys Acta* **1706**, 12-39 (2005).

19 Mullineaux, C. W. Function and evolution of grana. *Trends Plant Sci* **10**, 521-525 (2005).

20 Mustardy, L., Buttle, K., Steinbach, G. & Garab, G. The three-dimensional network of the thylakoid membranes in plants: quasihelical model of the granum-stroma assembly. *Plant Cell* **20**, 2552-2557 (2008).

21 Austin, J. R., 2nd, Frost, E., Vidi, P. A., Kessler, F. & Staehelin, L. A. Plastoglobules are lipoprotein subcompartments of the chloroplast that are permanently coupled to thylakoid membranes and contain biosynthetic enzymes. *Plant Cell* **18**, 1693-1703 (2006).

22 van Wijk, K. J. & Kessler, F. Plastoglobuli: Plastid microcompartments with integrated functions in metabolism, plastid developmental transitions, and environmental adaptation. *Annu Rev Plant Biol* **68**, 253-289 (2017).

23 Kessler, F., Schnell, D. & Blobel, G. Identification of proteins associated with plastoglobules isolated from pea (*Pisum sativum* L.) chloroplasts. *Planta* **208**, 107-113 (1999).

24 Lundquist, P. K., Poliakov, A., Bhuiyan, N. H., Zybailov, B., Sun, Q. & van Wijk, K. J. The functional network of the *Arabidopsis* plastoglobule proteome based on quantitative proteomics and genome-wide coexpression analysis. *Plant Physiol* **158**, 1172-1192 (2012).

25 Vidi, P. A., Kanwischer, M., Baginsky, S., Austin, J. R., Csucs, G., Dormann, P., Kessler, F. & Brehelin, C. Tocopherol cyclase (VTE1) localization and vitamin E accumulation in chloroplast plastoglobule lipoprotein particles. *J Biol Chem* **281**, 11225-11234 (2006).

26 Ytterberg, A. J., Peltier, J. B. & van Wijk, K. J. Protein profiling of plastoglobules in chloroplasts and chromoplasts. A surprising site for differential accumulation of metabolic enzymes. *Plant Physiol* **140**, 984-997 (2006).

27 Mirkovic, T., Ostroumov, E. E., Anna, J. M., van Grondelle, R., Govindjee & Scholes, G. D. Light absorption and energy transfer in the antenna complexes of photosynthetic organisms. *Chem Rev* **117**, 249-293 (2017).

28 Renger, G. & Kühn, P. Reaction pattern and mechanism of light induced oxidative water splitting in photosynthesis. *Biochim et Biophys Acta Bioenerg* **1767**, 458-471 (2007).

29 Kaminskaya, O., Renger, G. & Shuvalov, V. A. Effect of dehydration on light-induced reactions in photosystem II: Photoreactions of cytochrome *b559*. *Biochemistry* **42**, 8119-8132 (2003).

30 Nelson, N. & Yocum, C. F. Structure and function of photosystems I and II. *Annu Rev Plant Biol* **57**, 521-565 (2006).

31 Cao, P., Su, X., Pan, X., Liu, Z., Chang, W. & Li, M. Structure, assembly and energy transfer of plant photosystem II supercomplex. *Biochim Biophys Acta Bioenerg* **1859**, 633-644 (2018).

32 Li, X.-P., Müller-Moulé, P., Gilmore, A. M. & Niyogi, K. K. PsbS-dependent enhancement of feedback de-excitation protects photosystem II from photoinhibition. *Proc Nat Acad Sci U S A* **99**, 15222-15227 (2002).

33 Jensen, P. E., Bassi, R., Boekema, E. J., Dekker, J. P., Jansson, S., Leister, D., Robinson, C. & Scheller, H. V. Structure, function and regulation of plant photosystem I. *Biochim Biophys Acta* **1767**, 335-352 (2007).

34 Jordan, P., Fromme, P., Witt, H. T., Klukas, O., Saenger, W. & Krauss, N. Three-dimensional structure of cyanobacterial photosystem I at 2.5 Å resolution. *Nature* **411**, 909-917 (2001).

35 Jensen, P. E., Gilpin, M., Knoetzel, J. & Scheller, H. V. The PSI-K subunit of photosystem I is involved in the interaction between light-harvesting complex I and the photosystem I reaction center core. *J Biol Chem* **275**, 24701-24708 (2000).

36 Jensen, P. E., Haldrup, A., Zhang, S. & Scheller, H. V. The PSI-O subunit of plant photosystem I is involved in balancing the excitation pressure between the two photosystems. *J Biol Chem* **279**, 24212-24217 (2004).

37 Allen, J. F., de Paula, W. B., Puthiyaveetil, S. & Nield, J. A structural phylogenetic map for chloroplast photosynthesis. *Trends Plant Sci* **16**, 645-655 (2011).

38 Zhang, H., Primak, A., Cape, J., Bowman, M. K., Kramer, D. M. & Cramer, W. A. Characterization of the high-spin heme *x* in the cytochrome *b6f* complex of oxygenic photosynthesis. *Biochemistry* **43**, 16329-16336 (2004).

39 Baniulis, D., Yamashita, E., Zhang, H., Hasan, S. S. & Cramer, W. A. Structure-function of the cytochrome *b6f* complex. *Photochem Photobiol* **84**, 1349-1358 (2008).

40 Kurisu, G., Zhang, H., Smith, J. L. & Cramer, W. A. Structure of the cytochrome *b6f* complex of oxygenic photosynthesis: tuning the cavity. *Science* **302**, 1009-1014 (2003).

41 Stroebel, D., Choquet, Y., Popot, J. L. & Picot, D. An atypical haem in the cytochrome *b(6)f* complex. *Nature* **426**, 413-418 (2003).

42 Mitchell, P. The protonmotive Q cycle: A general formulation. *FEBS Lett* **59**, 137-139 (1975).

43 Tikhonov, A. N. The cytochrome *b6f* complex: Biophysical aspects of its functioning in chloroplasts. *Subcell Biochem* **87**, 287-328 (2018).

44 Seelert, H., Poetsch, A., Dencher, N. A., Engel, A., Stahlberg, H. & Müller, D. J. Proton-powered turbine of a plant motor. *Nature* **405**, 418-419 (2000).

45 Boekema, E. & Luecken, U. The structure of the CF1 part of the ATP-synthase complex from chloroplast. In: Oxygenic photosynthesis: The light reactions. Advances in photosynthesis and respiration. *(Ort D.R., Yocum C.F., Heichel I.F. Eds.)* Springer, Dordrecht, **4**, 487-492 (1996).

46 Allen, J. Photosynthesis of ATP-electrons, proton pumps, rotors, and poise. *Cell* **110**, 273-276 (2002).

47 Hahn, A., Vonck, J., Mills, D. J., Meier, T. & Kuhlbrandt, W. Structure, mechanism, and regulation of the chloroplast ATP synthase. *Science* **360** (2018).

48 Junge, W. & Nelson, N. ATP synthase. *Annu Rev Biochem* **84**, 631-657 (2015).

49 Staehelin, L. A. Chloroplast structure: from chlorophyll granules to supra-molecular architecture of thylakoid membranes. *Photosynth Res* **76**, 185-196 (2003).

50 Kirchhoff, H., Li, M. & Puthiyaveetil, S. Sublocalization of cytochrome *b6f* complexes in photosynthetic membranes. *Trends Plant Sci* **22**, 574-582 (2017).

51 Albertsson, P. A quantitative model of the domain structure of the photosynthetic membrane. *Trends Plant Sci* **6**, 349-358 (2001).

52 Cramer, W. A., Zhang, H., Yan, J., Kurisu, G. & Smith, J. L. Transmembrane traffic in the cytochrome *b6f* complex. *Annu Rev Biochem* **75**, 769-790 (2006).

53 Rochaix, J. D. Regulation of photosynthetic electron transport. *Biochim Biophys Acta* **1807**, 375-383 (2011).

54 Yamori, W. & Shikanai, T. Physiological functions of cyclic electron transport around photosystem I in sustaining photosynthesis and plant growth. *Annu Rev Plant Biol* **67**, 81-106 (2016).

55 Kawashima, R., Sato, R., Harada, K. & Masuda, S. Relative contributions of PGR5- and NDH-dependent photosystem I cyclic electron flow in the generation of a proton gradient in *Arabidopsis* chloroplasts. *Planta* **246**, 1045-1050 (2017).

56 Joliot, P. & Joliot, A. Cyclic electron flow in C3 plants. *Biochim Biophys Acta* **1757**, 362-368 (2006).

57 DalCorso, G., Pesaresi, P., Masiero, S., Aseeva, E., Schünemann, D., Finazzi, G., Joliot, P., Barbato, R. & Leister, D. A complex containing PGRL1 and PGR5 is involved in the switch between linear and cyclic electron flow in *Arabidopsis*. *Cell* **132**, 273-285 (2008).

58 Munekage, Y., Hashimoto, M., Miyake, C., Tomizawa, K.-I., Endo, T., Tasaka, M. & Shikanai, T. Cyclic electron flow around photosystem I is essential for photosynthesis. *Nature* **429**, 579-582 (2004).

59 Munekage, Y., Hojo, M., Meurer, J., Endo, T., Tasaka, M. & Shikanai, T. PGR5 is involved in cyclic electron flow around photosystem I and is essential for photoprotection in *Arabidopsis*. *Cell* **110**, 361-371 (2002).

60 Suorsa, M., Rossi, F., Tadini, L., Labs, M., Colombo, M., Jahns, P., Kater, M. M., Leister, D., Finazzi, G., Aro, E.-M., Barbato, R. & Pesaresi, P. PGR5-PGRL1-dependent cyclic electron

transport modulates linear electron transport rate in *Arabidopsis thaliana*. *Mol Plant* **9**, 271-288 (2016).

61 Endo, T., Ishida, S., Ishikawa, N. & Sato, F. Chloroplastic NAD(P)H dehydrogenase complex and cyclic electron transport around photosystem I. *Mol Cells* **25**, 158-162 (2008).

62 Ifuku, K., Endo, T., Shikanai, T. & Aro, E. M. Structure of the chloroplast NADH dehydrogenase-like complex: nomenclature for nuclear-encoded subunits. *Plant Cell Physiol* **52**, 1560-1568 (2011).

63 Peng, L., Yamamoto, H. & Shikanai, T. Structure and biogenesis of the chloroplast NAD(P)H dehydrogenase complex. *Biochim Biophys Acta* **1807**, 945-953 (2011).

64 Shikanai, T. Regulatory network of proton motive force: contribution of cyclic electron transport around photosystem I. *Photosynth Res* **129**, 253-260 (2016).

65 Finazzi, G., Rappaport, F., Furia, A., Fleischmann, M., Rochaix, J.-D., Zito, F. & Forti, G. Involvement of state transitions in the switch between linear and cyclic electron flow in *Chlamydomonas reinhardtii*. *EMBO reports* **3**, 280-285 (2002).

66 Niyogi, K. K. Safety valves for photosynthesis. *Curr Opin Plant Biol* **3**, 455-460 (2000).

67 Peltier, G. & Cournac, L. Chlororespiration. *Annu Rev Plant Biol* **53**, 523-550 (2002).

68 Tikhonov, A. N. Modeling electron and proton transport in chloroplasts. In: Chloroplasts: current research and future trends. *(Kirchhoff H. Eds.)* Caister Academic Press, Norfolk, UK. 101-134 (2016).

69 Nowicka, B. & Kruk, J. Occurrence, biosynthesis and function of isoprenoid quinones. *Biochim Biophys Acta* **1797**, 1587-1605 (2010).

70 Block, A., Fristedt, R., Rogers, S., Kumar, J., Barnes, B., Barnes, J., Elowsky, C. G., Wamboldt, Y., Mackenzie, S. A., Redding, K., Merchant, S. S. & Basset, G. J. Functional modeling identifies paralogous solanesyl-diphosphate synthases that assemble the side chain of plastoquinone-9 in plastids. *J Biol Chem* **288**, 27594-27606 (2013).

71 Kruk, J. & Karpinski, S. An HPLC-based method of estimation of the total redox state of plastoquinone in chloroplasts, the size of the photochemically active plastoquinone-pool and its redox state in thylakoids of *Arabidopsis*. *Biochim Biophys Acta* **1757**, 1669-1675 (2006).

72 Ksas, B., Legeret, B., Ferretti, U., Chevalier, A., Pospisil, P., Alric, J. & Havaux, M. The plastoquinone pool outside the thylakoid membrane serves in plant photoprotection as a reservoir of singlet oxygen scavengers. *Plant Cell Environ* **41**, 2277-2287 (2018).

73 Shapiguzov, A., Chai, X., Fucile, G., Longoni, P., Zhang, L. & Rochaix, J. D. Activation of the Stt7/STN7 kinase through dynamic interactions with the cytochrome *b6f* complex. *Plant Physiol* **171**, 82-92 (2016).

74 Escoubas, J. M., Lomas, M., LaRoche, J. & Falkowski, P. G. Light intensity regulation of *cab* gene transcription is signaled by the redox state of the plastoquinone pool. *Proc Natl Acad Sci U S A* **92**, 10237-10241 (1995).

75 Karpinski, S., Escobar, C., Karpinska, B., Creissen, G. & Mullineaux, P. M. Photosynthetic electron transport regulates the expression of cytosolic ascorbate peroxidase genes in *Arabidopsis* during excess light stress. *Plant Cell* **9**, 627-640 (1997).

76 Karpinski, S., Reynolds, H., Karpinska, B., Wingsle, G., Creissen, G. & Mullineaux, P. Systemic signaling and acclimation in response to excess excitation energy in *Arabidopsis*. *Science* **284**, 654-657 (1999).

77 Pfannschmidt, T., Allen, J. F. & Oelmüller, R. Principles of redox control in photosynthesis gene expression. *Plant Physiol* **112**, 1-9 (2001).

78 Pfannschmidt, T., Nilsson, A., Tullberg, A., Link, G. & Allen, J. F. Direct transcriptional control of the chloroplast genes *psbA* and *psaAB* adjusts photosynthesis to light energy distribution in plants. *IUBMB Life* **48**, 271-276 (1999).

79 Kruk, J., Jemiola-Rzeminska, M., Burda, K., Schmid, G. H. & Strzalka, K. Scavenging of superoxide generated in photosystem I by plastoquinol and other prenyllipids in thylakoid membranes. *Biochemistry* **42**, 8501-8505 (2003).

80 Kruk, J. & Trebst, A. Plastoquinol as a singlet oxygen scavenger in photosystem II. *Biochim Biophys Acta* **1777**, 154-162 (2008).

81 Ksas, B., Becuwe, N., Chevalier, A. & Havaux, M. Plant tolerance to excess light energy and photooxidative damage relies on plastoquinone biosynthesis. *Sci Rep* **5**, 10919 (2015).

82 Zbierzak, A. M., Kanwischer, M., Wille, C., Vidi, P. A., Giavalisco, P., Lohmann, A., Briesen, I., Porfirova, S., Brehelin, C., Kessler, F. & Dormann, P. Intersection of the tocopherol and plastoquinol metabolic pathways at the plastoglobule. *Biochem J* **425**, 389-399 (2010).

83 Krieger-Liszkay, A. Singlet oxygen production in photosynthesis. *J Exp Bot* **56**, 337-346 (2005).

84 Krieger-Liszkay, A., Fufezan, C. & Trebst, A. Singlet oxygen production in photosystem II and related protection mechanism. *Photosynth Res* **98**, 551-564 (2008).

85 Rinalducci, S., Pedersen, J. Z. & Zolla, L. Formation of radicals from singlet oxygen produced during photoinhibition of isolated light-harvesting proteins of photosystem II. *Biochim Biophys Acta* **1608**, 63-73 (2004).

86 Triantaphylides, C. & Havaux, M. Singlet oxygen in plants: production, detoxification and signaling. *Trends Plant Sci* **14**, 219-228 (2009).

87 Roach, T. & Krieger-Liszkay, A. Regulation of photosynthetic electron transport and photoinhibition. *Curr Protein Pept Sci* **15**, 351-362 (2014).

88 Takagi, D., Takumi, S., Hashiguchi, M., Sejima, T. & Miyake, C. Superoxide and singlet oxygen produced within the thylakoid membranes both cause photosystem I photoinhibition. *Plant Physiol* **171**, 1626-1634 (2016).

89 Triantaphylides, C., Krischke, M., Hoeberichts, F. A., Ksas, B., Gresser, G., Havaux, M., Van Breusegem, F. & Mueller, M. J. Singlet oxygen is the major reactive oxygen species involved in photooxidative damage to plants. *Plant Physiol* **148**, 960-968 (2008).

90 Minagawa, J. State transitions-the molecular remodeling of photosynthetic supercomplexes that controls energy flow in the chloroplast. *Biochim Biophys Acta* **1807**, 897-905 (2011).

91 Rochaix, J. D. Role of thylakoid protein kinases in photosynthetic acclimation. *FEBS Lett* **581**, 2768-2775 (2007).

92 Wollman, F. A. State transitions reveal the dynamics and flexibility of the photosynthetic apparatus. *EMBO J* **20**, 3623-3630 (2001).

93 Aro, E. M. & Ohad, I. Redox regulation of thylakoid protein phosphorylation. *Antioxid Redox Signal* **5**, 55-67 (2003).

94 Bellafiore, S., Barneche, F., Peltier, G. & Rochaix, J. D. State transitions and light adaptation require chloroplast thylakoid protein kinase STN7. *Nature* **433**, 892-895 (2005).

95 Depege, N., Bellafiore, S. & Rochaix, J. D. Role of chloroplast protein kinase Stt7 in LHCII phosphorylation and state transition in *Chlamydomonas*. *Science* **299**, 1572-1575 (2003).

96 Pesaresi, P., Pribil, M., Wunder, T. & Leister, D. Dynamics of reversible protein phosphorylation in thylakoids of flowering plants: the roles of STN7, STN8 and TAP38. *Biochim Biophys Acta* **1807**, 887-896 (2011).

97 Vener, A. V., van Kan, P. J., Rich, P. R., Ohad, I. & Andersson, B. Plastoquinol at the quinol oxidation site of reduced cytochrome *bf* mediates signal transduction between light and protein phosphorylation: thylakoid protein kinase deactivation by a single-turnover flash. *Proc Natl Acad Sci U S A* **94**, 1585-1590 (1997).

98 Zito, F., Finazzi, G., Delosme, R., Nitschke, W., Picot, D. & Wollman, F. A. The Qo site of cytochrome *b6f* complexes controls the activation of the LHCII kinase. *EMBO J* **18**, 2961-2969 (1999).

99 Pribil, M., Pesaresi, P., Hertle, A., Barbato, R. & Leister, D. Role of plastid protein phosphatase TAP38 in LHCII dephosphorylation and thylakoid electron flow. *PLoS Biol* **8**, e1000288 (2010).

100 Shapiguzov, A., Ingelsson, B., Samol, I., Andres, C., Kessler, F., Rochaix, J. D., Vener, A. V. & Goldschmidt-Clermont, M. The PPH1 phosphatase is specifically involved in LHCII dephosphorylation and state transitions in *Arabidopsis*. *Proc Natl Acad Sci U S A* **107**, 4782-4787 (2010).

101 Allen, J. F. & Forsberg, J. Molecular recognition in thylakoid structure and function. *Trends Plant Sci* **6**, 317-326 (2001).

102 Zhang, S. & Scheller, H. V. Light-harvesting complex II binds to several small subunits of photosystem I. *J Biol Chem* **279**, 3180-3187 (2004).

103 Mekala, N. R., Suorsa, M., Rantala, M., Aro, E. M. & Tikkanen, M. Plants actively avoid state transitions upon changes in light intensity: Role of light-harvesting complex II protein dephosphorylation in high light. *Plant Physiol* **168**, 721-734 (2015).

104 Ruban, A. V. Nonphotochemical chlorophyll fluorescence quenching: Mechanism and effectiveness in protecting plants from photodamage. *Plant Physiol* **170**, 1903-1916 (2016).

105 Joliot, P. A. & Finazzi, G. Proton equilibration in the chloroplast modulates multiphasic kinetics of nonphotochemical quenching of fluorescence in plants. *Proc Natl Acad Sci U S A* **107**, 12728-12733 (2010).

106 Maxwell, K. & Johnson, G. N. Chlorophyll fluorescence - a practical guide. *J Exp Bot* **51**, 659-668 (2000).

107 Krause, G. H. & E., W. Chlorophyll fluorescence and photosynthesis: The basics. *Annu Rev Plant Physiol Plant Mol Biol* **42**, 313-349 (1991).

108 Müller, P., Li, X. P. & Niyogi, K. K. Non-photochemical quenching. A response to excess light energy. *Plant Physiol* **125**, 1558-1566 (2001).

109 Li, X. P., Bjorkman, O., Shih, C., Grossman, A. R., Rosenquist, M., Jansson, S. & Niyogi, K. K. A pigment-binding protein essential for regulation of photosynthetic light harvesting. *Nature* **403**, 391-395 (2000).

110 Sylak-Glassman, E. J., Malnoe, A., De Re, E., Brooks, M. D., Fischer, A. L., Niyogi, K. K. & Fleming, G. R. Distinct roles of the photosystem II protein PsbS and zeaxanthin in the regulation of light harvesting in plants revealed by fluorescence lifetime snapshots. *Proc Natl Acad Sci U S A* **111**, 17498-17503 (2014).

111 Holt, N. E., Fleming, G. R. & Niyogi, K. K. Toward an understanding of the mechanism of nonphotochemical quenching in green plants. *Biochemistry* **43**, 8281-8289 (2004).

112 Holt, N. E., Zigmantas, D., Valkunas, L., Li, X. P., Niyogi, K. K. & Fleming, G. R. Carotenoid cation formation and the regulation of photosynthetic light harvesting. *Science* **307**, 433-436 (2005).

113 Yamamoto, H. Y., Bugos, R. C. & David Hieber, A. Biochemistry and molecular biology of the xanthophyll cycle. In: The photochemistry of carotenoids. *(Harry A. F., Andrew J. Y., George B., & Richard J. C. Eds.)* Springer Netherlands. 293-303 (1999).

114 Johnson, M. P., Perez-Bueno, M. L., Zia, A., Horton, P. & Ruban, A. V. The zeaxanthin-independent and zeaxanthin-dependent qE components of nonphotochemical quenching

involve common conformational changes within the photosystem II antenna in *Arabidopsis*. *Plant Physiol* **149**, 1061-1075 (2009).

115 Dall'Osto, L., Caffarri, S. & Bassi, R. A mechanism of nonphotochemical energy dissipation, independent from PsbS, revealed by a conformational change in the antenna protein CP26. *Plant Cell* **17**, 1217-1232 (2005).

116 Nilkens, M., Kress, E., Lambrev, P., Miloslavina, Y., Muller, M., Holzwarth, A. R. & Jahns, P. Identification of a slowly inducible zeaxanthin-dependent component of non-photochemical quenching of chlorophyll fluorescence generated under steady-state conditions in *Arabidopsis*. *Biochim Biophys Acta* **1797**, 466-475 (2010).

117 Ruban, A. V. Light harvesting control in plants. *FEBS Lett* **592**, 3030-3039 (2018).

118 Crouchman, S., Ruban, A. & Horton, P. PsbS enhances nonphotochemical fluorescence quenching in the absence of zeaxanthin. *FEBS Lett* **580**, 2053-2058 (2006).

119 Niyogi, K. K., Grossman, A. R. & Bjorkman, O. *Arabidopsis* mutants define a central role for the xanthophyll cycle in the regulation of photosynthetic energy conversion. *Plant Cell* **10**, 1121-1134 (1998).

120 Ruban, A. V., Johnson, M. P. & Duffy, C. D. The photoprotective molecular switch in the photosystem II antenna. *Biochim Biophys Acta* **1817**, 167-181 (2012).

121 Aro, E. M., Virgin, I. & Andersson, B. Photoinhibition of photosystem II. Inactivation, protein damage and turnover. *Biochim Biophys Acta* **1143**, 113-134 (1993).

122 Fufezan, C., Rutherford, A. W. & Krieger-Liszkay, A. Singlet oxygen production in herbicide-treated photosystem II. *FEBS Lett* **532**, 407-410 (2002).

123 Bonardi, V., Pesaresi, P., Becker, T., Schleiff, E., Wagner, R., Pfannschmidt, T., Jahns, P. & Leister, D. Photosystem II core phosphorylation and photosynthetic acclimation require two different protein kinases. *Nature* **437**, 1179-1182 (2005).

124 Tikkanen, M., Nurmi, M., Kangasjarvi, S. & Aro, E. M. Core protein phosphorylation facilitates the repair of photodamaged photosystem II at high light. *Biochim Biophys Acta* **1777**, 1432-1437 (2008).

125 Jarvi, S., Suorsa, M. & Aro, E. M. Photosystem II repair in plant chloroplasts - Regulation, assisting proteins and shared components with photosystem II biogenesis. *Biochim Biophys Acta* **1847**, 900-909 (2015).

126 Kruse, O., Zheleva, D. & Barber, J. Stabilization of photosystem two dimers by phosphorylation: implication for the regulation of the turnover of D1 protein. *FEBS Lett* **408**, 276-280 (1997).

127 Li, L., Aro, E. M. & Millar, A. H. Mechanisms of photodamage and protein turnover in photoinhibition. *Trends Plant Sci* **23**, 667-676 (2018).

128 Theis, J. & Schroda, M. Revisiting the photosystem II repair cycle. *Plant Signal Behav* **11**, e1218587 (2016).

129 Murata, N., Takahashi, S., Nishiyama, Y. & Allakhverdiev, S. I. Photoinhibition of photosystem II under environmental stress. *Biochim Biophys Acta* **1767**, 414-421 (2007).

130 Ohad, I., Berg, A., Berkowicz, S. M., Kaplan, A. & Keren, N. Photoinactivation of photosystem II: is there more than one way to skin a cat? *Physiol Plant* **142**, 79-86 (2011).

131 Melis, A. Photosystem-II damage and repair cycle in chloroplasts: what modulates the rate of photodamage? *Trends Plant Sci* **4**, 130-135 (1999).

132 Sonoike, K. Photoinhibition of photosystem I. *Physiol Plant* **142**, 56-64 (2011).

133 Gruszka, J., Pawlak, A. & Kruk, J. Tocochromanols, plastoquinol, and other biological prenyllipids as singlet oxygen quenchers-determination of singlet oxygen quenching rate constants and oxidation products. *Free Radic Biol Med* **45**, 920-928 (2008).

134 Kruk, J., Szymanska, R., Nowicka, B. & Dluzewska, J. Function of isoprenoid quinones and chromanols during oxidative stress in plants. *N Biotechnol* **33**, 636-643 (2016).

135 Lichtenthaler, H. K. Biosynthesis, accumulation and emission of carotenoids, α-tocopherol, plastoquinone, and isoprene in leaves under high photosynthetic irradiance. *Photosynth Res* **92**, 163-179 (2007).

136 Mène-Saffrané, L. & DellaPenna, D. Biosynthesis, regulation and functions of tocochromanols in plants. *Plant Physiol Biochem* **48**, 301-309 (2010).

137 Kobayashi, N. & DellaPenna, D. Tocopherol metabolism, oxidation and recycling under high light stress in *Arabidopsis*. *Plant J* **55**, 607-618 (2008).

138 Eugeni-Piller, L., Abraham, M., Dormann, P., Kessler, F. & Besagni, C. Plastid lipid droplets at the crossroads of prenylquinone metabolism. *J Exp Bot* **63**, 1609-1618 (2012).

139 Eugeni-Piller, L., Glauser, G., Kessler, F. & Besagni, C. Role of plastoglobules in metabolite repair in the tocopherol redox cycle. *Front Plant Sci* **5** (2014).

140 Ahmad, P., Jaleel, C. A., Salem, M. A., Nabi, G. & Sharma, S. Roles of enzymatic and nonenzymatic antioxidants in plants during abiotic stress. *Crit Rev Biotechnol* **30**, 161-175 (2010).

141 Asada, K. Ascorbate peroxidase – a hydrogen peroxide-scavenging enzyme in plants. *Physiol Plant* **85**, 235-241 (1992).

142 Dall'Osto, L., Cazzaniga, S., Havaux, M. & Bassi, R. Enhanced photoprotection by protein-bound vs free xanthophyll pools: a comparative analysis of chlorophyll *b* and xanthophyll biosynthesis mutants. *Mol Plant* **3**, 576-593 (2010).

143 Havaux, M., Dall'Osto, L., Cuine, S., Giuliano, G. & Bassi, R. The effect of zeaxanthin as the only xanthophyll on the structure and function of the photosynthetic apparatus in *Arabidopsis* thaliana. *J Biol Chem* **279**, 13878-13888 (2004).

144 Mozzo, M., Dall'Osto, L., Hienerwadel, R., Bassi, R. & Croce, R. Photoprotection in the antenna complexes of photosystem II: role of individual xanthophylls in chlorophyll triplet quenching. *J Biol Chem* **283**, 6184-6192 (2008).

145 Dall'Osto, L., Lico, C., Alric, J., Giuliano, G., Havaux, M. & Bassi, R. Lutein is needed for efficient chlorophyll triplet quenching in the major LHCII antenna complex of higher plants and effective photoprotection *in vivo* under strong light. BMC Plant Biol 6, 32, doi:10.1186/1471-2229-6-32 (2006).

146 Jahns, P. & Holzwarth, A. R. The role of the xanthophyll cycle and of lutein in photoprotection of photosystem II. *Biochim Biophys Acta* **1817**, 182-193 (2012).

147 Ramel, F., Birtic, S., Cuine, S., Triantaphylides, C., Ravanat, J. L. & Havaux, M. Chemical quenching of singlet oxygen by carotenoids in plants. *Plant Physiol* **158**, 1267-1278 (2012).

148 Telfer, A. Too much light? How β-carotene protects the photosystem II reaction centre. *Photochem Photobiol Sci* **4**, 950-956 (2005).

149 Falk, J. & Munné-Bosch, S. Tocochromanol functions in plants: antioxidation and beyond. *J Exp Bot* **61**, 1549-1566 (2010).

150 Havaux, M., Eymery, F., Porfirova, S., Rey, P. & Dormann, P. Vitamin E protects against photoinhibition and photooxidative stress in *Arabidopsis thaliana*. *Plant Cell* **17**, 3451-3469 (2005).

151 Krieger-Liszkay, A. & Trebst, A. Tocopherol is the scavenger of singlet oxygen produced by the triplet states of chlorophyll in the PSII reaction centre. *J Exp Bot* **57**, 1677-1684 (2006).

152 Munné-Bosch, S. The role of α-tocopherol in plant stress tolerance. *J Plant Physiol* **162**, 743-748 (2005).

153 Voll, L. M. & Abbasi, A. R. Are there specific *in vivo* roles for α- and γ-tocopherol in plants? *Plant Signal Behav* **2**, 486-488 (2007).

154 Spicher, L., Almeida, J., Gutbrod, K., Pipitone, R., Dormann, P., Glauser, G., Rossi, M. & Kessler, F. Essential role for phytol kinase and tocopherol in tolerance to combined light and temperature stress in tomato. *J Exp Bot* **68**, 5845-5856 (2017).

155 Ferretti, U., Ciura, J., Ksas, B., Rac, M., Sedlarova, M., Kruk, J., Havaux, M. & Pospisil, P. Chemical quenching of singlet oxygen by plastoquinols and their oxidation products in *Arabidopsis*. *Plant J* (2018).

156 Yadav, D. K., Kruk, J., Sinha, R. K. & Pospisil, P. Singlet oxygen scavenging activity of plastoquinol in photosystem II of higher plants: electron paramagnetic resonance spin-trapping study. *Biochim Biophys Acta* **1797**, 1807-1811 (2010).

157 Szymanska, R., Nowicka, B. & Kruk, J. Hydroxy-plastochromanol and plastoquinone-C as singlet oxygen products during photo-oxidative stress in *Arabidopsis*. *Plant Cell Environ* **37**, 1464-1473 (2014).

158 Jemioła-Rzemińska, M., Kruk, J. & Strzałka, K. Anisotropy measurements of intrinsic fluorescence of prenyllipids reveal much higher mobility of plastoquinol than α-tocopherol in model membranes. *Chem Phys Lipids* **123**, 233-243 (2003).

159 Nowicka, B. & Kruk, J. Plastoquinol is more active than α-tocopherol in singlet oxygen scavenging during high light stress of *Chlamydomonas reinhardtii*. *Biochim Biophys Acta* **1817**, 389-394 (2012).

160 Zbierzak, A. M., Kanwischer, M., Wille, C., Vidi, P. A., Giavalisco, P., Lohmann, A., Briesen, I., Porfirova, S., Brehelin, C., Kessler, F. & Dormann, P. Intersection of the tocopherol and plastoquinol metabolic pathways at the plastoglobule. *Biochem J* **425**, 389-399 (2009).

161 Nowicka, B., Gruszka, J. & Kruk, J. Function of plastochromanol and other biological prenyllipids in the inhibition of lipid peroxidation - A comparative study in model systems. *Biochim Biophys Acta* **1828**, 233-240 (2013).

162 Szymanska, R. & Kruk, J. Plastoquinol is the main prenyllipid synthesized during acclimation to high light conditions in *Arabidopsis* and is converted to plastochromanol by tocopherol cyclase. *Plant Cell Physiol* **51**, 537-545 (2010).

163 Mène-Saffrané, L., Jones, A. D. & DellaPenna, D. Plastochromanol-8 and tocopherols are essential lipid-soluble antioxidants during seed desiccation and quiescence in *Arabidopsis*. *Proc Natl Acad Sci U S A* **107**, 17815-17820 (2010).

164 Mène-Saffrané, L., Davoine, C., Stolz, S., Majcherczyk, P. & Farmer, E. E. Genetic removal of tri-unsaturated fatty acids suppresses developmental and molecular phenotypes of an *Arabidopsis* tocopherol-deficient mutant. Whole-body mapping of malondialdehyde pools in a complex eukaryote. *J Biol Chem* **282**, 35749-35756 (2007).

165 Cohen, M. & Bowler, E. Lamellar structure of the tobacco chloroplast. *Protoplasma* **42**, 414-416 (1953).

166 Greenwood, A. D., Leech, R. M. & Williams, J. P. Osmiophilic globules of chloroplasts. 1. Osmiophilic globules as a normal component of chloroplasts and their isolation and composition in *Vicia faba* L. *Biochim Biophys Acta* **78**, 148-162 (1963).

167 Lichtenthaler, H. K. Plastoglobuli and fine structure of plastids. *Endeavour* **27**, 144-149 (1968).

168 Lichtenthaler, H. K. & Peveling, E. Plastoglobuli and osmiophilic cytoplasmic lipid inclusions in green leaves of *Hoya carnosa* R Br. *Z Pflanzenphysiol* **56**, 153-165 (1967).

169 Bailey, J. L. & Whyborn, A. G. Osmiophilic globules of chloroplasts. II Globules of spinach-beet chloroplast. *Biochim Biophys Acta* **78**, 163-174 (1963).

170 Gaude, N., Bréhélin, C., Tischendorf, G., Kessler, F. & Dormann, P. Nitrogen deficiency in *Arabidopsis* affects galactolipid composition and gene expression and results in accumulation of fatty acid phytyl esters. *Plant J* **49**, 729-739 (2007).

171 Hansmann, P. & Sitte, P. Composition and molecular structure of chromoplast globules of *Viola tricolor*. *Plant Cell Rep* **1**, 111-114 (1982).

172 Lichtenthaler, H. K. Plastoglobuli of spinach - Their size and composition during chloroplast degeneration. *Protoplasma* **68**, 315-326 (1969).

173 Lichtenthaler, H. K. Plastoglobuli and lipoquinone content of chloroplasts from *Cereus peruvianus* (L) Mill. *Planta* **87**, 304-310 (1969).

174 Deruère, J., Romer, S., Dharlingue, A., Backhaus, R. A., Kuntz, M. & Camara, B. Fibril assembly and carotenoid overaccumulation in chromoplasts - a model for supramolecular lipoprotein structures. *Plant Cell* **6**, 119-133 (1994).

175 Pozueta-Romero, J., Rafia, F., Houlne, G., Cheniclet, C., Carde, J. P., Schantz, M. L. & Schantz, R. A ubiquitous plant housekeeping gene, *PAP*, encodes a major protein component of bell pepper chromoplasts. *Plant Physiol.* **115**, 1185-1194 (1997).

Chapter II

Plastoglobules: lipid droplets at the thylakoid membrane

Pralon Thibaut and Kessler Felix

Chloroplasts: Current Research and Future Trends. (Kirchhoff H. Eds.) Caister Academic Press, Norfolk, UK. 171-186 (2016).

Abstract

Plastoglobules (PG) are lipid droplets that are structurally and functionally associated with the thylakoid membranes of chloroplasts. PG thus effectively form a thylakoid membrane microdomain. The thylakoid membranes provide the environment for the photosynthetic light reactions. The thylakoid membranes in majority consist of bilayer forming galactolipids and also harbor neutral lipids, including carotenoids, chlorophylls, prenylquinones (plastoquinone, phylloquinone, tocopherols), and others. The neutral lipids participate directly in the photosynthetic light reactions, act as antioxidants or are metabolic products, respectively. The biosynthesis, abundance, redox state and other parameters of these compounds are tightly controlled. PG store these compounds but also actively participate in their metabolism. PG thereby contribute to continuous remodeling of the thylakoid membrane. This depends on the presence of an assortment of enzymes and regulatory kinases at PG that are involved in wide range of processes affecting thylakoid membrane composition. Here, we review the current state of the PG field.

2.1 Discovery of PG

2.1.1 Ultrastructure of the chloroplast reveals osmiophilic bodies, the plastoglobules

In the middle of the twentieth century, electron microscopy gave scientists a new tool to visualize plant subcellular organization. Soon, scientists began to describe the details of chloroplast ultrastructure in different photosynthetic organisms[1,2]. Among the discoveries were spherical particles that are ubiquitous in plastids. Owing to the presence of unsaturated lipids they were intensely contrasted by osmium tetroxide and therefore initially termed osmiophilic globules[3]. Their diameter varied from 10 to 500 nm depending on the plastid origin and developmental state[3,4]. The globules consist of a polar membrane lipid monolayer on the outside and neutral lipids on the inside[5]. In addition, proteins coat the surface of globules[6,7]. Therefore, structurally, the osmiophilic globules, now termed plastoglobules (PG), were categorized as lipoprotein particles or lipid droplets. Typical for lipid droplets, the lipid to protein ratio of PG is high resulting in a very low buoyant density. Due to their identification as lipid storing particles, the composition of the isolated PG became a topic of interest.

2.1.2 Plastoglobule lipid composition

In order to determine lipid composition, plastoglobules needed to be isolated. Taking advantage of their low density, plastoglobules could easily be isolated and separated from the denser envelope and thylakoid membranes by floatation centrifugation using sucrose density gradients. Lipid composition of isolated PG was then analyzed by thin-layer chromatography. First studies of the lipid composition of plastoglobules revealed the presence of triacylglycerol (TAG), plastoquinone/-ol, α-tocopherol (Vitamin E), galactolipids, but chlorophyll was notably absent[3,8]. Follow up investigations of the PG lipid composition largely confirmed the earlier results while adding some new compounds such as phylloquinone (Vitamin K_1)[9-11]. Recently, fatty acid phytyl esters (FAPE) were added to the PG lipid list[12] (Table 2.1). Triacylglycerol was found to be the major lipid constituent of chloroplast PG, whereas carotenoids and their esters were the most abundant in chromoplast PG[5,13-15]. So far, a complete PG lipidome using state of the art mass spectrometry techniques has not been determined. Therefore, additional, presumably less abundant lipid species may still be discovered. Apart from lipids, some early studies on PG composition also hinted at the presence of proteins[5,14]. In those days, however, the technology to identify and analyze the proteins was not yet sufficiently well developed.

Plastids	Lipid	References
Chloroplast	α-tocopherol (Vitamin E) Fatty acid phytyl esters (FAPE) Galactolipids Phylloquinone (Vitamin K_1) Plastochromanol-8 (PC-8) Plastoquinone/ol (PQ/PQH_2) Triacylglycerol (TAG)	Bailey and Whyborn (1963)[8], Gaude et al. (2007)[12], Greenwood et al. (1963)[3], Lichtenhaler and Peveling (1967)[10], Lichtenhaler and Sprey (1966)[11], Steinmüller and Tevini (1985)[14], Zbierzak et al. (2010)[54]
Chromoplast	α-tocopherol (Vitamin E) Carotenoids Carotenoid esters Plastoquinone (PQ) Triacylglycerol (TAG)	Deruère et al. (1994)[20], Hansmann and Sitte (1982)[5], Steinmüller and Tevini (1985)[14]
Gerontoplast	Fatty acid phytyl esters (FAPE) Triacylglycerol (TAG)	Gaude et al. (2007)[12], Tevini and Steinmüller (1985)[15]

Table 2.1. Main lipid founded in plastoglobules of different plastids.

2.1.3 Lipid trafficking between PG and the thylakoid membrane

Given the common nature of lipids in thylakoids and PG, an important question concerns the possibility and mechanism of lipid exchange between the two compartments. An electron tomographic study of plastoglobules revealed that PG are normally in contact with the margins of stromal thylakoids. High-resolution image analysis showed that the outer lipid leaflet of PG is contiguous with that of the thylakoid membrane[16]. The contact sites between PG and thylakoid membranes therefore result in a tight patch that connects the interior hydrophobic phase of PG with the thylakoid bilayer. This configuration could therefore allow the simultaneous transfer of polar membrane lipids and hydrophobic molecules between the two compartments thereby providing a physical basis for molecular trafficking between the two compartments and explanation for their molecular cooperation.

2.1.4 PG morphological changes in response to developmental transitions and stress adaptation

Using electron microscopy on various plant tissues, developmental states and stress conditions, plastid ultrastructural modifications implicating both PG and thylakoid membranes were observed. These changes provide striking visual evidence of physical membrane remodeling. For instance, the presence of numerous PG in proplastids and etioplasts that decrease in number during chloroplast formation while thylakoids emerge[4,17] led to the hypothesis of an involvement of PG in thylakoid membrane formation. During chloroplast senescence PG become supersized while the thylakoids progressively disappear[18,19] suggesting that PG participate in thylakoid disassembly. Similarly, during chromoplast development in red pepper fruit maturation, the disappearance of the thylakoid membranes concomitantly with the proliferation and enlargement of PG was observed. Ultimately, pigment-filled fibrils, derived from globular PG emerged[20]. The chloroplast to chromoplast transition in other species follows an analogous pattern but the PG themselves serve to store the pigments. In summary, the electron microscopic evidence implicates PG in several types of plastid developmental transitions: from etioplast to chloroplast, from chloroplast to gerontoplast and from chloroplast to chromoplast, respectively.

Electron microscopic observation of plastids after various stress treatments showed that ultrastructural changes in PG and the thylakoid membrane are not limited to developmental transitions. Various stress types such as high salt, drought, nitrogen deprivation, heat, high light as well as heavy metals increase the size and number of PG[12,21-24]. The aforementioned stress types result in leaf bleaching and altered photosynthetic parameters, which in turn reflect chlorophyll degradation and thylakoid membrane perturbation and disassembly. Thus, the various stress types to some extent reiterate senescence related phenotypes. As for the plastid developmental transitions, ultrastructural changes during stress adaptation provide evidence for the implication of PG in thylakoid lipid remodeling. One particularly striking example is *Arabidopsis* under nitrogen-depleted conditions[12]: by electron microscopy, thylakoids appear strongly diminished whereas PG become supersized. Here, the visible physical remodeling correlates with a reduction of chlorophyll and monogalactosyldiacylglycerol (MGDG) levels and an increase of triacylglycerol and fatty acid phytyl esters[25].

For a long time, however, the metabolic roles of PG (apart of course from lipid storage)[4,10,17] in plastid developmental transitions and in stress adaptations were unknown. Only with advent of modern molecular biology techniques evidence started to emerge indicating that it is the protein complement of PG that enables the active participation of PG in thylakoid membrane remodeling (Fig. 2.1).

2.1.5 PG protein composition

In the 1980s, proteins were detected in PG[5,14]. In red pepper chromoplasts, carotenoids are stored in globulo-tubular structures termed fibrils that contain an abundant 30 kDa protein that was termed fibrillin[20,26]. The amino acid sequence of fibrillin was determined by Deruère *et al.* (1994)[20] making it the first known PG protein. Related proteins, called PAP (Plastid-lipid Associated Proteins) belonging to the emerging fibrillin family were also identified and found to be major PG proteins in chloroplasts and chromoplasts of several species[6,7].

In the meantime, the PG proteomes from chloroplasts have been determined and refined revealing thirty consensus proteins[27] (Table 2.2). In addition, the proteome of red pepper chromoplast PG has been determined[28]. PG proteins can be classified in three main groups; (1) structural proteins (PAP/Fibrillins), (2) chloroplast metabolic enzymes, (3) unknown proteins[29]. Genome-wide coexpression analysis of the genes encoding PG proteins resulted in a modular network consisting of four distinct modules each containing PG proteins. Specific functional enrichment in each of the modules was attributed to chlorophyll degradation/senescence, isoprenoid biosynthesis, plastid proteolysis, redox regulators and phosphoregulators of electron flow[27].

The discovery of a surprising variety of associated proteins resulted in the new hypothesis proposing that PG do not only serve in lipid storage but also in lipid metabolism. Moreover, it appears that PG proteomes are functionally tailored to the plastid type. In chromoplast PG, for instance, enzymes involved in the synthesis and accumulation of colored carotenoids are specifically recruited[28]. In the following, we will review the identified and characterized PG proteins as well as their implication in lipid metabolism and remodeling of the thylakoid membrane during plastid developmental transitions and stress adaptation.

Known and characterized proteins in plastoglobules

Accession	Common name	Symbol	Function(s)
At4g04020	Fibrillin 1a	FBN1a; PGL35	PG structure
At4g22240	Fibrillin 1b	FBN1b; PGL33	
At2g35490	Fibrillin 2	FBN2; PGL40	
At3g23400	Fibrillin 4	FBN4; PGL30.4	
At4g32770	Tocopherol cyclase	VTE1	Tocopherol biosynthesis and regeneration
At5g08740	NAD(P)H dehydrogenase C1	NDC1	Phylloquinone biosynthesis, PC-8 biosynthesis; PQ redox state regulation
At4g25700	β-carotene β-hydroxylase	CrtR-β	Carotenoid metabolism
At3g04870	ζ-carotene desaturase	ZDS	
At3g10230	Lycopene β-cyclase	LYC-β	
At4g19170	Carotenoid cleavage dioxygenase 4	CCD4; NCED4	
At1g54570	Phytyl ester synthase 1	PES1; DGAT3	TAG and FAPEs biosynthesis
At3g26840	Phytyl ester synthase 2	PES2; DGAT4	
At4g31390	Activity of bc1-like kinase 1	ABC1K1	Prenylquinone biosynthesis and metabolic regulation
At1g79600	Activity of bc1-like kinase 3	ABC1K3	
At3g07700	Activity of bc1-like kinase 7	ABC1K7	

Uncharacterized plastoglobule proteins

Accession	*Common name*	*Symbol*	*Predicted function*
At3g58010	*Fibrillin 7a*	*FBN7a; PGL34*	*PG stucture*
At2g42130	*Fibrillin 7b*	*FBN7; PGL30*	
At2g46910	*Fibrillin 8*	*FBN8*	
At1g71810	*Activity of bc1-like kinase 5*	*ABC1K5*	*Regulation of metabolic process*
At3g24190	*Activity of bc1-like kinase 6*	*ABC1K6*	
At5g05200	*Activity of bc1-like kinase 9*	*ABC1K9*	
At1g32220	*Flavin reductase-related 1*		
At2g34460	*Flavin reductase-related 2*		
At1g78140	*UbiE methyltransferase-related 1*		*Prenyl lipid biosynthesis*
At2g41040	*UbiE methyltransferase-related 2*		
At3g10130	*SOUL domain protein*		*Tetrapyrale metabolism*
At1g06690	*Aldo/keto reductase*		*Sugar metabolism*
At4g39730	*PLAT/LH2-1*		*Lipid cleavage*
At3g27110	*M48 protease*		*Participation in senescence associated process*
At5g41120	*Esterase 1*		*TAG/FAPE biosynthesis*
At1g73750	*Unknown SAG*		*Participation in senescence associated process*
At4g13200	*Unknown 1*		*Carotenoid metabolism and thylakoid formation*
At3g43540	*Unknown 2*	*DUF1350*	*Unknown*

Table 2.2. Refined PG proteome according to Lundquist *et al.* (2012)[27] and overlapping significantly with Ytterberg *et al.* (2006)[28] and Vidi *et al.* (2006)[29].

2.2 PG proteins and metabolic activities

2.2.1 Fibrillins

Fibrillin was originally discovered through its association with carotenoid-sequestering fibrils of red pepper (*Capsicum annuum*) chromoplasts[20]. Despite their fibrillar appearance, fibrils are structurally closely related to plastoglobules having an outer polar lipid monolayer lined with proteins and enclosing a hydrophobic core containing colored carotenoids. Fibril carotenoids are mostly present as esters, capsanthin diester being the most abundant at more than 50% in red pepper[20]. It is interesting to note that in tomato chromoplasts no fibrils are present and plastoglobules take over their function[30]. The precise structure of carotenoid-containing structures has been attributed to the lipid to protein ratio. A high proportion of protein favors the formation of fibrillar rather than globular structures[31]. Fibrillin is the most abundant protein of carotenoid fibrils. Purified fibrillin protein was able to reconstitute fibrils when it was mixed with polar lipids and carotenoids at their natural stoichiometric ratio. The highest yields were achieved with the esterified xanthophylls, zeaxanthin diester and capsanthin diester[20]. Reconstitution did not occur in the absence of fibrillin. Based on the above findings, fibrillins were attributed a structural role in fibril formation. Overexpression of fibrillin in tobacco leaves led to an increase of plastoglobule numbers and clusters reinforcing the idea of structural role[23]. Homologues of fibrillin exist in many other species such as potato (plastid lipid associated proteins, PAP)[32] and pea (plastoglobulins, PGL)[6].

In *Arabidopsis*, quantitative proteomics indicated that fibrillins are the most abundant proteins of chloroplast PG, 4 homologs (FBN1a, -1b, -2 and -4) (At4g04020, At4g22240, At2g35490, At3g23400) making up almost 50% of the PG protein mass[27]. Interestingly also, the same study indicated that different fibrillin homologs partition to varying and predictable degrees between the plastoglobules and the thylakoid membrane. Low isoelectric points and a higher hydrophobicity index favored PG over thylakoid association.

A study on the apple *fib4* (the ortholog of *Arabidopsis* FBN4) knock down mutant revealed reduced accumulation of plastoquinone in PG while the total cellular plastoquinone remained constant. Fib4 contains a conserved lipocalin motif (DLDKLQGKWRLLY) that could potentially facilitate binding and transport of lipids[33,34]. These findings led to the hypothesis that fibrillins apart from a structural role may also have a role in metabolite trafficking between the thylakoid membrane and plastoglobules. Fibrillins such as Fib4 would therefore be expected to be present at the neck-like structure at the interface between PG and the thylakoid membrane.

The databases indicate that fibrillins are ancient, evolutionarily conserved proteins originating from cyanobacteria. Fibrillins may therefore be omnipresent in photosynthetic species[35]. While *Arabidopsis*

has many fibrillin homologs, *Synechocystis* sp. PCC 6803 only has two. Therefore, this cyanobacterial strain is an interesting model to test fibrillin function. The deletion of the two homologs of *Synechocystis* sp. PCC 6803 fibrillin (PGL1 and -2) was viable and photosynthetically active. However, the carotenoid composition was altered suggesting compromised resistance to high light stress[35]. In cyanobacteria lipid globules are rather rare, so their association with the fibrillins PGL1 and -2 was not readily apparent. It was therefore suggested that fibrillins in cyanobacteria may function in neutral lipid sequestration outside the PG context.

It is not known how proteins are targeted to PG but they do not have apparent targeting sequences. It has been shown for *Arabidopsis* PGL34/FBN7a (At3g58010)[36] that the entire protein with the exception of a small C-terminal sequence is required for assembly on PG. As PG are frequently observed at the stromal margins of thylakoids it has been proposed that the membrane curvature together perhaps with "lipid-associated proteins" such as the fibrillins may facilitate the budding of PG.

2.2.2 NDC1, a Type II NAD(P)H dehydrogenase required for phylloquinone biosynthesis

NDC1 (At5g08740) was identified as a bona fide PG protein in three independent proteomics studies[27-29]. NDC1 belongs to the family of monomeric Type II NAD(P)H-dependent dehydrogenases (NDH-2). Type II NAD(P)H dependent dehydrogenases serve as an alternative to the multi-subunit respiratory complex I (type-I NADH deshydrogenase (NDH-1)) to catalyze electron transfer from NADH to ubiquinone in the mitochondrial respiratory chain[37]. In *Arabidopsis*, a family of seven NDH-2 homologs exists. Six of these are located in mitochondria[38], but only one, NDC1, is present in chloroplasts.

NDC1 is conserved from cyanobacteria, which provides an evolutionary explanation for its presence in chloroplasts, although NDC1 was originally localized in mitochondria[38]. There is also evidence for dual mitochondrial and chloroplast localization of the protein[39,40]. In chloroplasts, not only proteomics but also fluorescence localization and subfractionation indicate that NDC1 sublocalizes to PG[40]. Ubiquinone, the usual substrate of NDH-2 enzymes, is not present in chloroplasts. But it was shown that NDC1 is a multifunctional enzyme accepting as substrates a variety of quinone derivatives such as decyl-ubiquinone and decyl-plastoquinone as well as isolated PG[40]. As NDC1 should well be able to use plastoquinone as substrate for NAD(P)H-dependent reduction, it is imaginable that NDC1 functions in cyclic electron flow around Photosystem I (PSI). In *Arabidopsis*, however, mutant analysis has revealed that the contribution of NDC1 to cyclic electron flow around PSI is negligible and that the chloroplast NDH complex is responsible for this task. But, in *Chlamydomonas* the chloroplast NDH complex is lacking and an NDH-2 homolog (Nda-2) has been implicated in cyclic electron flow[41].

Despite the lack of involvement in cyclic electron flow NDC1 affects the plastoquinone redox equilibrium: total plastoquinone in the *ndc1* mutant is significantly more oxidized than in the wild type[40]. Plastoquinone is distributed between the thylakoids and plastoglobules. The photochemically-active plastoquinone pool is localized in the thylakoid membrane but a large proportion of the plastoquinone is present in plastoglobules. Presumably, the plastoglobule-localized plastoquinone is selectively reduced by NDC1 without interfering with the plastoquinone participating in photosynthetic electron transport. This suggests that the thylakoid plastoquinone pool and the PG plastoquinone reservoir are well separated and do not rapidly equilibrate. The redox state of the plastoquinone pool is known to control the level of phosphorylation of the chloroplast light-harvesting complex II (LHCII)[42]. It will therefore be interesting to test whether and if to what extent NDC1 together with PG-localized plastoquinone contributes to plastoquinone redox regulation.

In a surprising twist, phylloquinone was completely absent from the *ndc1* mutant which instead accumulated demethylphylloquinone, lacking the 3-methyl group[40]. It is unclear why demethylphylloquinone accumulates in the *ndc1* mutant because the methylation step is known to be carried out by the AtMenG enzyme in *Arabidopsis*[43]. AtMenG is normally expressed in the *ndc1* mutant background. Despite the lack of phylloquinone, the *ndc1* mutant has no visible phenotype. In *Synechocystis*[44] and *Arabidopsis*[43] *menG* mutants demethylphylloquinone effectively replaces phylloquinone. In *Arabidopsis* however, the maximal photosynthetic efficiency was reduced in *atmenG* plants grown under high light. It therefore needs to be noted that despite the similarities the molecular phenotypes of *atmenG* and *ndc1* are not identical. Several hypothetical explanations for the role of NDC1 in phylloquinone synthesis may be proposed. One is that AtMenG-dependent methylation prefers reduced demethylphylloquinone as its substrate and the reduction of demethylphylloquinone therefore depends on NDC1. As we will see later, substrate reduction by NDC1 is also of importance for reactions catalyzed by tocopherol cyclase (VTE1, At4g32770). Another possibility is that NDC1 regulates AtMenG activity. For example, NDC1 could serve as platform to recruit AtMenG to the PHYLLO metabolon[45]. The PHYLLO metabolon consists of MenF, MenD, MenC, and MenH in a single polypeptide and catalyzes the preceding steps of phylloquinone biosynthesis. In support of this possibility, like NDC1-YFP both PHYLLO-DsRed and AtMenG-GFP fusion proteins gave punctate fluorescence within chloroplasts that were reminiscent of PG. To test this, it will be interesting to see whether the punctate patterns of the latter two fluorescent fusion proteins is disrupted in the *ndc1* mutant background.

2.2.3 Implication of PG in tocochromanol biosynthesis and metabolism

2.2.3.1 Role of PG in tocopherol biosynthesis

Tocochromanols (including tocopherol, tocotrienols and plastochromanol-8 (PC-8)) are important lipid antioxidants in the chloroplast protecting thylakoid membrane lipids from oxidation[46,47]. All of the enzyme activities of the tocopherol biosynthesis pathway were originally localized to the inner chloroplast envelope membrane where biosynthesis is thought to occur[48]. The tocopherol cyclase VTE1 (At4g32770) catalyzes the second to last step in α-tocopherol synthesis by introducing the chromanol ring. Surprisingly, however, proteomics studies indicated that the majority of VTE1 protein is localized in PG. This finding was confirmed by expression of a fluorescent VTE1-fusion protein, immunoelectron microscopy[16] and membrane fractionation studies[29]. In the *vte1* mutant, the substrate of VTE1 dimethylphytylbenzoquinone (DMPBQ) accumulated to a large extent in plastoglobules providing evidence for the implication of PG as a reaction site in the tocopherol cyclase step[49].

2.2.3.2 PG and VTE1 in the tocopherol redox cycle

The thylakoid membrane is exposed to the production of reactive oxygen species (ROS) due to the presence of the photosynthetic apparatus. Tocopherols act as antioxidants by rescuing membrane lipids from oxidation. Tocopherols scavenge lipid peroxy radicals yielding a tocopheroxyl radical followed by chromanol ring opening that results in α-tocoquinone. In the tocopherol repair cycle, α-tocoquinone is dehydrated resulting in trimethylphytylbenzoquinone (TMPBQ) before the re-introduction of chromanol ring by VTE1. The tocopherol redox cycle is believed to occur at the thylakoid membrane and in plastoglobules. In favor of this scenario, α-tocoquinone can be detected under high light conditions[50] and accumulates too much higher levels in the *ndc1* mutant background[51]. This finding suggests that VTE1 preferentially acts on a reduced substrate in the tocopherol repair cycle.

2.2.3.3 PG and VTE1 in plastochromanol-8 synthesis

While tocopherols and tocotrienols have been well studied, knowledge on plastochromanol-8, that is derived from plastoquinol by tocopherol cyclase activity, is rather scarce despite its wide presence in crop species[52]. Together with tocopherol, PC-8 protects *Arabidopsis* seed oil from oxidation and is essential for seed longevity[53]. PC-8 has a chromanol-containing headgroup identical to that of γ-tocopherol but the longer solanesyl side chain of plastoquinone. Surprisingly, overexpression of VTE1 led to the accumulation of large quantities of PC-8 rather than tocopherol. A large proportion of the

plastochromanol accumulated in PG[54]. In the VTE1 overexpressing line, plastoglobules were more numerous and present in larger clusters than in the wild type. Interestingly also, PC-8 levels were reduced in *ndc1* mutant background. This suggests that also in the case of PC-8, VTE1 prefers reduced plastoquinol as the substrate.

2.2.3.4 PG and metabolite trafficking within the chloroplast

Localization of VTE1 at PG while the other enzymes of the tocopherol pathway are localized at the inner envelope membrane suggests that metabolites are trafficked from the inner envelope membrane to PG and back to complete the pathway. This would particularly concern DMPBQ, the substrate of VTE1 and γ-tocopherol, the substrate of the VTE4 methylase that is localized at the inner envelope membrane[54]. How likely is this to occur? Fascinating experimentation in *Arabidopsis*, fittingly described as transorganellar complementation, demonstrated that VTE1 when targeted to the endoplasmic reticulum (ER) is still able to complement the *vte1* mutant[55]. The work by Mehrshahi *et al.* (2013)[55] thus indicates that metabolites are sufficiently mobile for DMPBQ to reach the ER and γ-tocopherol to return to the chloroplast. Presumably, this does not implicate specific transport proteins localized at the chloroplast envelope membrane but an interorganellar pathway relying on membrane connections between the ER and the chloroplast outer envelope membrane that allows to complete the tocopherol cyclase reaction outside the chloroplast[55]. These connections may implicate a shared outer lipid layer between the chloroplast and the ER[55] not unlike the one observed between PG and the thylakoid membrane. If DMPBQ can reach the ER, it appears likely that DMPBQ can also reach PG to complete the tocopherol cyclase reaction. Still, the question remains why the tocopherol cyclase reaction would be located in PG and not at the inner envelope membrane. One reason may lie in the fact that VTE1 catalyzes chromanol ring formation also in other molecules than DMPBQ. This concerns TMPBQ, that is recycled to α-tocopherol at the end of the tocopherol redox cycle[51] and plastoquinone that is converted to plastochromanol-8 by VTE1[54]. It has been shown that chromanol ring formation preferentially occurs in the reduced state of the substrate in the case of tocopherol[56]. NDC1 which is present in PG has the ability to reduce a variety of quinolic substrates. Owing to the presence of NDC1, PG may present a favorable, reductive reaction environment in which chromanol ring formation by VTE1 may readily occur.

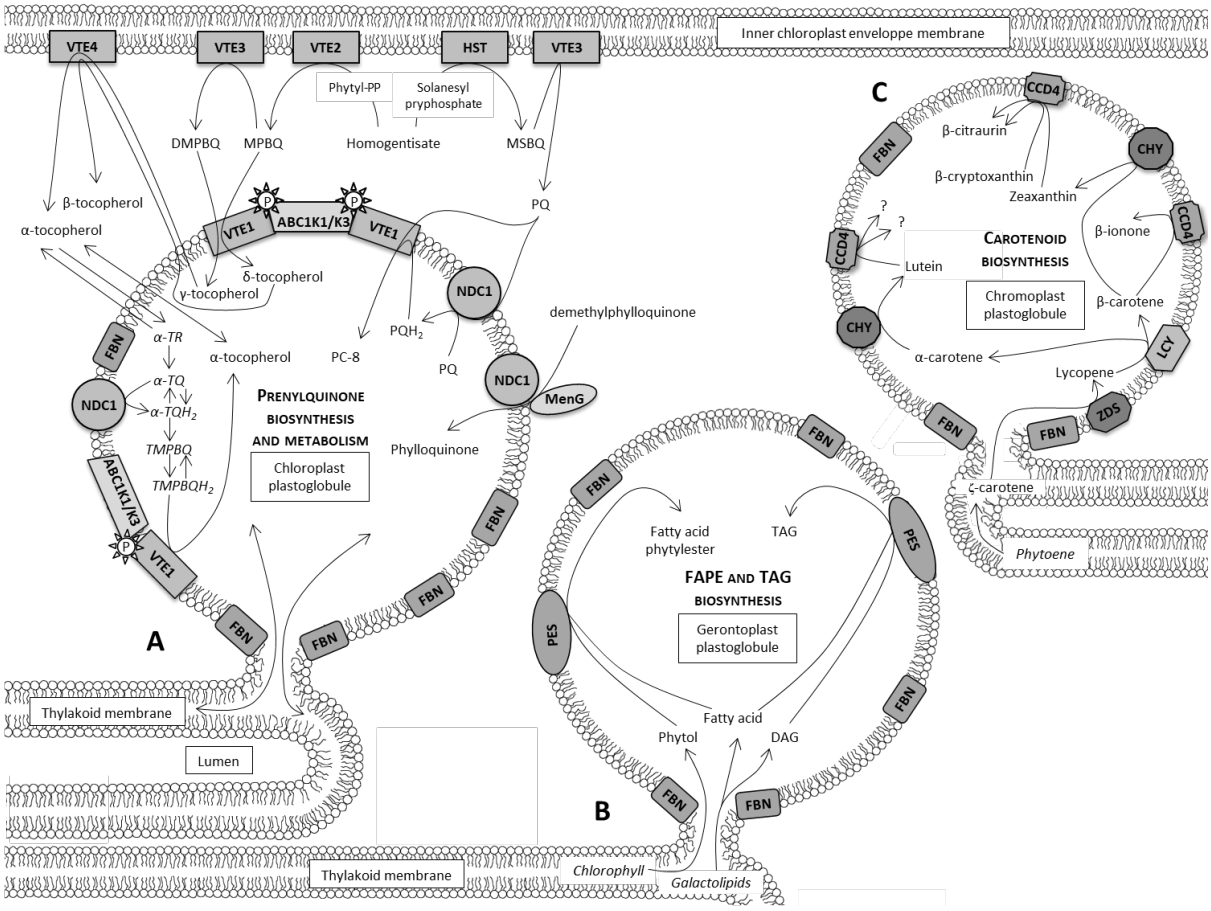

Figure 2.1. Lipid metabolism in plastoglobules. (A) Prenylquinone biosynthesis and metabolism in chloroplast plastoglobules. NDC1 is required for phylloquinone biosynthesis. NDC1 is also implicated in plastochromanol (PC-8) biosynthesis and in tocopherol recycling by reducing substrates, plastoquinol and TMPBQ, to their quinol forms. VTE1 uses reduced substrates for the biosynthesis of plastochromanol and tocopherol recycling. ABC1K1 kinase is required for increased tocopherol production under highlight. ABC1K3 kinase is required for normal PC-8 accumulation and tocopherol recycling. Both ABC1K1 and -K3 do so by acting on VTE1 activity, presumably by phosphorylation. **(B)** During senescence-induced thylakoid disassembly, fatty acid phytyl esters and triacylglycerols are synthetized by phytyl ester synthase 1 and 2 (PES1 and -2) in gerontoplast plastoglobules. **(C)** In chromoplast plastoglobules LCY, CHY, ZDS are recruited to promote carotenoid biosynthesis and accumulation. CCD4 participates in flower color production and volatile emission.

ABC1K, activity of bc1-like kinase; α-TQH_2, α-tocopherol-quinol; α-TQ, α-tocopherol-quinone; α-TR, α-tocopheroxyl-radical; CCD4, carotenoid cleavage dioxygenase 4; CHY, β-carotene β-hydroxylase; DMPBQ, dimethylphytylbenzoquinone; FAPE, fatty acid phytyl ester; FBN, fibrillins; HST, homogentisate prenyl transferase; LCY, lycopene β-cyclase; MenG, demethylmenaquinone methyl transferase; MPBQ, methylphytylbenzoquinone; MSBQ, methylsolanylbenzoquinone; NDC1, NAD(P)H dehydrogenase C1; P, phosphorylation; PC-8, plastochromanol-8; PES, phytyl ester synthases; PQ, plastoquinone-9; PQH_2, plastoquinol-9; TAG, triacylglycerol; VTE1, tocopherol cyclase, vitamin E deficient 1; VTE2, homogentisate phytyl transferase, vitamin E deficient 2; VTE3, tocopherol methyltransferase, vitamin E deficient 3; VTE4, γ-tocopherol methyltransferase, vitamin E deficient 4; ZDS, ζ-carotene desaturase.

2.2.4 Roles of PG in carotenoid metabolism

PG play a key role in chloroplast to chromoplast transition. During this transition chlorophyll is degraded, thylakoids are disassembled and replaced by large carotenoid-containing plastoglobules in tomato[30] or fibrils in red pepper fruit[20], to give two examples. In red pepper chromoplasts, four enzymes implicated in carotenoid biosynthesis are specifically recruited to PG: these are ζ-carotene desaturase (ZDS), lycopene β-cyclase (LCY) and two β-carotene β-hydroxylases (CHY)[28]. ZDS introduces conjugated double bonds in ζ-carotene contributing to the synthesis of lycopene, a red pigment of tomato fruit[57]. LCY catalyzes the formation of ionone rings at either ends of lycopene resulting in α- or β-carotene. CHY catalyzes the addition of hydroxy groups to the ionone rings giving the xanthophyll derivatives lutein and zeaxanthin, respectively[58-60]. Hypothetically, the PG location of these enzymes may facilitate substrate channeling and subsequent accumulation of the carotenoid products within PG.

Carotenoids are subject to oxidative cleavage by Carotenoid Cleavage Dioxygenases (CCDs) giving rise to a large variety of so-called apocarotenoids[61]. Apocarotenoids take on a multitude of physiological functions including those of phytohormones (abscisic acid, strigolactones), pollinator attracting volatiles (β-ionone, geranial) and chloroplast to nucleus retrograde signaling (β-cyclocitral)[62-65]. Of the known CCDs only CCD4 (At4g19170) has been identified in PG[27-29].

Homologs of CCD4 carry out a variety of cleavage reactions in different species and tissues. For instance, the *Chrysanthemum morifolium* homolog CmCCD4 produces white color in chrysanthemum flowers. It presumably does so by degrading lutein that is abundant in *cmccd4* mutant yellow flowers[66]. Although the association of chrysanthemum CmCCD4 with PG has not been demonstrated it appears likely that its products accumulate in the chromoplast PG[67]. Similarly, CitCCD4 in the Satsuma mandarin fruit is responsible for the accumulation of the orange-colored pigment β-citraurin by specific cleavage of β-cryptoxanthin and zeaxanthin[68]. During *Crocus sativa* stigma development CsCCD4 cleaves β-carotene into β-ionone and β-cyclocitral[69,70].

In an elegant genetic screen, *Arabidopsis* AtCCD4 was found to degrade carotenoids during seed maturation as well as leaf senescence[71]. *ccd4* mutant seeds accumulate β-carotene which consequently was identified as a probable substrate of AtCCD4. Lack of β-carotene (Provitamin A) in food is the leading cause for vitamin A deficiency that may cause xerophthalmia and total blindness[72]. In the past, genetic engineering has been used to introduce β-carotene biosynthetic pathway into the "Golden rice" endosperm[73]. The research on *Arabidopsis* CCD4 opens up exciting new perspectives for provitamin A biofortification using smart breeding in seed crops[71].

AtCCD4 is strongly induced during senescence and degrades β-carotene under dark-induced senescence conditions[71]. While many steps of chlorophyll degradation have been elucidated, this is an essential enzyme known to be implicated in carotenoid degradation. It will be interesting to see whether and which CCD4 homologs are implicated in the color production in the fall foliage of perennials.

2.2.5 Phytol ester synthases: mediators of thylakoid remodeling during senescence and nitrogen deprivation

During senescence and under stress conditions such as nitrogen deprivation PG become supersized while the extent of thylakoid membranes is reduced[74]. Typically, chlorophyll and galactolipids are catabolized under these conditions. In the second step of chlorophyll degradation, free phytol is liberated from pheophytine by the pheophytine pheophorbide hydrolase (PPH)[75,76]. Free phytol is considered toxic and does not accumulate. In a salvage pathway, free phytol is converted to phytol diphosphate by phytol kinase (VTE5) and incorporated into tocopherols[77]. Alternatively free phytol may be incorporated in to fatty acid phytyl esters (FAPE) by esterification with free fatty acids stemming from galactolipid hydrolysis[12]. Free fatty acids may also be used to synthesize triacylgycerol. Together FAPE and TAG may account for PG supersizing during senescence and under nitrogen stress[74]. Therefore, the two conditions present a striking case for thylakoid lipid remodeling, both at the biochemical and ultrastructural levels.

Interestingly, two enzymes, phytyl ester synthases 1 and 2 (PES1 and-2) (At1g54570 and At3g26840) largely responsible for the formation of FAPE and TAG were identified as components of the PG proteome. PES1 and -2 are both able to transfer fatty acids from galactolipids directly to free phytol and diacylglycerol. PES1 and -2 belong to the seven-member diacylglycerol acyltransferase (DGAT) family in *Arabidopsis* and are both strongly induced during senescence and nitrogen starvation. The *pes1pes2* double mutant had strongly reduced levels of phytyl esters under nitrogen starvation indicating that the two enzymes are predominant in FAPE synthesis[25]. Complementation of the H1246 yeast strain lacking acyltransferase activity showed that both PES1 and -2 restored TAG and sterol ester synthesis. 14:0 Acyl-CoA was the preferred substrate in the yeast system, but monogalactosyldiacylglycerol also worked as an acyl donor[78]. Finally, chlorophyll degradation and thylakoid membrane disassembly were delayed in the *pes1pes2* double mutant. In summary, the evidence makes a compelling case for the participation of PES1 and -2 in thylakoid membrane remodeling during senescence and under nitrogen starvation.

Homologues of phytyl ester synthase also play an important role in carotenoid ester biosynthesis and chromoplast biogenesis in flower organs. It has recently been demonstrated in tomato that PYP1 (Pale Yellow Petal 1) is required for the accumulation in petals and anthers of high levels of xanthophylls that were mostly neoxanthin and violaxanthin esterified with myristic and palmitic acids[79]. Xanthophyll esters were absent from *pyp1* mutant alleles, which also had a reduced total carotenoid content and perturbed chromoplasts.

2.2.6 ABC1-like kinases, metabolic regulators in PG

The plant kinase family is very large, but surprisingly few kinases are known to reside in chloroplasts[80]. Of the chloroplast kinases, the family of ABC1-like kinases constitutes the largest group: nine homologs are known or predicted to be in chloroplasts, six of which were localized to PG using proteomics. Next to the fibrillins the ABC1-like kinases are the most abundant group of PG proteins both in number and in contribution to total PG protein mass[27].

The first ABC1-like kinase was discovered in yeast mitochondria and is required for the Activity of the Cytochrome BC1 complex[81]. It is also known as COQ8 (coenzyme Q biosynthesis). The *abc1/coq8* mutant is respiration deficient and was found to lack ubiquinone[82]. An analogous phenotype was caused by mutation of the bacterial ubiB gene, a homolog of ABC1/COQ8 that also lacks ubiquinone and instead accumulates the octaprenylphenol biosynthetic intermediate[83]. In humans, the mutation of the ABC1/COQ8 homologs ADCK3 and ADCK4 (ABC1 domain-containing kinase) are linked to disease such as cerebellar ataxia[84] and steroid-resistant nephrotic syndrome[85]. The symptoms have been attributed to reduced ubiquinone levels and in some cases can be alleviated by ubiquinone supplementation. COQ8 probably functions as a regulatory kinase in the ubiquinone biosynthesis pathway. In favor of this hypothesis, COQ3, -5 and -7 of the ubiquinone biosynthesis pathway were phosphorylated in an ABC1/COQ8 dependent manner[86].

Given the known role of ABC1-like kinases in mitochondrial ubiquinone biosynthesis, the strong presence of ABC1-like kinases in chloroplasts (termed ABC1Ks) seems surprising and begs the question of their function. By analogy to mitochondrial ABC1-like kinases an implication in chloroplast prenylquinone metabolism may be proposed. Reverse genetic analyses provided confirmatory evidence for this hypothesis: in the *abc1k1* mutant (At4g31390), α-, γ- and δ-tocopherol levels were lower after high light treatment than in the wild type[87]. At the same time, α-TQ, the α-tocopherol oxidation product was increased suggesting a defect in the tocopherol repair cycle. In the *abc1k3* mutant (At1g79600), no effect was observed on α-tocopherol levels, but PC-8 was reduced and α-TQ increased[88] suggesting a defect in VTE1-dependant metabolic steps but excluding tocopherol

biosynthesis. The common denominator of the *abc1k1* and *-k3* molecular phenotypes is their dependence on VTE1 activities. In fact, the observed mutant effects could be explained by deregulation of VTE1. Indeed, VTE1 behaves as an *in vitro* substrate of recombinant ABC1K1 as well as ABC1K3[88]. In addition, VTE1 is an experimentally confirmed phosphoprotein having a phosphorylation hotspot near its N-terminus (PhosphAt database, University of Hohenheim, http://phosphat.uni-hohenheim.de/).

However, the activities of the ABC1K family extend beyond plastid prenylquinone metabolism. In the *abc1k1* mutant, β-carotene levels were reduced even under moderate light conditions. After exposure to highlight and return to moderate light conditions, the *abc1k1* mutant failed to accumulate starch normally producing higher amounts of soluble sugars instead[87].

The ABC1K1 was initially identified as *pgr6* (Proton Gradient Regulation 6) in a genetic screen for *Arabidopsis* mutants with reduced NPQ and hence increase chlorophyll fluorescence. *pgr* mutants are defective in photosynthetic electron transport and in pH gradient generation across the thylakoid membrane[89]. Currently it is not clear why the *abc1k1* mutant has a *pgr* phenotype. Potentially, the *pgr* phenotype may be a consequence of the metabolic perturbation occurring in the *abc1k1* mutant. Alternatively, ABC1K1 may directly phosphorylate target(s) participating in the photosynthetic electron transport chain at the level of the cytochrome *b6f* complex.

The existence of additional targets of the ABC1-like kinases is supported by a study showing that ABC1K1 and -K3 form a complex[90]. The study consequently focused on the double mutant and found the double mutant to degreen under different types of stress and to senesce prematurely. This phenotype was accompanied by remodeling of the PG proteome and the recruitment of lipoxygenases 3 and 4 (At1g17420 and At1g72520) to PG. These two enzymes participate in the jasmonate biosynthetic pathway that is highly active during senescence and nitrogen stress conditions. This may reflect the increased galactolipid turnover that would be expected under the aforementioned conditions. As a consequence of the reduced ability of *abc1k1/abc1k3* to adapt to stress, reactive oxygen species production may be elevated. This notion is supported by the increased levels of β-cyclocitral that in turn mediate retrograde signaling from the chloroplast to the nucleus[65,90].

ABC1K8/OSA1 is located at the chloroplast envelope membrane and is up-regulated upon cadmium exposure. *abc1k8* mutants (At5g64940) are more sensitive to a variety of stress types including cadmium and high light. The ABC1K7/SIA1 homolog has been implicated in salt stress tolerance[91], overexpression resulting in higher tolerance. The *abc1k7* (At3g07700) and *abc1k8* mutants also synthesized lower levels of highly unsaturated DGDG and MGDG[92]. ABC1K7 and ABC1K8 were previously implicated in oxidative stress resistance as the respective mutants accumulated more ferritin, superoxide and had reduced tolerance to ROS. Interestingly, *abc1k8* and particularly the

abc1k7/abc1k8 double mutant accumulated increased levels of DGDG oxylipins that are product of ROS and a source for the synthesis of jasmonate. In this context it is interesting to note that the jasmonate pathway is recruited to PG in the *abc1k1/abc1k3* double mutant. It is therefore possible that the ABC1K1, -3, -7 and -8 cooperate in the regulation of thylakoid membrane disassembly and jasmonate production during senescence.

2.2.7 Uncharacterized PG proteins

Despite the advances made in recent years, PG still hold numerous secrets. A good number of the PG proteins have not been characterized so far and may hold clues to previously unidentified PG functions. Combinations of reverse genetics with –omics tools have proven to be very successful in the functional analysis of PG proteins and will probably continue to do so in the future.

Among the uncharacterized PG proteins are several fibrillins (FBN7a, FBN7b, FBN8) (At3g58010, At2g4213, At2g46910). The functions of fibrillins in the chloroplast remain poorly understood. Therefore the characterization of additional fibrillins may reveal precious new information on their specific roles role in development and under various stresses. In particular it will be interesting to see whether the classification of fibrillins as structural proteins holds up to experimental scrutiny and to test whether fibrillins play a larger role in metabolite trafficking between the PG and thylakoid compartments.

Recent research on the ABC1-like kinases provided evidence for the role of ABC1K1, –K3, -K7 and -K8 in regulation of range of chloroplast metabolic pathways. Three ABC1-like kinases (ABC1K5, -K6, -K9) (At1g71810, At3g24190, At5g05200) associated with PG remain to be explored. Their characterization may well reveal other aspects of chloroplast metabolism and organellar processes that are under the control of the ABC1-like kinase family. Phosphorylation is a reversible process and therefore phosphatases may be expected to play a role in ABC1-like kinase regulatory cycles. While no phosphatases were found in the PG proteome it is likely that they exist elsewhere in the chloroplast.

A number of uncharacterized and predicted metabolic enzymes also remain in the PG proteome. Among these are two UbiE-related methyltransferases (At1g78140, At2g41040). UbiE (known as CoQ5 in yeast) is a methyltransferase required for ubiquinone biosynthesis in bacteria and mitochondria. Based on the analogy between ubiquinone and the chloroplast prenylquinones, it is tempting to hypothesize, that the UbiE-related methyltransferases participate in an unrecognized methylation step in PG prenyl lipid metabolism.

A third predicted esterase/lipase/thioesterase (At5g41120) highly homologous to PES1 and PES2 is present in the PG proteome. This protein is an excellent candidate for a third phytyl ester synthase, responsible for the residual accumulation of FAPE in the *pes1pes2* double mutant[25].

Two uncharacterized PG proteins, an unknown SAG (Senescence Associated Gene) (At1g73750) and a predicted M48 protease (At3g27110) are highly upregulated during senescence and may shed new light on PG functions during senescence[27].

Yet other uncharacterized proteins, such as PLAT/LH2-1 (At4g39730) are likely to be involved in lipid metabolism in PG. Furthermore, additional undiscovered PG proteins may exist. Some of these proteins may associate with PG only under specific conditions. Others may only loosely associate with PG and dissociate during the purification procedure. The advances in mass spectrometric technology may also allow the detection of very low abundance PG proteins in the near future.

2.3 Future applications

2.3.1 Recombinant protein production

Plants have the potential for almost unlimited production of recombinant proteins[93]. In particular, the transformation of the chloroplast genome and protein expression inside chloroplasts of so-called transplastomic plants results in high protein yields[94]. Plastoglobules have also been explored for their potential as a destination for recombinant proteins[36]. The proposed advantage of PG is their low density that would allow enriching a recombinant protein in PG by floatation centrifugation before proceeding to protein purification. Transplastomic plants have been engineered to produce chimeric proteins of the mature form of the fibrillin PGL35/FBN1a fused to HIV p24 (PGL35-HIVp24) as well as hepatitis C virus core protein (PGL35-HCV)[95]. The PGL35-HIVp24 fusion protein partitioned between PG and thylakoid membranes. Targeting proteins to PG and thylakoids by the means of transplastomic fibrillin fusion proteins may be optimized in the future to become an effective tool in plant biotechnology.

2.3.2 Metabolic engineering in fruit and leaves

Several PG lipid components are vitamins (tocopherols and phylloquinone) or commercially important pigment crop traits such as lycopene and other carotenoids. Enzymes implicated in their biosynthesis and metabolism reside at the PG surface. It may therefore be possible to modify the nature and abundance of PG lipid components in leaves, flowers and fruit. An example of metabolic engineering is CCD4 in *chrysanthemum* flowers. The *chrysanthemum* flowers are normally white. The

Chrysanthemum ccd4 mutant of has yellow instead of white flowers due to the accumulation of lutein. The *Arabidopsis ccd4* mutant has enhanced carotenoid levels. Engineering or selecting crop varieties with reduced CCD4 activity represents a potential short cut to new "golden" crop varieties that hold promise to combat xerophthalmia in developing countries. Systematic tilling of PG genes crop species will very likely turn up new alleles of potential commercial interest. For instance, mutants in the regulatory ABC1-like kinases are known to affect prenyl lipid levels as well as senescence. It may therefore be possible to identify ABC1K-like alleles that are enhanced for tocopherol and carotenoid content or feature delayed senescence and therefore accumulate more biomass.

References

1 Cohen, M. & Bowler, E. Lamellar structure of the tobacco chloroplast. *Protoplasma* **42**, 414-416 (1953).

2 Wolken, J. J. & Palade, G. E. Fine structure of chloroplasts in two flagellates. *Nature* **170**, 114-115 (1952).

3 Greenwood, A. D., Leech, R. M. & Williams, J. P. Osmiophilic globules of chloroplasts: I. Osmiophilic globules as a normal component of chloroplasts and their isolation and composition in *Vicia faba* L. *Biochim. Biophys. Acta* **78**, 148-162 (1963).

4 Lichtenthaler, H. K. Plastoglobuli and fine structure of plastids. *Endeavour* **27**, 144-149 (1968).

5 Hansmann, P. & Sitte, P. Composition and molecular structure of chromoplast globules of *Viola tricolor*. *Plant Cell Rep* **1**, 111-114 (1982).

6 Kessler, F., Schnell, D. & Blobel, G. Identification of proteins associated with plastoglobules isolated from pea (*Pisum sativum* L.) chloroplasts. *Planta* **208**, 107-113 (1999).

7 Pozueta-Romero, J., Rafia, F., Houlne, G., Cheniclet, C., Carde, J. P., Schantz, M. L. & Schantz, R. A ubiquitous plant housekeeping gene, *PAP*, encodes a major protein component of bell pepper chromoplasts. *Plant Physiol* **115**, 1185-1194 (1997).

8 Bailey, J. L. & Whyborn, A. G. Osmiophilic globules of chloroplasts. II. Globules of spinach-beet chloroplast. *Biochim Biophys Acta* **78**, 163-174 (1963).

9 Lichtenthaler, H. K. Plastoglobuli und Plastidenstruktur. *Ber Dtsch Bot Ges* **79**, 82-88 (1966).

10 Lichtenthaler, H. K. & Peveling, E. Plastoglobuli in verschiedenen Differenzierungsstadien der Plastiden bei *Allium cepa* L. *Planta* **72**, 1-13 (1967).

11 Lichtenthaler, H. K. & Sprey, B. Uber Die osmiophilen lobularen Lipideinschlusse der Chloroplasten. *Z Naturforsch B* **21**, 690-697 (1966).

12 Gaude, N., Bréhélin, C., Tischendorf, G., Kessler, F. & Dormann, P. Nitrogen deficiency in *Arabidopsis* affects galactolipid composition and gene expression and results in accumulation of fatty acid phytyl esters. *Plant J* **49**, 729-739 (2007).

13 Lichtenthaler, H. K. Plastoglobuli and lipoquinone content of chloroplasts from *Cereus peruvianus* (L.) Mill. *Planta* **87**, 304-310 (1969).

14 Steinmüller, D. & Tevini, M. Composition and function of plastoglobuli. I. Isolation and purification from chloroplasts and chromoplasts. *Planta* **163**, 201-207 (1985).

15 Tevini, M. & Steinmüller, D. Composition and function of plastoglobuli. II. Lipid-composition of leaves and plastoglobuli during beech leaf senescence. *Planta* **163**, 91-96 (1985).

16 Austin, J. R., Frost, E., Vidi, P. A., Kessler, F. & Staehelin, L. A. Plastoglobules are lipoprotein subcompartments of the chloroplast that are permanently coupled to thylakoid membranes and contain biosynthetic enzymes. *Plant Cell* **18**, 1693-1703 (2006).

17 Sprey, B. & Lichtenthaler, H. K. Zur Frage Der Beziehungen zwischen Plastoglobuli und Thylakoidgenese in Gerstenkeimlingen. *Z Naturforsch B* **21**, 697-699 (1966).

18 Lichtenthaler, H. K. Plastoglobuli of spinach - Their size and composition during chloroplast degeneration. *Protoplasma* **68**, 315-326 (1969).

19 Tuquet, C. & Newman, D. W. Aging and regreening in soybean cotyledons. 1. Ultrastructural-changes in plastids and plastoglobuli. *Cytobios* **29**, 43-59 (1980).

20 Deruère, J., Romer, S., Dharlingue, A., Backhaus, R. A., Kuntz, M. & Camara, B. Fibril assembly and carotenoid overaccumulation in chromoplasts - a model for supramolecular lipoprotein structures. *Plant Cell* **6**, 119-133 (1994).

21 Ben Salem-Fnayou, A., Bouamama, B., Ghorbel, A. & Mliki, A. Investigations on the leaf anatomy and ultrastructure of grapevine (*Vitis vinifera*) under heat stress. *Microsc Res Tech* **74**, 756-762 (2011).

22 Locy, R. D., Chang, C. C., Nielsen, B. L. & Singh, N. K. Photosynthesis in salt-adapted heterotrophic tobacco cells and regenerated plants. *Plant Physiol* **110**, 321-328 (1996).

23 Rey, P., Gillet, B., Romer, S., Eymery, F., Massimino, J., Peltier, G. & Kuntz, M. Over-expression of a pepper plastid lipid-associated protein in tobacco leads to changes in plastid ultrastructure and plant development upon stress. *Plant J* **21**, 483-494 (2000).

24 Zhang, R., Wise, R. R., Struck, K. R. & Sharkey, T. D. Moderate heat stress of *Arabidopsis thaliana* leaves causes chloroplast swelling and plastoglobule formation. *Photosynth Res* **105**, 123-134 (2010).

25 Lippold, F., vom Dorp, K., Abraham, M., Holzl, G., Wewer, V., Yilmaz, J. L., Lager, I., Montandon, C., Besagni, C., Kessler, F., Stymne, S. & Dormann, P. Fatty acid phytyl ester synthesis in chloroplasts of *Arabidopsis*. *Plant Cell* **24**, 2001-2014 (2012).

26 Knoth, R., Hansmann, P. & Sitte, P. Chromoplasts of *Palisota barteri*, and the molecular structure of chromoplast tubules. *Planta* **168**, 167-174 (1986).

27 Lundquist, P. K., Poliakov, A., Bhuiyan, N. H., Zybailov, B., Sun, Q. & van Wijk, K. J. The functional network of the *Arabidopsis* plastoglobule proteome based on quantitative proteomics and genome-wide coexpression analysis. *Plant Physiol* **158**, 1172-1192 (2012).

28 Ytterberg, A. J., Peltier, J. B. & van Wijk, K. J. Protein profiling of plastoglobules in chloroplasts and chromoplasts. A surprising site for differential accumulation of metabolic enzymes. *Plant Physiol* **140**, 984-997 (2006).

29 Vidi, P. A., Kanwischer, M., Baginsky, S., Austin, J. R., Csucs, G., Dormann, P., Kessler, F. & Brehelin, C. Tocopherol cyclase (VTE1) localization and vitamin E accumulation in chloroplast plastoglobule lipoprotein particles. *J Biol Chem* **281**, 11225-11234 (2006).

30 Simkin, A. J., Gaffe, J., Alcaraz, J. P., Carde, J. P., Bramley, P. M., Fraser, P. D. & Kuntz, M. Fibrillin influence on plastid ultrastructure and pigment content in tomato fruit. *Phytochemistry* **68**, 1545-1556 (2007).

31 Wuttke, H. G. Chromoplasts in *Rosa rugosa*: Development and chemical characterization of tubular elements. *Z. Naturforsch.* **C 31**, 456-460 (1976).

32 Langenkamper, G., Manac'h, N., Broin, M., Cuine, S., Becuwe, N., Kuntz, M. & Rey, P. Accumulation of plastid lipid-associated proteins (fibrillin/CDSP34) upon oxidative stress, ageing and biotic stress in *Solanaceae* and in response to drought in other species. *J Exp Bot* **52**, 1545-1554 (2001).

33 Singh, D. K., Laremore, T. N., Smith, P. B., Maximova, S. N. & McNellis, T. W. Knockdown of *FIBRILLIN4* gene expression in apple decreases plastoglobule plastoquinone content. *PloS One* **7**, e47547 (2012).

34 Singh, D. K., Maximova, S. N., Jensen, P. J., Lehman, B. L., Ngugi, H. K. & McNellis, T. W. *FIBRILLIN4* is required for plastoglobule development and stress resistance in apple and *Arabidopsis*. *Plant Physiol* **154**, 1281-1293 (2010).

35 Cunningham, F. X., Jr., Tice, A. B., Pham, C. & Gantt, E. Inactivation of genes encoding plastoglobuli-like proteins in *Synechocystis* sp. PCC 6803 leads to a light-sensitive phenotype. *J Bacteriol* **192**, 1700-1709 (2010).

36 Vidi, P. A., Kessler, F. & Bréhélin, C. Plastoglobules: a new address for targeting recombinant proteins in the chloroplast. *BMC Biotechnol* **7**:4 (2007).

37 Feng, Y., Li, W. F., Li, J., Wang, J. W., Ge, J. P., Xu, D., Liu, Y. J., Wu, K. Q., Zeng, Q. Y., Wu, J. W., Tian, C. L., Zhou, B. & Yang, M. J. Structural insight into the type-II mitochondrial NADH dehydrogenases. *Nature* **491**, 478-482 (2012).

38 Michalecka, A. M., Svensson, A. S., Johansson, F. I., Agius, S. C., Johanson, U., Brennicke, A., Binder, S. & Rasmusson, A. G. *Arabidopsis* genes encoding mitochondrial type II NAD(P)H dehydrogenases have different evolutionary orgin and show distinct responses to light. *Plant Physiol* **133**, 642-652 (2003).

39 Carrie, C., Murcha, M. W., Kuehn, K., Duncan, O., Barthet, M., Smith, P. M., Eubel, H., Meyer, E., Day, D. A., Millar, A. H. & Whelan, J. Type II NAD(P)H dehydrogenases are targeted to mitochondria and chloroplasts or peroxisomes in *Arabidopsis thaliana*. *FEBS Lett* **582**, 3073-3079 (2008).

40 Eugeni-Piller, L., Besagni, C., Ksas, B., Rumeau, D., Brehelin, C., Glauser, G., Kessler, F. & Havaux, M. Chloroplast lipid droplet type II NAD(P)H quinone oxidoreductase is essential for prenylquinone metabolism and vitamin K_1 accumulation. *Proc Natl Acad Sci U S A* **108**, 14354-14359 (2011).

41 Jans, F., Mignolet, E., Houyoux, P. A., Cardol, P., Ghysels, B., Cuine, S., Cournac, L., Peltier, G., Remacle, C. & Franck, F. A type II NAD(P) H dehydrogenase mediates light-independent plastoquinone reduction in the chloroplast of *Chlamydomonas*. *Proc Natl Acad Sci U S A* **105**, 20546-20551 (2008).

42 Allen, J. F., Bennett, J., Steinback, K. E. & Arntzen, C. J. Chloroplast protein-phosphorylation couples plastoquinone redox state to distribution of excitation-energy between photosystems. *Nature* **291**, 25-29 (1981).

43 Lohmann, A., Schottler, M. A., Brehelin, C., Kessler, F., Bock, R., Cahoon, E. B. & Dormann, P. Deficiency in phylloquinone (vitamin K_1) methylation affects prenyl quinone distribution, photosystem I abundance, and anthocyanin accumulation in the *Arabidopsis* AtmenG mutant. *J Biol Chem* **281**, 40461-40472 (2006).

44 Sakuragi, Y., Zybailov, B., Shen, G. Z., Jones, A. D., Chitnis, P. R., van der Est, A., Bittl, R., Zech, S., Stehlik, D., Golbeck, J. H. & Bryant, D. A. Insertional inactivation of the *menG* gene, encoding 2-phytyl-1,4-naphthoquinone methyltransferase of *Synechocystis* sp. PCC 6803, results in the incorporation of 2-phytyl-1,4-naphthoquinone into the A_1 site and alteration of the equilibrium constant between A_1 and Fx in photosystem I. *Biochemistry* **41**, 394-405 (2002).

45 Gross, J., Cho, W. K., Lezhneva, L., Falk, J., Krupinska, K., Shinozaki, K., Seki, M., Herrmann, R. G. & Meurer, J. A plant locus essential for phylloquinone (vitamin K_1) biosynthesis originated from a fusion of four eubacterial genes. *J Biol Chem* **281**, 17189-17196 (2006).

46 Dormann, P. Functional diversity of tocochromanols in plants. *Planta* **225**, 269-276 (2007).

47 Mène-Saffrané, L. & DellaPenna, D. Biosynthesis, regulation and functions of tocochromanols in plants. *Plant Physiol Biochem* **48**, 301-309 (2010).

48 Schultz, G. & Soll, J. [Biosynthesis of alpha-tocopherol (vitamin E), phylloquinone (2-methyl-3-phytylnaphtoquinone, vitamin K_1) and other prenylquinones in plants. On the problem of inability of the biosynthesis in animals--a survey (author's transl)]. *Dtsch Tierarztl Wochenschr* **87**, 410-412 (1980).

49 Eugeni-Piller, L., Abraham, M., Dormann, P., Kessler, F. & Besagni, C. Plastid lipid droplets at the crossroads of prenylquinone metabolism. *J Exp Bot* **63**, 1609-1618 (2012).

50 Kobayashi, N. & DellaPenna, D. Tocopherol metabolism, oxidation and recycling under high light stress in *Arabidopsis*. *Plant J* **55**, 607-618 (2008).

51 Eugeni-Piller, L., Glauser, G., Kessler, F. & Besagni, C. Role of plastoglobules in metabolite repair in the tocopherol redox cycle. *Front Plant Sci* **5**, 298 (2014).

52 Kruk, J., Szymanska, R., Cela, J. & Munné-Bosch, S. Plastochromanol-8: fifty years of research. *Phytochemistry* **108**, 9-16 (2014).

53 Mène-Saffrané, L., Jones, A. D. & DellaPenna, D. Plastochromanol-8 and tocopherols are essential lipid-soluble antioxidants during seed desiccation and quiescence in *Arabidopsis*. *Proc Natl Acad Sci U S A* **107**, 17815-17820 (2010).

54 Zbierzak, A. M., Kanwischer, M., Wille, C., Vidi, P. A., Giavalisco, P., Lohmann, A., Briesen, I., Porfirova, S., Bréhélin, C., Kessler, F. & Dörmann, P. Intersection of the tocopherol and plastoquinol metabolic pathways at the plastoglobule. *Biochem J* **425**, 389-399 (2010).

55 Mehrshahi, P., Stefano, G., Andaloro, J. M., Brandizzi, F., Froehlich, J. E. & DellaPenna, D. Transorganellar complementation redefines the biochemical continuity of endoplasmic reticulum and chloroplasts. *Proc Natl Acad Sci U S A* **110**, 12126-12131 (2013).

56 Grutter, C., Alonso, E., Chougnet, A. & Woggon, W. D. A biomimetic chromanol cyclization leading to α-tocopherol. *Angew Chem Int Ed Engl* **45**, 1126-1130 (2006).

57 Ben-Shaul, Y. & Naftali, Y. The development and ultrastructure of lycopene bodies in chromoplasts of *Lycopersicum esculentum*. *Protoplasma* **67**, 333-344 (1969).

58 Nogueira, M., Mora, L., Enfissi, E. M. A., Bramley, P. M. & Fraser, P. D. Subchromoplast sequestration of carotenoids affects regulatory mechanisms in tomato lines expressing different carotenoid gene combinations. *Plant Cell* **25**, 4560-4579 (2013).

59 Liu, L. H., Shao, Z. Y., Zhang, M. & Wang, Q. M. Regulation of carotenoid metabolism in tomato. *Mol Plant* **8**, 28-39 (2015).

60 Ruiz-Sola, M. A. & Rodríguez-Concepción, M. Carotenoid biosynthesis in *Arabidopsis*: A colorful pathway. In: The *Arabidopsis* book, **10**:e0158 (2012).

61 Auldridge, M. E., McCarty, D. R. & Klee, H. J. Plant carotenoid cleavage oxygenases and their apocarotenoid products. *Curr Opin Plant Biol* **9**, 315-321 (2006).

62 Gomez-Roldan, V., Fermas, S., Brewer, P. B., Puech-Pages, V., Dun, E. A., Pillot, J. P., Letisse, F., Matusova, R., Danoun, S., Portais, J. C., Bouwmeester, H., Becard, G., Beveridge, C. A., Rameau, C. & Rochange, S. F. Strigolactone inhibition of shoot branching. *Nature* **455**, 189-194 (2008).

63 Hirayama, T. & Shinozaki, K. Perception and transduction of abscisic acid signals: keys to the function of the versatile plant hormone ABA. *Trends Plant Sci* **12**, 343-351 (2007).

64 Jia, C. G., Zhang, L. P., Liu, L. H., Wang, J. S., Li, C. Y. & Wang, Q. M. Multiple phytohormone signalling pathways modulate susceptibility of tomato plants to *Alternaria alternata* f. sp. *lycopersici*. *J Exp Bot* **64**, 637-650 (2013).

65 Ramel, F., Birtic, S., Ginies, C., Soubigou-Taconnat, L., Triantaphylides, C. & Havaux, M. Carotenoid oxidation products are stress signals that mediate gene responses to singlet oxygen in plants. *Proc Natl Acad Sci U S A* **109**, 5535-5540 (2012).

66 Zhu, C., Bai, C., Sanahuja, G., Yuan, D., Farre, G., Naqvi, S., Shi, L., Capell, T. & Christou, P. The regulation of carotenoid pigmentation in flowers. *Arch Biochem Biophys* **504**, 132-141 (2010).

67 Yoshioka, S., Aida, R., Yamamizo, C., Shibata, M. & Ohmiya, A. The carotenoid cleavage dioxygenase 4 (*CmCCD4a*) gene family encodes a key regulator of petal color mutation in C*hrysanthemum*. *Euphytica* **184**, 377-387 (2012).

68 Ma, G., Zhang, L. C., Matsuta, A., Matsutani, K., Yamawaki, K., Yahata, M., Wahyudi, A., Motohashi, R. & Kato, M. Enzymatic formation of β-citraurin from β-cryptoxanthin and zeaxanthin by carotenoid cleavage dioxygenase4 in the flavedo of citrus fruit. *Plant Physiol* **163**, 682-695 (2013).

69 Rubio-Moraga, A., Rambla, J. L., Fernandez-de-Carmen, A., Trapero-Mozos, A., Ahrazem, O., Orzaez, D., Granell, A. & Gomez-Gomez, L. New target carotenoids for CCD4 enzymes are revealed with the characterization of a novel stress-induced carotenoid cleavage dioxygenase gene from *Crocus sativus*. *Plant Mol Biol* **86**, 555-569 (2014).

70 Rubio, A., Rambla, J. L., Santaella, M., Gomez, M. D., Orzaez, D., Granell, A. & Gomez-Gomez, L. Cytosolic and plastoglobule-targeted carotenoid dioxygenases from *Crocus sativus* are both involved in β-ionone release. *J Biol Chem* **283**, 24816-24825 (2008).

71 Gonzalez-Jorge, S., Ha, S. H., Magallanes-Lundback, M., Gilliland, L. U., Zhou, A. L., Lipka, A. E., Nguyen, Y. N., Angelovici, R., Lin, H. N., Cepela, J., Little, H., Buell, C. R., Gore, M. A. & DellaPenna, D. CAROTENOID CLEAVAGE DIOXYGENASE4 is a negative regulator of β-carotene content in *Arabidopsis* seeds. *Plant Cell* **25**, 4812-4826 (2013).

72 Sommer, A. Xerophthalmia, keratomalacia and nutritional blindness. *Int Ophthalmol* **14**, 195-199 (1990).

73 Ye, X. D., Al-Babili, S., Kloti, A., Zhang, J., Lucca, P., Beyer, P. & Potrykus, I. Engineering the provitamin A (β-carotene) biosynthetic pathway into (carotenoid-free) rice endosperm. *Science* **287**, 303-305 (2000).

74 Besagni, C. & Kessler, F. A mechanism implicating plastoglobules in thylakoid disassembly during senescence and nitrogen starvation. *Planta* **237**, 463-470 (2013).

75 Schelbert, S., Aubry, S., Burla, B., Agne, B., Kessler, F., Krupinska, K. & Hörtensteiner, S. Pheophytin pheophorbide hydrolase (Pheophytinase) is involved in chlorophyll breakdown during leaf senescence in *Arabidopsis*. *Plant Cell* **21**, 767-785 (2009).

76 Zhang, W., Liu, T. Q., Ren, G. D., Hörtensteiner, S., Zhou, Y. M., Cahoon, E. B. & Zhang, C. Y. Chlorophyll degradation: the tocopherol biosynthesis-related phytol hydrolase in *Arabidopsis* seeds is still missing. *Plant Physiol* **166**, 70-79 (2014).

77 Ischebeck, T., Zbierzak, A. M., Kanwischer, M. & Dormann, P. A salvage pathway for phytol metabolism in *Arabidopsis*. *J Biol Chem* **281**, 2470-2477 (2006).

78 Pan, X., Siloto, R. M., Wickramarathna, A. D., Mietkiewska, E. & Weselake, R. J. Identification of a pair of phospholipid: diacylglycerol acyltransferases from developing flax (*Linum usitatissimum* L.) seed catalyzing the selective production of trilinolenin. *J Biol Chem* **288**, 24173-24188 (2013).

79 Ariizumi, T., Kishimoto, S., Kakami, R., Maoka, T., Hirakawa, H., Suzuki, Y., Ozeki, Y., Shirasawa, K., Bernillon, S., Okabe, Y., Moing, A., Asamizu, E., Rothan, C., Ohmiya, A. & Ezura, H. Identification of the carotenoid modifying gene PALE YELLOW PETAL 1 as an essential factor in xanthophyll esterification and yellow flower pigmentation in tomato (*Solanum lycopersicum*). *Plant J* **79**, 453-465 (2014).

80 Bayer, R. G., Stael, S., Rocha, A. G., Mair, A., Vothknecht, U. C. & Teige, M. Chloroplast-localized protein kinases: a step forward towards a complete inventory. *J Exp Bot* **63**, 1713-1723 (2012).

81 Bousquet, I., Dujardin, G. & Slonimski, P. P. *ABC1*, a novel yeast nuclear gene has a dual function in mitochondria: it suppresses a cytochrome *b* mRNA translation defect and is essential for the electron transfer in the *bc1* complex. *EMBO J* **10**, 2023-2031 (1991).

82 Do, T. Q., Hsu, A. Y., Jonassen, T., Lee, P. T. & Clarke, C. F. A defect in coenzyme Q biosynthesis is responsible for the respiratory deficiency in *Saccharomyces cerevisiae abc1* mutants. *J Biol Chem* **276**, 18161-18168 (2001).

83 Poon, W. W., Davis, D. E., Ha, H. T., Jonassen, T., Rather, P. N. & Clarke, C. F. Identification of *Escherichia coli ubiB*, a gene required for the first monooxygenase step in ubiquinone biosynthesis. *J Bacteriol* **182**, 5139-5146 (2000).

84 Lagier-Tourenne, C., Tazir, M., Lopez, L. C., Quinzii, C. M., Assoum, M., Drouot, N., Busso, C., Makri, S., Ali-Pacha, L., Benhassine, T., Anheim, M., Lynch, D. R., Thibault, C., Plewniak, F., Bianchetti, L., Tranchant, C., Poch, O., DiMauro, S., Mandel, J. L., Barros, M. H., Hirano, M. & Koenig, M. ADCK3, an ancestral kinase, is mutated in a form of recessive ataxia associated with coenzyme Q10 deficiency. *Am J Hum Genet* **82**, 661-672 (2008).

85 Ashraf, S., Gee, H. Y., Woerner, S., Xie, L. X., Vega-Warner, V., Lovric, S., Fang, H., Song, X., Cattran, D. C., Avila-Casado, C., Paterson, A. D., Nitschke, P., Bole-Feysot, C., Cochat, P., Esteve-Rudd, J., Haberberger, B., Allen, S. J., Zhou, W., Airik, R., Otto, E. A., Barua, M., Al-Hamed, M. H., Kari, J. A., Evans, J., Bierzynska, A., Saleem, M. A., Bockenhauer, D., Kleta, R., El Desoky, S., Hacihamdioglu, D. O., Gok, F., Washburn, J., Wiggins, R. C., Choi, M., Lifton, R. P., Levy, S., Han,

Z., Salviati, L., Prokisch, H., Williams, D. S., Pollak, M., Clarke, C. F., Pei, Y., Antignac, C. & Hildebrandt, F. *ADCK4* mutations promote steroid-resistant nephrotic syndrome through CoQ_{10} biosynthesis disruption. *J Clin Invest* **123**, 5179-5189 (2013).

86 Xie, L. T. X., Hsieh, E. J., Watanabe, S., Allan, C. M., Chen, J. Y., Tran, U. C. & Clarke, C. F. Expression of the human atypical kinase ADCK3 rescues coenzyme Q biosynthesis and phosphorylation of Coq polypeptides in yeast *coq8* mutants. *Biochim Biophys Acta Mol Cell Biol Lipids* **1811**, 348-360 (2011).

87 Martinis, J., Glauser, G., Valimareanu, S., Stettler, M., Zeeman, S. C., Yamamoto, H., Shikanai, T. & Kessler, F. ABC1K1/PGR6 kinase: a regulatory link between photosynthetic activity and chloroplast metabolism. *Plant J* **77**, 269-283 (2014).

88 Martinis, J., Glauser, G., Valimareanu, S. & Kessler, F. A chloroplast ABC1-like kinase regulates vitamin E metabolism in *Arabidopsis*. *Plant Physiol* **162**, 652-662 (2013).

89 Shikanai, T., Munekage, Y., Shimizu, K., Endo, T. & Hashimoto, T. Identification and characterization of *Arabidopsis* mutants with reduced quenching of chlorophyll fluorescence. *Plant Cell Physiol* **40**, 1134-1142 (1999).

90 Lundquist, P. K., Poliakov, A., Giacomelli, L., Friso, G., Appel, M., McQuinn, R. P., Krasnoff, S. B., Rowland, E., Ponnala, L., Sun, Q. & van Wijk, K. J. Loss of plastoglobule kinases ABC1K1 and ABC1K3 causes conditional degreening, modified prenyl-lipids, and recruitment of the jasmonic acid pathway. *Plant Cell* **25**, 1818-1839 (2013).

91 Yang, S., Zhang, Q., Li, T., Du, J., Yang, S. & Yang, C. AtSIA1, an ABC1-like kinase, regulates salt response in *Arabidopsis*. *Biologia* **67**, 1107-1111 (2012).

92 Manara, A., DalCorso, G., Guzzo, F. & Furini, A. Loss of the atypical kinases ABC1K7 and ABC1K8 changes the lipid composition of the chloroplast membrane. *Plant Cell Physiol* **56**, 1193-1204 (2015).

93 Ma, J. K., Drake, P. M., Chargelegue, D., Obregon, P. & Prada, A. Antibody processing and engineering in plants, and new strategies for vaccine production. *Vaccine* **23**, 1814-1818 (2005).

94 Bock, R. Genetic engineering of the chloroplast: novel tools and new applications. *Curr Opin Biotechnol* **26**, 7-13 (2014).

95 Shanmugabalaji, V., Besagni, C., Piller, L. E., Douet, V., Ruf, S., Bock, R. & Kessler, F. Dual targeting of a mature plastoglobulin/fibrillin fusion protein to chloroplast plastoglobules and thylakoids in transplastomic tobacco plants. *Plant Mol Biol* **81**, 13-25 (2013).

2.4 Addendum to Chapter II "Plastoglobules: lipid droplets at the thylakoid membrane"

Since 2016, new proteins of plastoglobules, PG18 (At4g13200) and PGM48 (At3g27110) have been characterized. Therefore, this addendum was added to update the chapter II, which corresponds to a published book chapter. In addition, a few explanatory remarks concerning atypical kinases were added to complete the subchapter 2.2.6.

2.4.1 The plastoglobular protein 18

The activity of the plastoglobular protein 18 (PG18; At4g13200), previously named unknown 1, is important for plant development. It has no predicted functional domains and is of very low abundance[1]. The *pg18* mutant exhibited pale green leaves and growth inhibition when compared to wild type. At the ultrastructural level, *pg18* chloroplasts were smaller, had larger thylakoid grana stacks, shorter thylakoid stroma lamellae and less PG per chloroplast. This suggested its implication in plastoglobule and thylakoid formation during chloroplast biogenesis. In addition, changes in photosynthetic complex stoichiometry associated with diminished accumulation of carotenoid and chlorophyll levels, and an increase of xanthophyll pigments in *pg18* drastically affected photosynthetic efficiency. Despite the intriguing phenotypes, the precise function of PG18 is still unclear. Its proposed role in plastoglobules is to act on thylakoid organization during chloroplast[2].

2.4.2 The M48 protease

Due to degradation by CCD4 (carotenoid cleavage oxygenase) the total amount of carotenoids decreases during leaf senescence, but carotenoids in PG initially increase in early senescence to finally drop in late senescence[3]. Recently, it has been shown that the M48 protease (PGM48; At3g27110) positively regulates leaf senescence[4]. Absence or overexpression of PGM48 in *Arabidopsis* triggered delay or acceleration of senescence, respectively. Interestingly, in the PGM48 overexpressing line, the level of CCD4 was diminished. Furthermore, a yeast two-hybrid assay indicated an interaction between PGM48 and CCD4. This suggested that CCD4 is a substrate of the M48 protease[4]. Together, CCD4 and PGM48 are thought to control carotenoid breakdown during senescence.

Furthermore, by possibly degrading other PG proteins, PGM48 might affect PG composition and promote senescence by yet unknown retrograde signaling pathways. Therefore, it was proposed that PGM48 plays a larger role in senescence by activating or increasing regulators inducing senescence

(related with ethylene, jasmonic acid, abscisic acid or salicylic acid) or by reducing negative regulators (associated with brassinosteroid and cytokinin pathways)[4].

2.4.3 Explanatory remarks on atypical kinases

Protein kinases play essential roles in most cellular activities such as metabolic regulation or signaling. They modify target proteins by catalyzing the addition of phosphate groups from ATP to hydroxyl groups (-OH) of the side chains of specific amino acids (serine, threonine and tyrosine residues), known as phosphorylation. This modification on the target proteins (*e.g.* enzymes, receptors) induce conformational changes modulating for instance activity, localization or association with other molecules.

Protein kinases belong to the protein kinase-like superfamily and possess a conserved basic kinase catalytic core structure, including the ATP binding and the phosphotransfer reaction regions[5]. Protein kinases can be attributed to two main groups: 1) the typical kinases that have common "classical" sequence motifs and occur predominantly in eukaryotes; and 2) the atypical kinases, common in prokaryotes, that do not have all of the classical motifs[5-7].

Belonging to the atypical protein kinases, the Activity of the Cytochrome BC1 complex kinase (ABC1K) family does not bear any relationship with ATP-binding cassette (ABC) family.

The ABC1 atypical kinase gene family was conserved among bacteria, archaea and eukaryotes during the evolution, and became considerably enlarged in photosynthetic organisms[7,8], suggesting important roles of the ABC1 atypical kinases in cellular activities.

References

1 Lundquist, P. K., Poliakov, A., Bhuiyan, N. H., Zybailov, B., Sun, Q. & van Wijk, K. J. The functional network of the *Arabidopsis* plastoglobule proteome based on quantitative proteomics and genome-wide coexpression analysis. *Plant Physiol* **158**, 1172-1192 (2012).

2 Espinoza-Corral, R., Heinz, S., Klingl, A., Jahns, P., Lehmann, M., Meurer, J., Nickelsen, J., Soll, J. & Schwenkert, S. Plastoglobular protein 18 is involved in chloroplast function and thylakoid formation. *J Exp Bot* **70**, 3981-3993 (2019).

3 Tevini, M. & Steinmuller, D. Composition and function of plastoglobuli .2. Lipid-composition of leaves and plastoglobuli during beech leaf senescence. *Planta* **163**, 91-96 (1985).

4 Bhuiyan, N. H. & van Wijk, K. J. Functions and substrates of plastoglobule-localized metallopeptidase PGM48. *Plant Signal Behav* **12**, e1331197 (2017).

5 Scheeff, E. D. & Bourne, P. E. Structural evolution of the protein kinase-like superfamily. *PLoS Comput Biol* **1**, e49 (2005).

6 Kannan, N., Taylor, S. S., Zhai, Y., Venter, J. C. & Manning, G. Structural and functional diversity of the microbial kinome. *PLoS Biol* **5**, e17 (2007).

7 Lundquist, P. K., Davis, J. I. & van Wijk, K. J. ABC1K atypical kinases in plants: filling the organellar kinase void. *Trends Plant Sci* **17**, 546-555 (2012).

8 Lohscheider, J. N. & Rio Bartulos, C. Plastoglobules in algae: A comprehensive comparative study of the presence of major structural and functional components in complex plastids. *Mar Genomics* **28**, 127-136 (2016).

Aims of this work

Photosynthesis is the key to life on earth and therefore the understanding of the process and its regulatory pathways are essential. The ABC1K1 atypical kinase of PG (also known as Proton Gradient Regulation 6/PGR6) is a known regulatory factor in photosynthesis but its functional mechanisms are unknown. The primary aim of my work was to elucidate the functional mechanisms of ABC1K1 as well as those of its closely related homolog ABC1K3.

ABC1K1/PGR6 and ABC1K3 are not only involved in photosynthesis regulation but also in prenyl lipid metabolism. Under long-term high light conditions the Arabidopsis *abc1k3* mutant was incapable of accumulating normal levels of plastochromanol-8 but did not show any strong photosynthetic defect (Martinis *et al.* 2013). Under the same stress conditions, the *abc1k1/pgr6* mutant accumulated diminished levels of tocopherols and exhibited reduced photosynthetic electron transport as well as weak non-photochemical quenching (Martinis *et al.* 2014). Moreover, two independent studies (Lundquist *et al.* 2013; Huang *et al.* 2015) have been carried out on *abc1k1/abc1k3* double mutants. However, their conclusions were divergent. While one study concluded that the lack of these two proteins in the double mutant caused additive defects leading to pronounced defects in adult plants under high light, the second reaches the conclusion that ABC1K1/PGR6 and ABC1K3 act in an opposing manner, the *abc1k3* mutation alleviating the *abc1k1/pgr6* phenotype in the double mutant. It is therefore important to clarify the nature of the *abc1k1/abc1k3* double mutant phenotype, which may also contribute to the understanding of the function of both ABC1K1/PGR6 and ABC1K3.

As many years of research on ABC1k1 have not yet led to its functional elucidation this constitutes the main challenge of my thesis. Another important challenge is to unravel how ABC1K1/PGR6 and ABC1k3 functionally interact to modulate photosynthetic activity.

Since ABC1K1/PGR6 and ABC1K3 are proteins enriched in plastoglobules, and *abc1k1/pgr6* mutant has a photosynthetic phenotype, we hypothesize that the two proteins are elements of an unknown regulatory mechanism of photosynthesis. In particular, I will test the hypothesis that the two atypical kinases act on lipid distribution between plastoglobules and thylakoid membrane. Plastoquinone is of particular interest here as variations in its concentrations are known to affect photosynthesis strongly.

Therefore, the goals of this PhD project are the following:

- identify primary cause(s) leading to the *abc1k1/pgr6* phenotype. To determine its implication in the *abc1k1/pgr6* phenotype, analysis of the photoactive and non-photoactive pools of plastoquinone will be performed.
- specify role(s) of ABC1K1/PGR6 in photosynthesis regulation under different light conditions by measuring and analysing photosynthetic parameters, such as electron transport capacity, non-photochemical quenching, state transitions, cytochrome *b6f* activity and P_{700} re-oxidation.
- identification of direct as well as indirect targets of the ABC1K1/PGR6-kinase will contribute to the elucidation of molecular mechanisms. Anti-phospho-threonine antibodies and Phos-tag™ gels will be used for the identification of phosphoproteins.
- analyse the *abc1k1/abc1k3* double mutant to evaluate the ability of the *abc1k3* mutant to complement the *abc1k1/pgr6* photosynthetic phenotype and to define the role(s) of ABC1K3 in photosynthesis regulation.

Chapter III

Plastoquinone homeostasis by *Arabidopsis* Proton Gradient Regulation 6 is essential for photosynthetic efficiency

Pralon Thibaut, Shanmugabalaji Venkatasalam, Longoni Paolo, Glauser Gaetan, Ksas Brigitte, Collombat Joy, Desmeules Saskia, Havaux Michel, Finazzi Giovanni, Kessler Felix

Communication Biology 2, 220 (2019)

Abstract

Photosynthesis produces organic carbon via a light-driven electron flow from H_2O to CO_2 that passes through a pool of plastoquinone molecules. These molecules are either present in the photosynthetic thylakoid membranes, participating to photochemistry (photoactive pool), or stored (non-photoactive pool) in thylakoid-attached lipid droplets, the plastoglobules. The photoactive pool acts also as a signal of photosynthetic activity allowing the adaptation to changes in light condition. Here we show that, in *Arabidopsis thaliana*, PGR6 (PROTON GRADIENT REGULATION 6), a predicted atypical kinase located at plastoglobules, is required for plastoquinone homeostasis *i.e.* to maintain the photoactive plastoquinone pool. In *pgr6* mutant, the photoactive pool is depleted and becomes limiting under high light, affecting short-term acclimation and photosynthetic efficiency. In the long term, *pgr6* seedlings fail to adapt to high light, and develop a conditional variegated leaf phenotype. Therefore, PGR6 activity, by regulating plastoquinone homeostasis, is required to cope with high light.

3.1 Introduction

Oxygenic photosynthesis exploits light energy to generate an electron flow from H_2O to NADPH, which is used for the production of organic molecules from CO_2. This process requires the coordinated activity of several membrane embedded complexes: photosystem II (PSII), the cytochrome b_6f and photosystem I (PSI) which are functionally connected by diffusible electron carriers[1,2]. A membrane-soluble prenyl quinone, plastoquinone (PQ), ensures the electron transport between PSII, and cytochrome b_6f [1-3]. High light intensities generate stress at the photosynthetic apparatus with PSII being particularly exposed to damage. By transferring electrons to cytochrome b_6f PQ releases the light excitation pressure on PSII and as a consequence, prevents light induced damage on the photosynthetic apparatus. However, only part of the total PQ participates in electron flow. This portion (the photoactive PQ pool) can be quantified by measuring its reduction by PSII[4,5] or its oxidation by PSI[6] via the cytochrome b_6f complex upon light exposure. The remaining portion of the total PQ is not directly involved in photochemistry. This is defined as the non-photoactive PQ pool since it cannot be reduced by PSII or oxidised by PSI. This second pool of PQ is largely stored in lipid droplets associated with the thylakoid membranes: the plastoglobules[7]. The non-photoactive pool is involved in biosynthetic pathways occurring within the chloroplast (*e.g.* plastochromanol-8 biosynthesis[8]) and at the same time acts as an indispensable reservoir of PQ to refill the photoactive pool. In fact, when a plant experiences light intensities exceeding its electron transport capacity (high light) the photoactive PQ pool is damaged[9,10]. By replenishing it, the presence of a sufficient non-photoactive PQ pool reservoir ensures photosynthetic efficiency under prolonged stressful light conditions[4,11,12].

The Proton Gradient Regulation (PGR) family comprises mutants displaying a perturbation of photosynthetic electron transport[13], which in turn compromises the formation of a proton gradient across the thylakoid membranes. The proton gradient not only aliments ATP synthesis but also induces non-photochemical quenching (NPQ) of chlorophyll fluorescence upon high light exposure. *PGR6* (PROTON GRADIENT REGULATION 6) codes for a predicted atypical **a**ctivity of **b**c1 **c**omplex kinase 1 (ABC1K1) that is localized inside the chloroplast and associated with plastoglobules[14-16]. The *pgr6* mutant is defective in NPQ and maximal photosynthetic electron transport rate [13,17]. Moreover, loss of PGR6 leads to developmental defects such as impaired cotyledon greening and hypocotyl elongation under pure red light, which were reported to be independent from phytochrome-dependent light signalling pathways[18]. Upon several days of high light exposure, the *pgr6* mutant is characterized by growth and specific metabolic defects, such as low carotenoid accumulation and impaired sugar metabolism, which have been reported for adult plants[17,19].

In this study, we show that the *pgr6* primary defect consists in the misregulation of the homeostatic relationship between the photoactive PQ pool and the non-photoactive PQ pool. By relating

photophysiological measurements to the analysis of photochemically active and non-active PQ pools in wild type, *pgr6* and a mutant of PQ biosynthesis, we conclude that PGR6 is required to maintain the balance between the two pools already during a short (3 hours) exposure to high light. This primary *pgr6* phenotype brings on the downstream defects in chloroplast physiology and plant development, which result in leaf variegation in high light exposed seedlings.

3.2 Results

3.2.1 Short-term photosynthetic defects in *pgr6*

Phenotypic observation of young seedlings grown under continuous high light (500 µmol m^{-2} s^{-1}) revealed that the *pgr6* mutation resulted in a chloroplast developmental issue that became visible as a conditional variegation of young leaves (Fig. 3.1a). Conversely, the same mutant plants did not show any visible phenotype when grown under continuous low light intensity (80 µmol m^{-2} s^{-1}). This variegation is reminiscent of the phenotype previously reported in plants affected in protein turnover[20], reoxidation of PQ[21] or chloroplast to nucleus signalling[22]. Thus, this observation suggests that PGR6 is part of a mechanism essential for chloroplast development under high light.

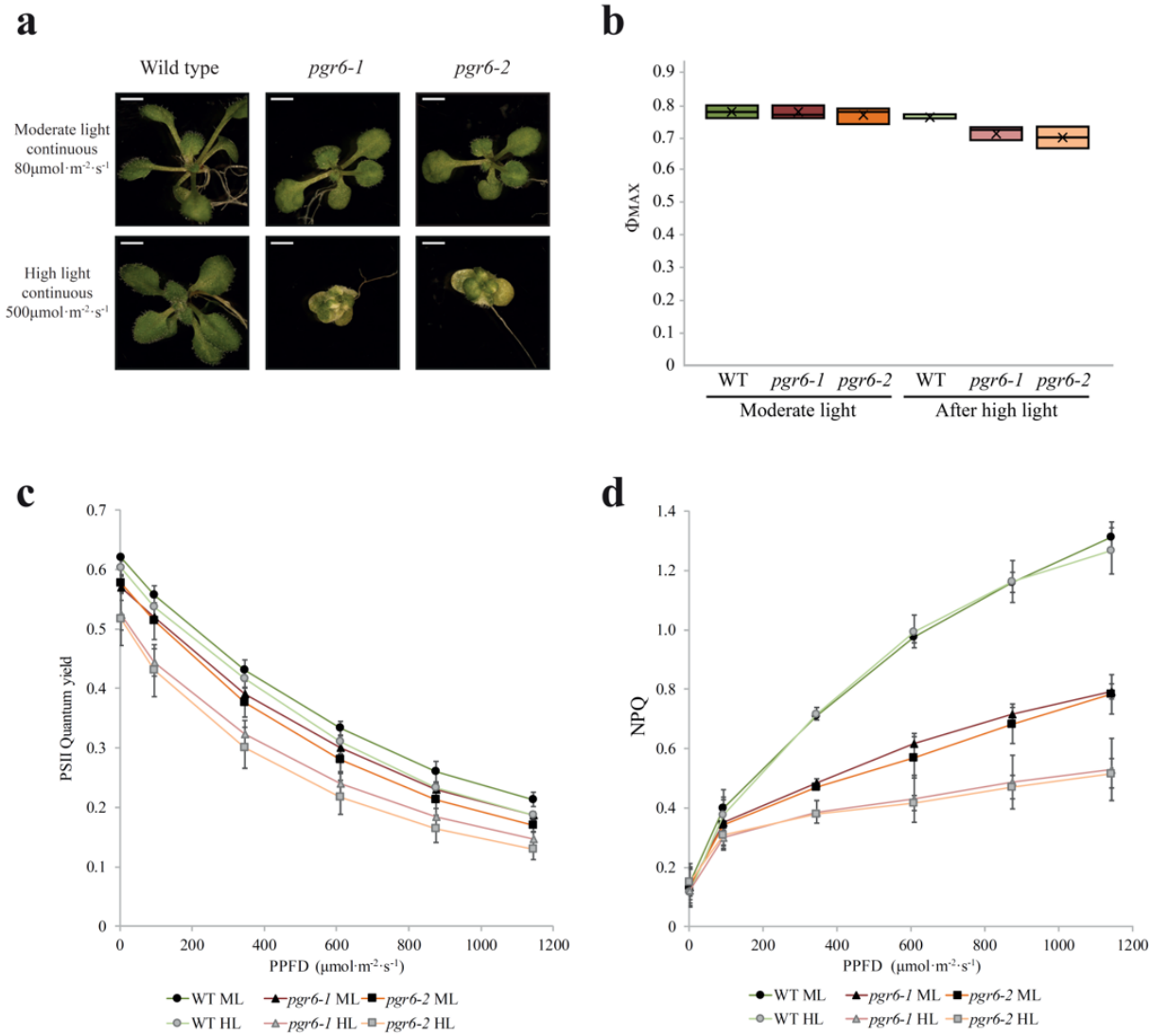

Figure 3.1. *pgr6* mutant has a conditional variegated phenotype and is affected in photosystem II efficiency. (a) Visible phenotype of 14 days seedlings of wild type, *pgr6-1* and *pgr6-2* mutants grown on 0.5x MS medium under 80 µmol m^{-2} s^{-1} (upper panel) and 500 µmol m^{-2} s^{-1} (lower panel) in 24h continuous light; scale bar = 2 mm. 24 days old plants grown on soil in short day cycle (8h light /16h dark) were used to assess the photosynthetic efficiency of wild type (WT), *pgr6-1* and *pgr6-2* under moderate light (120 µmol m^{-2} s^{-1}) (ML, dark colors) and after 3 hours of high light (500 µmol m^{-2} s^{-1}) (HL, light colors). After 10 minutes of dark relaxation, variable room temperature chlorophyll fluorescence was measured on whole plants exposed to these light conditions to determine the following parameters: **(b)** PSII maximum quantum yield (Φ_{MAX} = Fv/Fm). **(c)** PSII quantum yield (Φ_{PSII} = (Fm' – Fs)/Fm') at increasing light intensities, whiskers and box plot shows the minimum, first quartile, median, average, third quartile, and maximum of each data set. **(d)** non-photochemical quenching (NPQ = (Fm – Fm')/Fm') after one minute of exposure at different light intensities. These measures were performed with a Fluorcam (MF800 – PSI) with blue light LEDs (470 nm). Each value represents the average of a pot containing 2-3 plants. Error bars indicate ±SD (n=3 biologically independent samples).

To pinpoint the *pgr6* primary defect, while limiting the secondary effects that may arise from this initial perturbation[17,19], we grew wild type and mutant plants under moderate light conditions (120 µmol m^{-2} s^{-1}, 8h light/16h dark) for 5 weeks and then exposed them to a relatively short high light treatment (3h, 500 µmol m^{-2} s^{-1}). This did not cause lasting damage to the photosynthetic apparatus, as shown by the maximum PSII efficiency ($\Phi_{MAX}=F_V/F_M$), which remained similar in both *pgr6* lines and wild type plants (Fig. 3.1b). However, both the PSII quantum yield (Φ_{PSII}) and the non-photochemical quenching (NPQ) were clearly lower in both *pgr6* mutant lines compared to wild type (Fig. 3.1c, 3.1d). The photosynthetic defects observed in *pgr6* after 3h high light were not due to alterations in the composition and/or abundance of photosynthetic complexes that were present at comparable levels of representative subunits of PSII (D1 (PsbA) and PsbO), PSI (PsaD and PsaC), light harvesting complex (LHCII) (Lhcb2), cytochrome b_6f (cyt *b6f*) (PetC), and the ATPase (AtpC) (Supplementary figure 3.1).

3.2.2 Loss of PGR6 affects state transition kinases activity

When shifted to high light plants acclimate via changes in the phosphorylation patterns of their photosynthetic protein complexes. High light leads to the inactivation of State Transition kinase 7 (STN7) that phosphorylates the PSII antenna and a concomitant increase in the phosphorylation of the PSII core proteins by State Transition kinase 8 (STN8)[23]. Since PGR6 is a predicted atypical kinase that may phosphorylate chloroplast proteins[14-17], we investigated whether the observed modifications in the Φ_{PSII} and NPQ parameters reflect a modification in the phosphorylation of the photosynthetic complexes. We analysed the phosphorylation patterns of major thylakoid proteins in wild type, *pgr6-1* and *pgr6-2* by anti-phosphothreonine immunoblotting and discovered that phosphorylation of both LHCII and PSII was clearly lower in both *pgr6* lines after 3h high light compared to wild type (Fig. 3.2a), while there was no visible difference under moderate light. We found that the phosphorylation of the two major LHCII subunits (Lhcb1 and Lhcb2), as assessed by phosphorylation-dependent band shift using Phostag™-gels, was severely decreased in *pgr6* upon high light exposure. This result suggests that in *pgr6* the activity of the STN7 kinase is more severely down-regulated compared to wild type (Fig. 3.2b). Indeed, STN7 is the principal responsible for the phosphorylation of the trimeric LHCII, triggering the migration of mobile LHCII trimers between the two PSs in a process known as state transitions[24]. STN7 activity depends on the reduction of photoactive PQ at cytb_6f [25-27] and PGR6 is associated with plastoglobules (thylakoid-attached lipid droplets) that are believed to function as PQ reservoir[7,14-16]. We therefore reasoned that the observed changes in the phosphorylation patterns might reflect a perturbation in PQ redox state and/or availability in this mutant rather than a direct effect of PGR6 kinase activity.

We thus investigated the impact of the *pgr6* mutation on state transitions. To follow the antenna movement *in vivo* we measured the chlorophyll fluorescence at room temperature in plants while switching from red supplemented with far-red light (which triggers LHCII dephosphorylation leading to state 1) to red light only (which enhances phosphorylation in state 2)[28]. Decrease in the fluorescence level upon light switch is a proxy for the antenna movement and is absent in the state transitions mutant *stn7* [24]. Consistent with the phosphorylation data, we found that both *pgr6* and wild type have the same capacity to undergo the state 1 to state 2 transition, when grown under and exposed only to moderate light (Fig. 3.2c). However, the transition from state 1 to state 2 was inhibited in *pgr6* but not in wild type after 3h high light (Fig. 3.2c, 3.2d), supporting the idea that the loss of PGR6 causes a conditional state transitions defect, which may be observed only after high light exposure.

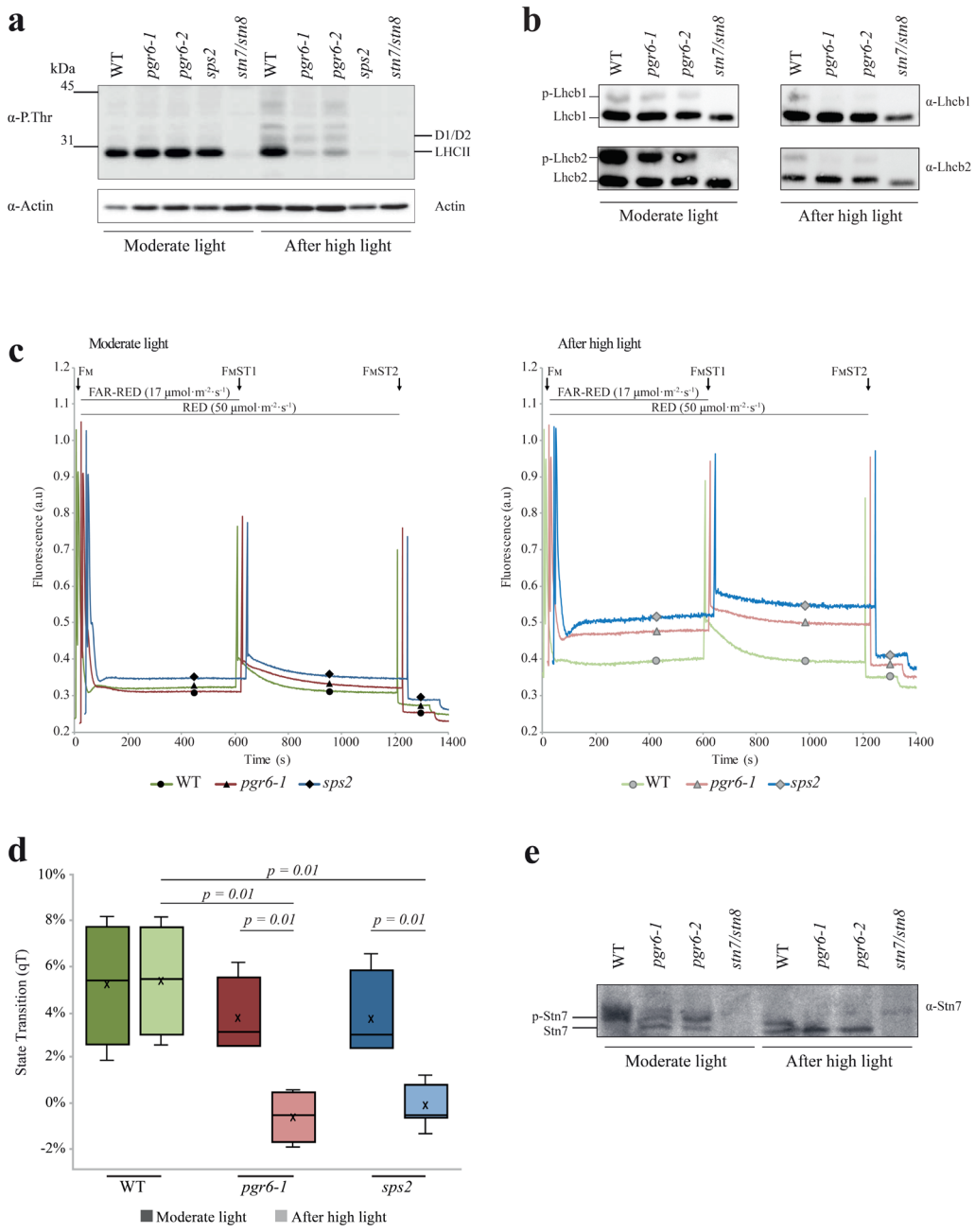

Figure 3.2. Thylakoid protein phosphorylation and state transitions are disturbed after high light treatment in *pgr6* background. (a) Total protein extracts of 4 weeks-old wild type (WT), *pgr6-1*, *pgr6-2*, *sps2* and *stn7/stn8* analysed by immunoblotting with anti-phosphothreonine antibody; the principal thylakoid phospho-proteins are indicated on the right according to their size. Core photosystem II proteins D1 (PsbA) and D2 (PsbD) are indicated as a single band due their poor resolution. Actin was used as a loading control. **(b)** Lhcb1 and Lhcb2 phosphorylation levels were visualised after separation on Phostag™-pendant acrylamide gels. The upper band corresponds to the phosphorylated form (p-), *stn7/stn8* double mutant is a non-phosphorylated control. **(c)** Average transient of the variable room temperature chlorophyll fluorescence measured during the transition from red (660 nm) supplemented with far-red light (720 nm) State 1 to pure red light State 2 (n=4 independent pots containing 2-3 plants). The fluorescence curves from *pgr6* and *sps2* are shifted on the x-axis to allow visualizing the FMST1 and FMST2 values. The x-axis time scale refers to the wild type curve. **(d)** Calculated quenching related to state transitions (qT = (FMST1 – FMST2) / FM), expressed as the percentage of FM that is dissipated by the state 1 to state 2 transition, of wild type (WT), *pgr6-1* and *sps2* under moderate light (120 µmol m^{-2} s^{-1}) (ML) and after 3 hours of high light (500 µmol m^{-2} s^{-1}) (HL). Whiskers and box plot shows the minimum, first quartile, median, average, third quartile, and maximum of each data set (n=4 biologically independent samples); p-values are calculated via a two-tailed Student's t-test. **(e)** STN7 phosphorylation level visualised after separation on Phostag™-pendant acrylamide gels. The upper band corresponds to the phosphorylated form (p-), a protein sample from *stn7/stn8* double mutant was loaded as a control for the antibody specificity.

It has been reported that the activation of STN7 kinase involves its own phosphorylation[26,27]. Therefore, we analysed the phosphorylation pattern of the STN7 protein using Phostag™-gels, and found that it was less phosphorylated in *pgr6* after high light treatment (Fig. 3.2e), once again in agreement with a perturbation of state transitions (*i.e.* STN7 activity). Interestingly, the phosphorylation of the PSII reaction center proteins (*i.e*. D1 (PsbA) and D2 (PsbD)), which mostly depends on STN8[24,29], was also affected in *pgr6.* 3h high light exposure resulted in a lower phosphorylation level of D1 (PsbA) and D2 (PsbD) in *pgr6* compared to wild type (Fig. 3.2a, Supplementary figure 3.2). Although the regulation of STN8 has not been fully clarified yet, this observation suggests that the activities of the two state transition kinases are linked and possibly both dependent on the status of the photosynthetic electron transport chain or that they have overlapping target proteins[30]. A decrease in PSII phosphorylation may affect the repair cycle of the core protein D1 (PsbA) thereby decreasing the maximum efficiency of PSII[31]. This did not appear to be the underlying cause of the long-term *pgr6* phenotype, as short high light exposure did not cause a measurable decrease in the maximum yield of PSII (Fig. 3.1b) or increase of the basal level of fluorescence in the dark (F_O). Both parameters are dependent on PSII activity and are affected if there is a defect in its repair cycle[32] (Supplementary figure 3.2).

3.2.3 Loss of PGR6 affects the photoactive plastoquinone pool

To address whether the defects in protein phosphorylation and state transitions are linked to a decrease in PQ availability, we compared the photosynthetic behaviour of *pgr6* to that of *sps2* (solanesyl phosphate synthase 2 mutant). In *sps*2, a mutant partially defective in PQ biosynthesis, the total PQ and, as a consequence, the photoactive PQ pools are decreased[4]. In particular, the shortage of photoactive PQ should diminish the electron capacity of the electron transport chain (ETC) affecting the photosynthetic efficiency. This would result in lower electron transport rate, and therefore a reduced quantum yield of the PSII (Φ_{PSII}), and NPQ induction[4] (Supplementary figure 3.3). Since *sps2* by its nature is PQ-limited, it can be used as a term of comparison to pinpoint a *pgr6* defect due to PQ availability. The first observation was that in *sps2*, as in *pgr6*, the thylakoid proteins are strongly dephosphorylated after 3h high light (Fig. 3.2a). This result supports the hypothesis linking the down-regulation of the STN7 and STN8 activity and perturbation of PQ availability. To directly assess the capacity of the ETC, we measured chlorophyll *a* fluorescence induction kinetics and calculated the electron transport capacity from the normalised area above the fluorescence traces[33] (Fig. 3.3a). The rationale for this choice is that the area above the fluorescence kinetics is a proxy of the average number of turnovers of each PSII reaction center, *i.e.* of the number of electrons that this photosystem is able to inject into the ETC. It thus provides quantitative data on all the ETC electron acceptors,

including the PSII internal electron acceptors (Q_A and Pheophytin), the plastocyanin downstream of the cytochrome b_6f complex and the PQ connected to PSII (the photochemically active pool). Using this approach, we found that the ETC electron capacity is not different between *pgr6* and wild type when plants were grown under moderate light. This suggests that the photoactive PQ pool has the same electron capacity in *pgr6* and wild type at least under moderate light. On the other hand, we detected a smaller electron capacity in *sps2* mutant, consistent with a constitutive lack of PQ in this line. Upon 3h of high light exposure both *pgr6* and *sps2* mutants showed a diminished electron transport capacity (Fig. 3.3a). This finding suggests that increasing light intensity diminishes the photoactive PQ pool in *pgr6,* thus the phenotype was similar to *sps2* from a functional point of view. To substantiate the hypothesis that the changes in the ETC observed after 3 hours of high light are linked to the lack of photoactive PQ, we quantified changes in the electron fluxes in the different genotypes using a previously established kinetic model based on fluorescence induction kinetics (the JIP-test)[33,34] . We found that the maximum quantum yield of primary photochemistry in PSII (ΦPo) did not vary between wild type and *pgr6* under moderate light (Supplementary figure 3.4), consistent with the previous measurements (Fig. 3.1b). However, the quantum yield of the electron transport flux after Q_A (ΦET2o) and the yield of electron transport to PSI electron acceptors (ΦRE1o) were already lower in *pgr6* mutants compared to wild type. After 3h of high light exposure, the maximum yield was again not affected by the *pgr6* mutation, however both parameters related to the transport from PSII to PSI (ΦET2o and ΦRE1o) were even further decreased in the two *pgr6* mutant lines (ΦET2o: 0.28±0.04; 0.28±0.07) (ΦRE1o: 0.08±0.02; 0.07±0.03) compared to wild type (ΦET2o: 0.38±0.03; ΦRE1o: 0.13±0.02). Similarly, the PQ-limited *sps2* plants showed lower electron transport efficiency (lower ΦET2o and ΦRE1o) under both light conditions (Supplementary figure 3.4). This analysis points to a constitutive lower capacity of the mutants to perform electron transport from PSII to PSI, which is consistent with a perturbation of the photoactive PQ pool in *pgr6*. However, this defect becomes symptomatic only upon exposure to high light. A direct measurement in *pgr6* of the fraction of the PSII reaction centers incapable of transferring electrons to the ETC (closed) by variable room temperature fluorescence upon exposure to increasing light intensities[35], also supports this hypothesis. In fact, the steady state fluorescence was higher in the mutant confirming that the PSII reaction centers were systematically more closed in *pgr6* than in the wild type (Supplementary figure 3.5). Closure of PSII reaction centers is the expected consequence of a limitation of the electron transfer to the photoactive PQ pool [35]. It is worth noting that said effect is already measurable in plants not exposed to high light, suggesting that the electron transport efficiency is constitutively defective in *pgr6.*

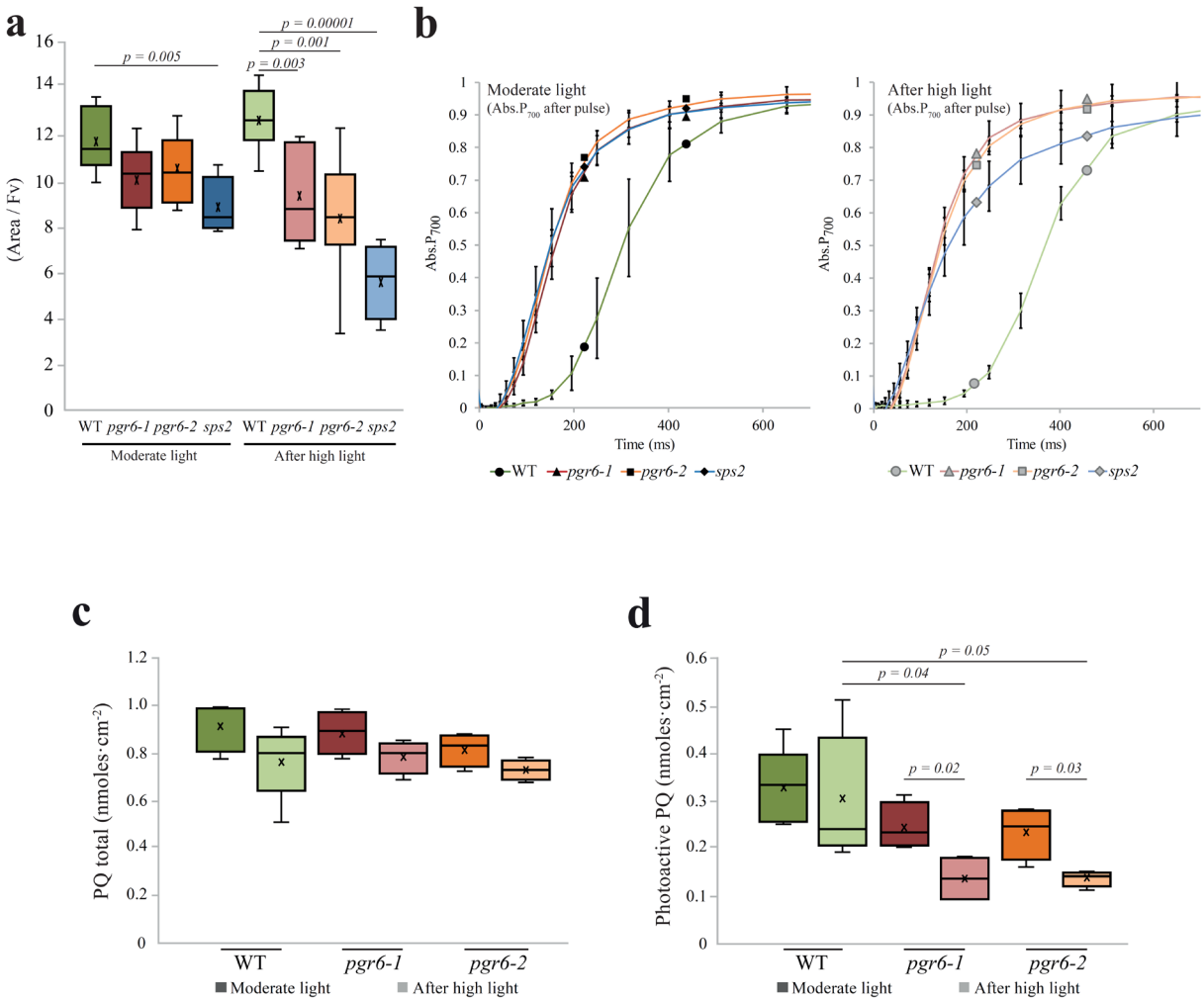

Figure 3.3. *pgr6* mutant shows a limitation in photosynthetic electron carriers. Wild type (WT), *pgr6-1*, *pgr6-2* and *sps2* plants were grown under moderate light intensity and sampled under growth light conditions (Moderate light) or after the exposure to 3 hours at 500 µmol m^{-2} s^{-1} (After high light). **(a)** Normalised area above the rapid fluorescence induction curve measured after 15 minutes of incubation in dark. This value estimates the number of available electron carriers per reaction center (Area/Fv). Whiskers and box plot shows the minimum, first quartile, median, average, third quartile, and maximum of each data set (n=8 for wild type, *pgr6-2*, n=6 for *pgr6-1*, n=4 for *sps2* biologically independent samples). **(b)** Analysis of P_{700} re-oxidation kinetics induced by far-red light after a saturating light pulse (Time 0 = far-red ON). The oxidation status was measured by the increase in absorption at 810 nm on fully expanded leaves of each genotype. Error bars indicate ±SD (n=9 biologically independent samples). **(c)** Leaf discs from wild type (WT), *pgr6-1* and *pgr6-2* plants were collected under moderate light (120 µmol m^{-2} s^{-1}) and after 3 hours of high light (500 µmol m^{-2} s^{-1}), the average total plastoquinone (oxidised + reduced PQ) content was measured in nmoles cm^{-2}. **(d)** The oxidised and reduced PQ amount was measured in leaf discs exposed either to 2 minutes far-red light (5.5 µmol m^{-2} s^{-1}) to fully oxidise the photoactive PQ pool or to 15 seconds saturating flash (2000 µmol m^{-2} s^{-1}) to fully reduce the photoactive PQ. The total photoactive PQ pool was calculated from the difference between these two conditions. Average values are reported as PQ nmoles cm^{-2}. Whiskers and box plot shows the minimum, first quartile, median, average, third quartile, and maximum of each data set (n=4 biologically independent samples); p-values are calculated via a two-tailed Student's t-test.

A limitation in the size of the photoactive PQ pool should also have a downstream effect on PSI, by decreasing the number of electrons available to reduce its primary electron donor (P_{700}) upon light-driven oxidation. This hypothesis can be tested by comparing the lag-time of P_{700}^{+} oxidation in conditions under which the ETC is completely oxidised (devoid of transportable electrons so that only the one electron present inside the PSI will account for the delay) or fully reduced by a saturating flash. The ratio between these two values provides the number of electrons contained in the whole ETC per PSI[6]. We measured these parameters using time resolved redox spectroscopy to quantify the *pgr6*-induced defect[6]. Wild type plants, acclimated to moderate light, had a maximum of 19±2 electrons per PSI, which is a number consistent with previous reports estimating the number of electron carriers[36], whereas in both *pgr6* lines background there were only 8±1 electrons per PSI. After 3h of high light exposure, the ETC of the wild type plant contained 13±2 electrons per PSI while only 4±1 and 3±1 were present in *pgr6-1* and *pgr6-2* respectively (Fig. 3.3b, Table 3.1). These results demonstrate that the electron transport chain capacity is limited in *pgr6* and that this defect is accentuated by the high light treatment. Interestingly, the same effect was observed in the *sps2* background (Table 3.1).

Moderate Light				
	Wild type	*pgr6-1*	*pgr6-2*	*sps2*
Lag time after far red (ms)	8.78±0.79	9.89±1.06	8.57±1.15	7.32±1.06
Lag time after pulse (ms)	165.88±2.93 [a]	**74.34±5.93 [b]**	**69.38±5.81 [b]**	**64.54±5.92 [b]**
Calculated pulse e^- number	19.35±1.95 [f]	**7.53±0.41 [g]**	**8.16±0.68 [g]**	**9.19±2.23 [g]**

After High Light				
	Wild type	*pgr6-1*	*pgr6-2*	*sps2*
Lag time after far red (ms)	17.14±4.37	15.68±2.94	15.01±2.69	17.67±0.98
Lag time after pulse (ms)	213.03±12.68 [c]	**54.04±13.72 [d]**	**47.36±14.05[d,e]**	**14.75±3.27 [e]**
Calculated pulse e^- number	13.21±2.33 [h]	**3.69±1.51 [i]**	**3.30±1.31 [i]**	**0.83±0.16 [i]**

Table 3.3. The electron transport capacity per photosystem I is limited in *pgr6*. Electron (e^-) capacity of the electron transport chain per photosystem I calculated from the P_{700} oxidation lag time after a saturation pulse normalised over the lag time of the oxidation after dark. Values statistically different from the wild type for each condition are in bold. Superscript letters are used to indicate statistically different groups by Student's t-test ($p<0.05$) (n=4 for Wild type, *pgr6-1*, n=3 for *pgr6-2*, *sps2* biologically independent samples).

In summary, the spectroscopic data for both *pgr6* and *sps2* are consistent with a scenario in which the limitation of photoactive PQ results in diminished electron transport. Importantly also, the cytochrome b_6f turnover rate[37] was affected in neither *pgr6* nor *sps2*, featuring wild type kinetics after exposure to 3h of high light (Supplementary figure 3.6). This indicates that the very high affinity of this complex for

plastoquinone *in vivo* ensures maximum turnover even under conditions when the PQ pool is lowered[38].

To biochemically determine the size of the photoactive PQ pool, the amounts of reduced and oxidised PQ were measured by HPLC in leaves in which the photoactive PQ was either fully oxidised by two minutes of far-red light, or fully reduced by saturating white light[4,5,11,12]. Total PQ in *pgr6* was indistinguishable from the wild type (Fig. 3.3c), and the photoactive PQ was 0.33 ± 0.08 nmoles cm^{-2} in wild type and 0.24 ± 0.05 and 0.23 ± 0.06 nmoles cm^{-2} in *pgr6-1* and *pgr6-2* respectively under moderate light (Fig. 3.3d). However, after 3h high light, the photoactive PQ in *pgr6* mutants decreased significantly (Student t-test, p=0.05) to 0.14 ± 0.05 nmoles cm^{-2} and 0.14 ± 0.02 nmoles cm^{-2}, while the wild type photoactive PQ pool remained stable around 0.30 ± 0.13 nmoles cm^{-2} (Fig. 3.3d). Furthermore, no major difference was observed in the levels of the hydroxyl-plastoquinone, a molecule that accumulates when PQ is depleted by oxidative stress, between wild type, *pgr6* and *sps2* [12] (Supplementary figure 3.7). These results demonstrate that high light treatment depletes photoactive PQ in *pgr6*. Since total PQ was not measurably different under either moderate or high light conditions, no accumulation of the oxidation product hydroxyl-plastoquinone had occurred and the photoactive pool was smaller, we expected the non-photoactive PQ pool in the plastoglobules to be increased. Consistently, higher levels of PQ were present in the plastoglobules isolated from *pgr6* and this difference was accentuated after 3h high light (Supplementary figure 3.8).

3.3 Discussion

Knock-out mutants of *PGR6* are characterised by conditional defects in growth and development, including the pale cotyledon phenotype previously reported under constant red light[18] and the variegated phenotype under high light reported here (Fig. 3.1a). So far, no molecular explanation for the observed defects was provided, besides proposing that either the lower photosynthetic efficiency[17] or the misregulation of the prenyl-lipid metabolism[19] in *pgr6* are the cause of the biochemical phenotype upon prolonged high light. In this work, we analysed plants grown under moderate non-phenotype-inducing light and assessed their photosynthetic traits after a limited exposure to high light. We observed that 3 hours of high light were sufficient to trigger a clear photosynthetic defect in *pgr6,* suggesting that the underlying cause was either already present before the treatment or could be attributed to the lack of fast adaptive responses. Photosynthetic complexes were affected neither in amount nor in activity, suggesting that the defect is not a direct consequence of protein perturbation (Supplementary figure 3.1 and Fig. 3.6).

A first level of response to photosynthetic imbalance is through the phosphorylation network of the thylakoid proteins controlled, mostly, by the kinases STN7 and STN8 and their counteracting phosphatases[23,30]. Due to the STN7 and STN8-dependent phosphorylation, the photosynthetic apparatus is capable to cope with rapid changes in the environmental conditions by maintaining an optimal photosynthetic efficiency (*e.g.* state transitions) and cope with damages to the photosystems (*e.g.* regulation of D1 repair cycle)[39,40]. In high light, the overall thylakoid protein phosphorylation was decreased in *pgr6* compared to the wild type. Lower activity of the STN7 kinase is expected in plants shifted to high light, however, the analysis of the phosphorylation pattern indicated lower activities of both STN7 and STN8 kinases in *pgr6* (Fig. 3.2). The activity of both STN kinases is linked to the redox status of the PQ pool. Therefore, this defect can potentially be explained by an influence of PGR6 on PQ. Although we cannot fully exclude that PGR6 is a direct regulator of the STN kinases, this scenario seems a rather unlikely explanation for the photosynthetic defects observed in *pgr6*. Indeed, even the double knock-out mutant of the STN kinases (*stn7/stn8*), which has an even lower level of phosphorylation of the target proteins than *pgr6*, does not display a defect in electron transport comparable to that of *pgr6* (Supplementary figure 3.2). Furthermore, *sps2*, which is genetically deprived of PQ, displays a phosphorylation defect similar to *pgr6* (Fig. 3.2).

The evidence so far points toward PQ as a key molecule regulated by PGR6 activity. Biochemical and biophysical analyses were performed to assess whether there is a limitation of the photoactive PQ pool in *pgr6* (Fig. 3.3). The comparison between wild type, *pgr6* and *sps2* offers a suitable experimental system to test this model. Indeed, when the photoactive PQ pool is genetically limited, as in *sps2*, the PSII input will be in excess over the electron capacity of the PQ pool at lower light intensity than in wild

type (Supplementary figure 3.3). As a result, the fraction of closed PSII, unable to donate electrons to the photoactive PQ, will increase and thus limit the photosynthetic efficiency compared to wild type.

These data show that here the role of PGR6 is to maintain the size of the photoactive PQ pool, *i.e.* the PQ available for the photosynthetic ETC. The lack of PGR6 does not result in a visible phenotype under moderate light indicating that its activity is not essential under this light condition[13]. This can be rationalized assuming that the loss of photoactive PQ depends on the electron flux from the PSII. The electron flow is the result of the photon input (*i.e.* light intensity) minus the portion of absorbed photons dissipated as heat (NPQ)[41]. It is only during high light that the photoactive PQ pool will receive electrons in excess of the electron flow capacity and therefore an efficient supply of PQ from a reservoir (non-photoactive PQ pool) is required for its homeostasis[12]. In this model, the role of PGR6 is to ensure a rapid refill of the photoactive PQ pool, which is essential in high electron fluencies (high light) (Fig. 3.4). Consequently, in a *pgr6* mutant upon high light exposure, the photoactive PQ pool will be depleted limiting the amount of the electron carriers available for photosynthesis. Hydroxylation of the photoactive PQ may be the cause of said depletion, which becomes phenotypic when combined with an inefficient supply of newly synthetized PQ from storage compartments to the photoactive pool[12]. However, no detectable difference in the level of accumulation of the hydroxyl-plastoquinone has been observed between *pgr6* and the wild type (Supplementary figure 3.7). Although the most likely storage compartments capable of efficiently and quickly refilling the photoactive PQ are the plastoglobules, the contribution of the envelope-located PQ cannot be excluded.

The depletion of the photoactive PQ pool observed in *pgr6* upon exposure to 3h high light may account for the reported electron transport limitation and resembles that of *sps2*. The observation that total PQ is not affected and there is no accumulation of hydroxyl-plastoquinone in *pgr6* after 3h of high light supports the model in which the cause for photoactive PQ pool depletion is the lack of an efficient refill from the PQ reservoir[12]. The lower refill ratio can be explained by a lower mobility of PQ in *pgr6*. PQ mobility constraints would also explain the measurable increase in the fraction of closed PSII reaction centers (1-qP) and NPQ observed in *pgr6* plants grown under moderate light, where the photoactive PQ pool size is unaffected (Fig. 3.1, 3.3, Supplementary figure 3.5) and the lower yield of electron transport from PSII to PQ (ΦET2o) (Supplementary figure 3.4). Additional evidence comes from measuring the electron transport as the output of the ETC at the level of P_{700} (PSI) oxidation. The output defect of *pgr6* and *sps2* appears to be much larger than the lack of photoactive PQ measured biochemically. This is exceedingly evident in the *sps2* mutant, where the depletion of PQ caused by high light resulted in a drop of the measured electron transport to less than 1 electron, suggesting that the ETC is almost completely blocked (Table 3.1). However, there is still a measurable amount of available electron acceptors for PSII and therefore of available PQ molecules (Fig. 3.3a). The

observation is consistent with previous studies on the *sps2* mutant[4] and becomes highly relevant in the context of the defect in *pgr6*: the photoactive PQ pool appears only slightly diminished (Fig. 3.3d) but electron transport is disproportionately affected (Fig. 3.1c, Fig. 3.3a, 3.3b). This is consistent with the previous model, showing that a lower concentration of PQ in the photoactive pool cannot efficiently overcome the diffusion barriers affecting its access to the photosynthetic complexes[42]. Furthermore, by limiting its own mobility in the thylakoid membranes[42], the exchange with the non-photoactive PQ pool will be impaired. Therefore, a combination of adequate photoactive PQ pool size, PQ mobility and refill rate are required to ensure PQ homeostasis and photosynthetic efficiency. Perturbation of the electron flow through the photoactive PQ, which is also the molecular vector for proton transfer across the thylakoid membrane, will limit the trans-thylakoid proton gradient needed to activate the thermal dissipation of excess absorbed light (NPQ)[43]. With a lower NPQ, the ETC will become even more over-reduced since the electron input from PSII cannot be adequately controlled. This creates a negative loop that will further exacerbate the electron transport defect. The finding that both *pgr6* and *sps2* share common defects at the level of electron transport and NPQ (Fig. 3.1, Supplementary figure 3.3) is also in accordance with this model. In the long term (*i.e.* several days of high light) these combined defects increase the high light dependent degradation of PQ[12] and will result in the depletion of the total PQ that was previously reported in *sps2*[11,12] and *pgr6* [17].

A defect in PQ mobility and availability may also explain the previously reported defect in carotenoid accumulation in *pgr6* [17,19]: Oxidised PQ functions as a sink for the electrons removed during the desaturase reactions of carotenoid biosynthesis; a limitation in the access, mobility and/or concentration of PQ may hamper this process and would lead to a lower level of carotenoid production. The consequence of this scenario would be similar to the one of *immutans* (*im*) which lacks the terminal PQ oxidase (PTOX)[21]. Interestingly, this mutant is also characterized by a variegated light-dependent phenotype similar to the one observed in *pgr6* exposed to high light. Finally, alteration of the size (and accessibility) of the photoactive PQ pool, would explain long-term effects of *pgr6* on chloroplast to nucleus communication, thus providing a rationale for the pale cotyledon phenotype reported when grown under constant red light[44].

In conclusion, our results indicate that, in order to maintain photoactive PQ as well as photosynthetic efficiency while preventing long-term photodamage[17,19] under high light, plants have evolved a PQ homeostasis mechanism controlled by the PGR6 kinase (Fig. 3.4). The observed depletion of photoactive PQ in *pgr6* after 3h high light explains the diminished STN7 activity on LHCII together with the measured effects on state transitions. Also, the Proton Gradient Regulation phenotype considering that the lack of photoactive PQ will generate a smaller trans-thylakoid proton gradient which is needed to activate the NPQ mechanism[43], and the lack of this protective mechanism results in increased

chlorophyll fluorescence, which is the signature phenotype of all *pgr* mutants[13]. Considering its subcellular localization on plastoglobules, it is tempting to hypothesise that the role of PGR6 is to control the release of PQ from plastoglobules supplying the ETC in the thylakoid membrane[12]. In support of this model there was a measurable increase in PQ concentration in *pgr6* plastoglobules compared to wild type suggesting PQ trapping in the non-photoactive pool (Supplementary figure 3.8).

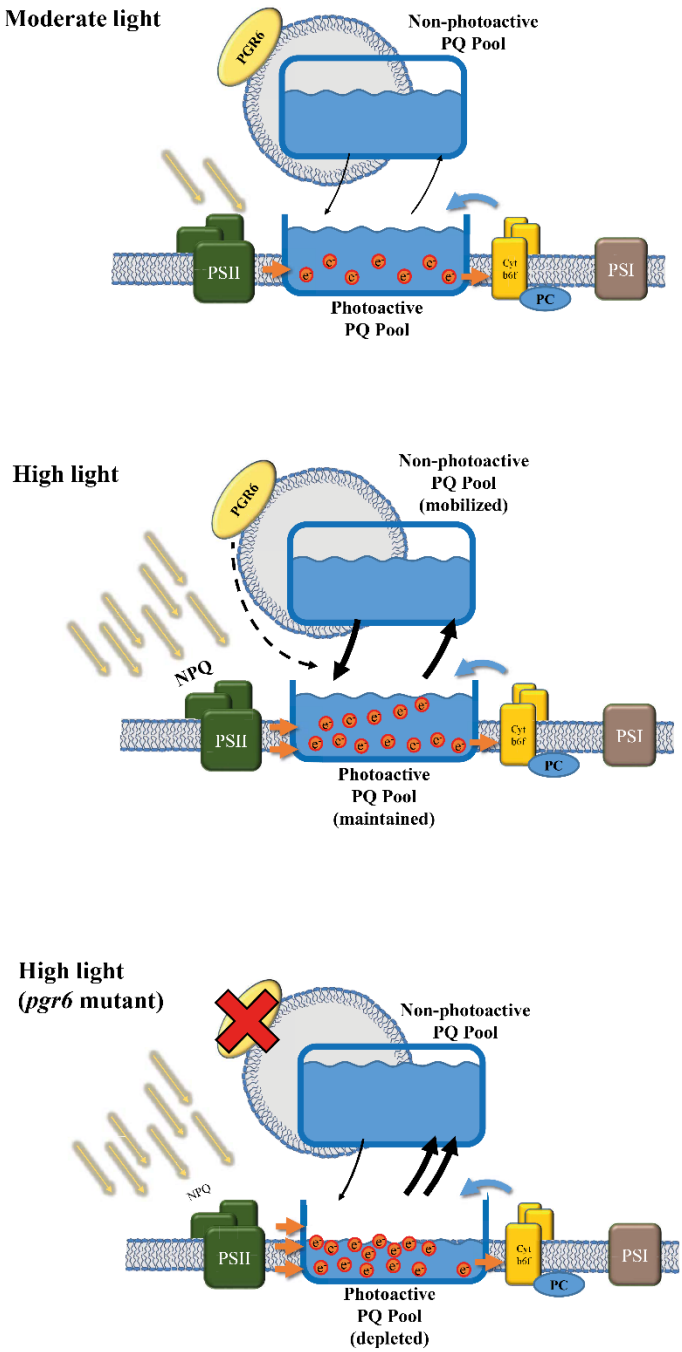

Figure 3.4. Schematic representation of the regulation mediated by PGR6. Under moderate light intensity, the electron input from the PSII is compensated by the activity of cytochrome *b6f* complex. Under this condition, the action of the two complexes is in equilibrium and maintains the photoactive PQ pool in balance thus allowing a continuous electron transport. When the light exceeds the electron transport capacity (high light) the electron input from the PSII is higher than the output from the cytochrome *b6f*, this effect is partially mitigated by the thermal dissipation of light excess (NPQ). Under high light, the maintenance of the photoactive PQ depends as well on the mobilization of the reservoir, *i.e.* the PQ stored in the non-photoactive pool. This mobilization is possible thanks to the activity of PGR6, which regulates this redistribution thus allowing the preservation of the photoactive PQ pool under high light. In the absence of PGR6 the input from the non-photoactive pool is limited and therefore insufficient to replenish the photoactive PQ pool, furthermore, the lower NPQ induction causes an even stronger over-reduction of the PQ pool, which further increases the loss of the photoactive PQ. These combined defects result in a reduction of growth and in developmental issues observed in *pgr6* mutant plants. Orange dots represent the electrons contained inside the pool, orange arrows represent the movement of the reduced PQ and blue arrows represent the movement of the oxidised form, while black arrows represent the rate of exchange between the photoactive and the non-photoactive PQ pools.

References

1 Tikhonov, A. N. pH-Dependent regulation of electron transport and ATP synthesis in chloroplasts. *Photosynth Res* **116**, 511-534 (2013).

2 Rochaix, J. D. Regulation of photosynthetic electron transport. *Biochim Biophys Acta* **1807**, 375-383 (2011).

3 Van Eerden, F. J., Melo, M. N., Frederix, P., Periole, X. & Marrink, S. J. Exchange pathways of plastoquinone and plastoquinol in the photosystem II complex. *Nat Commun* **8**, 15214 (2017).

4 Block, A., Fristedt, R., Rogers, S., Kumar, J., Barnes, B., Barnes, J., Elowsky, C. G., Wamboldt, Y., Mackenzie, S. A., Redding, K., Merchant, S. S. & Basset, G. J. Functional modeling identifies paralogous solanesyl-diphosphate synthases that assemble the side chain of plastoquinone-9 in plastids. *J Biol Chem* **288**, 27594-27606 (2013).

5 Kruk, J. & Karpinski, S. An HPLC-based method of estimation of the total redox state of plastoquinone in chloroplasts, the size of the photochemically active plastoquinone-pool and its redox state in thylakoids of *Arabidopsis*. *Biochim Biophys Acta* **1757**, 1669-1675 (2006).

6 Joliot, P. & Joliot, A. Cyclic electron flow in C3 plants. *Biochim Biophys Acta* **1757**, 362-368 (2006).

7 van Wijk, K. J. & Kessler, F. Plastoglobuli: plastid microcompartments with integrated functions in metabolism, plastid developmental transitions, and environmental adaptation. *Annu Rev Plant Biol* **68**, 253-289 (2017).

8 Kruk, J., Szymanska, R., Cela, J. & Munné-Bosch, S. Plastochromanol-8: fifty years of research. *Phytochemistry* **108**, 9-16 (2014).

9 Giacometti, G. M., Barbato, R., Chiaramonte, S., Friso, G. & Rigoni, F. Effects of ultraviolet-B radiation on photosystem II of the cyanobacterium *Synechocystis* sp. PCC 6083. *Eur J Biochem* **242**, 799-806 (1996).

10 Trebst, A. & Pistorius, E. Photosynthetische Reaktionen in UV-bestrahlten Chloroplasten. *Z Naturforsch B* **20**, 885-889 (1965).

11 Ksas, B., Becuwe, N., Chevalier, A. & Havaux, M. Plant tolerance to excess light energy and photooxidative damage relies on plastoquinone biosynthesis. *Sci Rep* **5**, 10919 (2015).

12 Ksas, B., Legeret, B., Ferretti, U., Chevalier, A., Pospisil, P., Alric, J. & Havaux, M. The plastoquinone pool outside the thylakoid membrane serves in plant photoprotection as a reservoir of singlet oxygen scavengers. *Plant Cell Environ* **41**, 2277-2287 (2018).

13 Shikanai, T., Munekage, Y., Shimizu, K., Endo, T. & Hashimoto, T. Identification and characterization of *Arabidopsis* mutants with reduced quenching of chlorophyll fluorescence. *Plant Cell Physiol* **40**, 1134-1142 (1999).

14 Lundquist, P. K., Poliakov, A., Bhuiyan, N. H., Zybailov, B., Sun, Q. & van Wijk, K. J. The functional network of the *Arabidopsis* plastoglobule proteome based on quantitative proteomics and genome-wide coexpression analysis. *Plant Physiol* **158**, 1172-1192 (2012).

15 Vidi, P. A., Kanwischer, M., Baginsky, S., Austin, J. R., Csucs, G., Dormann, P., Kessler, F. & Brehelin, C. Tocopherol cyclase (VTE1) localization and vitamin E accumulation in chloroplast plastoglobule lipoprotein particles. *J Biol Chem* **281**, 11225-11234 (2006).

16 Ytterberg, A. J., Peltier, J. B. & van Wijk, K. J. Protein profiling of plastoglobules in chloroplasts and chromoplasts. A surprising site for differential accumulation of metabolic enzymes. *Plant Physiol* **140**, 984-997 (2006).

17 Martinis, J., Glauser, G., Valimareanu, S., Stettler, M., Zeeman, S. C., Yamamoto, H., Shikanai, T. & Kessler, F. ABC1K1/PGR6 kinase: a regulatory link between photosynthetic activity and chloroplast metabolism. *Plant J* **77**, 269-283 (2014).

18 Yang, M., Huang, H., Zhang, C., Wang, Z., Su, Y., Zhu, P., Guo, Y. & Deng, X. W. *Arabidopsis* atypical kinase ABC1K1 is involved in red light-mediated development. *Plant Cell Rep* **35**, 1213-1220 (2016).

19 Lundquist, P. K., Poliakov, A., Giacomelli, L., Friso, G., Appel, M., McQuinn, R. P., Krasnoff, S. B., Rowland, E., Ponnala, L., Sun, Q. & van Wijk, K. J. Loss of plastoglobule kinases ABC1K1 and ABC1K3 causes conditional degreening, modified prenyl-lipids, and recruitment of the jasmonic acid pathway. *Plant Cell* **25**, 1818-1839 (2013).

20 Kato, Y., Miura, E., Ido, K., Ifuku, K. & Sakamoto, W. The variegated mutants lacking chloroplastic FtsHs are defective in D1 degradation and accumulate reactive oxygen species. *Plant Physiol* **151**, 1790-1801 (2009).

21 Wetzel, C. M., Jiang, C. Z., Meehan, L. J., Voytas, D. F. & Rodermel, S. R. Nuclear-organelle interactions: the immutans variegation mutant of *Arabidopsis* is plastid autonomous and impaired in carotenoid biosynthesis. *Plant J* **6**, 161-175 (1994).

22 Zagari, N., Sandoval-Ibanez, O., Sandal, N., Su, J., Rodriguez-Concepcion, M., Stougaard, J., Pribil, M., Leister, D. & Pulido, P. SNOWY COTYLEDON 2 promotes chloroplast development and has a role in leaf variegation in both *Lotus japonicus* and *Arabidopsis thaliana*. *Mol Plant* **10**, 721-734 (2017).

23 Mekala, N. R., Suorsa, M., Rantala, M., Aro, E. M. & Tikkanen, M. Plants actively avoid state transitions upon changes in light intensity: role of light-harvesting complex II protein dephosphorylation in high light. *Plant Physiol* **168**, 721-734 (2015).

24 Bellafiore, S., Barneche, F., Peltier, G. & Rochaix, J. D. State transitions and light adaptation require chloroplast thylakoid protein kinase STN7. *Nature* **433**, 892-895 (2005).

25 Rochaix, J. D. Redox regulation of thylakoid protein kinases and photosynthetic gene expression. *Antioxid Redox Signal* **18**, 2184-2201 (2013).

26 Shapiguzov, A., Chai, X., Fucile, G., Longoni, P., Zhang, L. & Rochaix, J. D. Activation of the Stt7/STN7 kinase through dynamic interactions with the cytochrome *b6f* complex. *Plant Physiol* **171**, 82-92 (2016).

27 Trotta, A., Suorsa, M., Rantala, M., Lundin, B. & Aro, E. M. Serine and threonine residues of plant STN7 kinase are differentially phosphorylated upon changing light conditions and specifically influence the activity and stability of the kinase. *Plant J* **87**, 484-494 (2016).

28 Pietrzykowska, M., Suorsa, M., Semchonok, D. A., Tikkanen, M., Boekema, E. J., Aro, E. M. & Jansson, S. The light-harvesting chlorophyll *a/b* binding proteins Lhcb1 and Lhcb2 play complementary roles during state transitions in *Arabidopsis*. *Plant Cell* **26**, 3646-3660 (2014).

29 Bonardi, V., Pesaresi, P., Becker, T., Schleiff, E., Wagner, R., Pfannschmidt, T., Jahns, P. & Leister, D. Photosystem II core phosphorylation and photosynthetic acclimation require two different protein kinases. *Nature* **437**, 1179-1182 (2005).

30 Schonberg, A., Rodiger, A., Mehwald, W., Galonska, J., Christ, G., Helm, S., Thieme, D., Majovsky, P., Hoehenwarter, W. & Baginsky, S. Identification of STN7/STN8 kinase targets reveals connections between electron transport, metabolism and gene expression. *Plant J* **90**, 1176-1186 (2017).

31 Tikkanen, M., Nurmi, M., Kangasjarvi, S. & Aro, E. M. Core protein phosphorylation facilitates the repair of photodamaged photosystem II at high light. *Biochim Biophys Acta* **1777**, 1432-1437 (2008).

32 Bailey, S., Thompson, E., Nixon, P. J., Horton, P., Mullineaux, C. W., Robinson, C. & Mann, N. H. A critical role for the Var2 FtsH homologue of *Arabidopsis thaliana* in the photosystem II repair cycle *in vivo*. *J Biol Chem* **277**, 2006-2011 (2002).

33 Strasser, R. J., Tsimilli-Michael, M., Qiang, S. & Goltsev, V. Simultaneous *in vivo* recording of prompt and delayed fluorescence and 820-nm reflection changes during drying and after rehydration of the resurrection plant *Haberlea rhodopensis*. *Biochim Biophys Acta* **1797**, 1313-1326 (2010).

34 Kalaji, H. M., Oukarroum, A., Alexandrov, V., Kouzmanova, M., Brestic, M., Zivcak, M., Samborska, I. A., Cetner, M. D., Allakhverdiev, S. I. & Goltsev, V. Identification of nutrient deficiency in maize and tomato plants by *in vivo* chlorophyll *a* fluorescence measurements. *Plant Physiol Biochem* **81**, 16-25 (2014).

35 Maxwell, K. & Johnson, G. N. Chlorophyll fluorescence - a practical guide. *J Exp Bot* **51**, 659-668 (2000).

36 Graan, T. & Ort, D. R. Quantitation of the rapid electron donors to P_{700}, the functional plastoquinone pool, and the ratio of the photosystems in spinach chloroplasts. *J Biol Chem* **259**, 14003-14010 (1984).

37 Finazzi, G., Rappaport, F., Furia, A., Fleischmann, M., Rochaix, J. D., Zito, F. & Forti, G. Involvement of state transitions in the switch between linear and cyclic electron flow in *Chlamydomonas reinhardtii*. *EMBO Rep* **3**, 280-285 (2002).

38 Finazzi, G., Buschlen, S., de Vitry, C., Rappaport, F., Joliot, P. & Wollman, F. A. Function-directed mutagenesis of the cytochrome *b6f* complex in *Chlamydomonas reinhardtii*: involvement of the cd loop of cytochrome *b6* in quinol binding to the Q(o) site. *Biochemistry* **36**, 2867-2874 (1997).

39 Pesaresi, P., Pribil, M., Wunder, T. & Leister, D. Dynamics of reversible protein phosphorylation in thylakoids of flowering plants: the roles of STN7, STN8 and TAP38. *Biochim Biophys Acta* **1807**, 887-896 (2011).

40 Tikkanen, M., Grieco, M., Kangasjarvi, S. & Aro, E. M. Thylakoid protein phosphorylation in higher plant chloroplasts optimizes electron transfer under fluctuating light. *Plant Physiol* **152**, 723-735 (2010).

41 Genty, B., Harbinson, J., Briantais, J. M. & Baker, N. R. The relationship between non-photochemical quenching of chlorophyll fluorescence and the rate of photosystem 2 photochemistry in leaves. *Photosynth Res* **25**, 249-257 (1990).

42 Lavergne, J. & Joliot, P. Restricted diffusion in photosynthetic membranes. *Trends Biochem Sci* **16**, 129-134 (1991).

43 Müller, P., Li, X. P. & Niyogi, K. K. Non-photochemical quenching. A response to excess light energy. *Plant Physiol* **125**, 1558-1566 (2001).

44 Huang, H., Yang, M., Su, Y., Qu, L. & Deng, X. W. *Arabidopsis* atypical kinases ABC1K1 and ABC1K3 act oppositely to cope with photodamage under red light. *Mol Plant* **8**, 1122-1124 (2015).

45 Eugeni-Piller, L., Glauser, G., Kessler, F. & Besagni, C. Role of plastoglobules in metabolite repair in the tocopherol redox cycle. *Front Plant Sci* **5**, 298 (2014).

46 Martinis, J., Kessler, F. & Glauser, G. A novel method for prenylquinone profiling in plant tissues by ultra-high pressure liquid chromatography-mass spectrometry. *Plant Methods* **7**, 23 (2011).

Supplementary figures

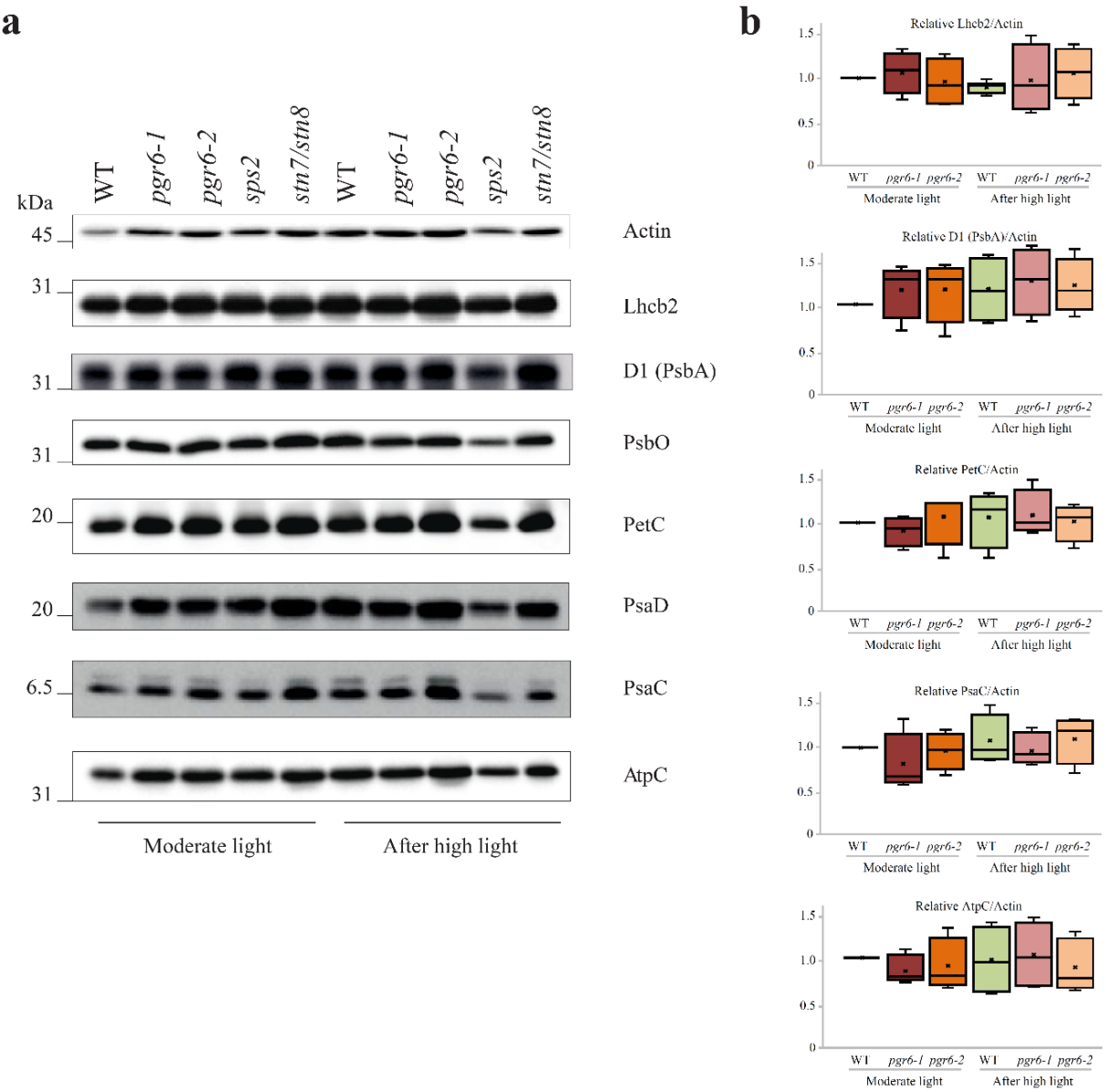

Supplementary figure 3.1. Abundance of photosynthetic complexes is not affected in *pgr6* mutants. Total protein extract of light-exposed leaves under moderate light (120 µmol m^{-2} s^{-1}) and after 3h of high light (500 µmol m^{-2} s^{-1}) from wild type (WT), *pgr6-1*, *pgr6-2*, *sps2* and *stn7/stn8* adult plants were separated in SDS-PAGE. **(a)** Upon transfer on nitrocellulose membrane, representative subunits of the principal photosynthetic complexes were immuno-detected. Lhcb2 for the major LHCII, D1 (PsbA) and PsbO for PSII, PetC for cytochrome *b6f*, PsaD and PsaC for PSI, and AtpC for ATP synthase. Actin was used as a loading control. **(b)** For WT as well as *pgr6-1* and *-2* representative proteins for each photosynthetic complex were quantified using gel image analysis software (ImageQuant GE healthcare) and normalized to actin, whiskers and box plot shows the minimum, first quartile, median, average, third quartile, and maximum of each data set (n=4 biologically independent samples.

a

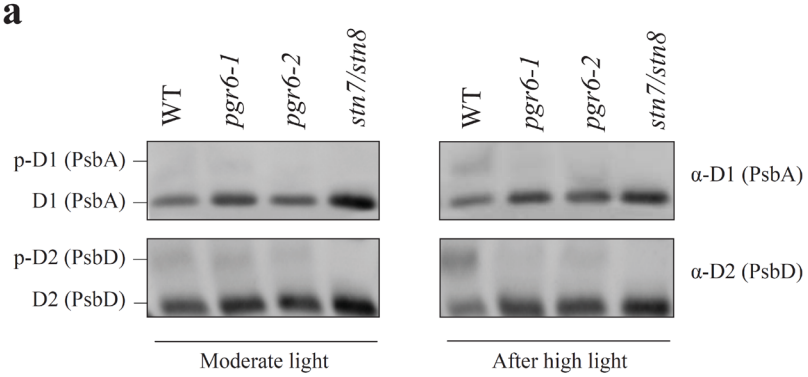

b

	WT	*pgr6-1*	*pgr6-2*	*stn7/stn8*
Fo (ML)	41.32 ± 1.34	43.86 ± 1.79	45.02 ± 1.82	48.10 ± 2.83
Fo (HL)	39.55 ± 2.07	41.27 ± 2.72	43.46 ± 1.63	43.18 ± 1.12

c

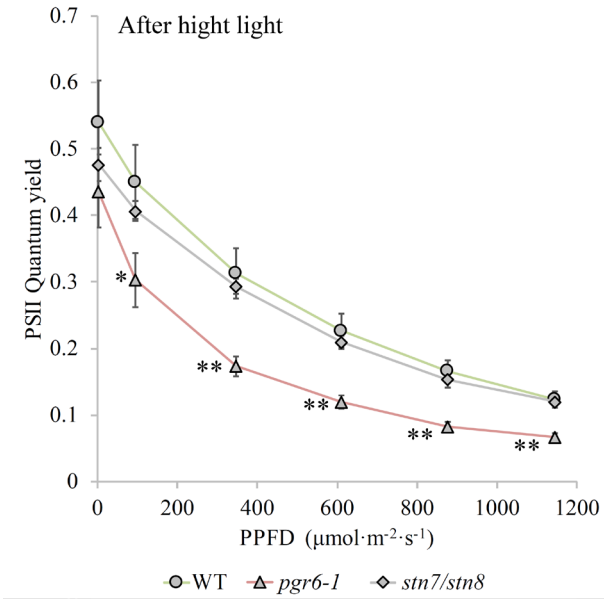

d

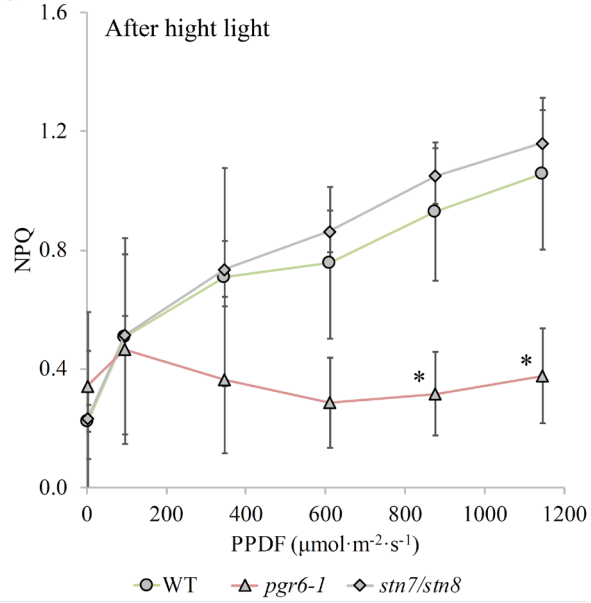

Supplementary figure 3.2. Reduced phosphorylation of thylakoid proteins does not strongly affect PSII functionality in *pgr6* mutants after short high light treatment. Total proteins of wild type (WT), *pgr6-1*, *pgr6-2* and *stn7/stn8* adult plants before (Moderate light) and after high light treatment were separated on Phostag™-pendant acrylamide gels. **(a)** D1 (PsbA) and D2 (PsbD) phosphorylation level visualised using D1 (PsbA) and D2 (PsbD) antibodies, the upper band corresponds to the phosphorylated form (p-), a protein sample from *stn7/stn8* double mutant was loaded as a non-phosphorylated control. **(b)** Average Fo values measured after 10 minutes of dark relaxation in wild type (WT), *pgr6-1*, *pgr6-2* and *stn7/stn8*. The plants were kept under moderate light (120 µmol m^{-2} s^{-1}) (ML) or under high light (500 µmol m^{-2} s^{-1}) for 3h (HL). PSII quantum yield **(c)** and the NPQ **(d)** measured in plants exposed to 3h of HL for WT, *pgr6-1* and *stn7/stn8*. The measurements were performed with Fluorcam (MF800 – PSI). ±SD (n=3) (Student's t-test, ** : p<0.01; * : p<0.05).

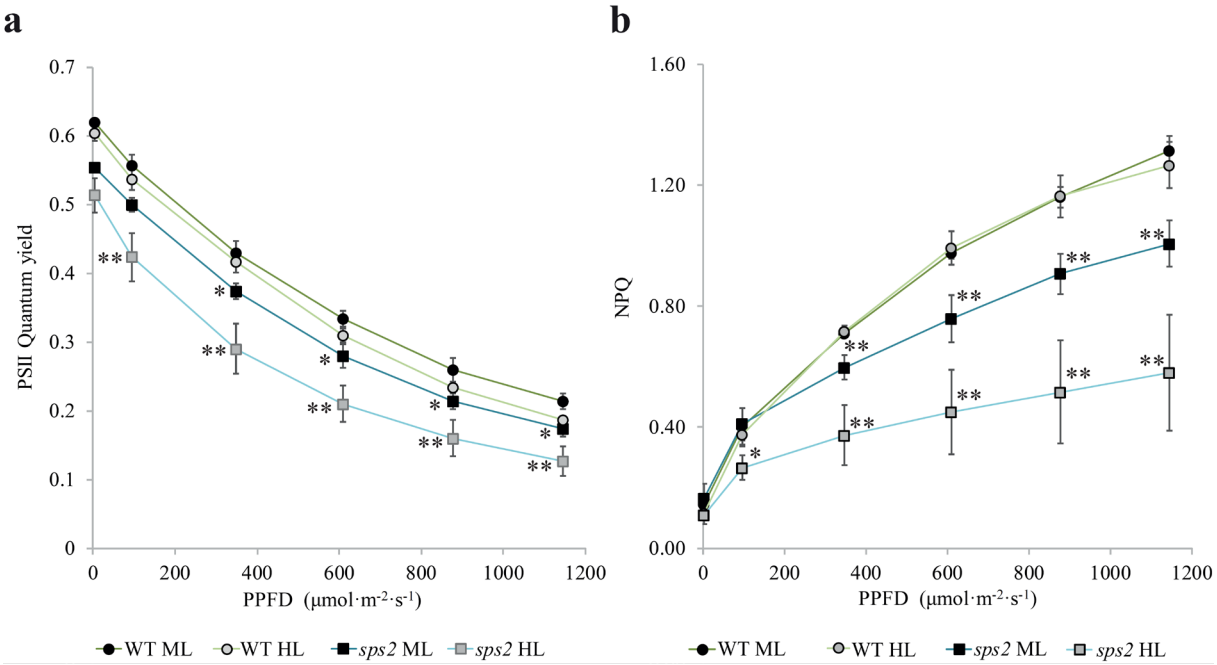

Supplementary figure 3.3. Mutant of PQ biosynthesis (*sps2*) is affected in photosystem II quantum yield and thermal dissipation. 24 days old plants grown on soil in short day cycle (8h light /16h dark) were used to assess the photosynthetic efficiency of wild type (WT) and *sps2* under moderate light (120 µmol m^{-2} s^{-1}) (ML, dark colors) and after 3 hours of high light (500 µmol m^{-2} s^{-1}) (HL, light colors). After 10 minutes of dark relaxation variable room temperature chlorophyll fluorescence was measured on whole plants exposed to these light conditions to determine the following parameters: **(a)** PSII quantum yield (Φ_{PSII} = (F_M' – F_S)/F_M') at increasing light intensities and **(b)** non-photochemical quenching (NPQ = (F_M – F_M')/F_M') after one minute of exposure at different light intensities. These measures were performed with a Fluorcam (MF800 – PSI) with blue light LEDs (470 nm). Each value represents the average of a pot containing 2-3 plants. Error bars indicate ±SD between different pots (n=3). Asterisks indicate statistically different points in which the difference between *sps2* and the WT exposed to the same light treatment (Student's t-test, ** : p<0.01; * : p<0.05).

a

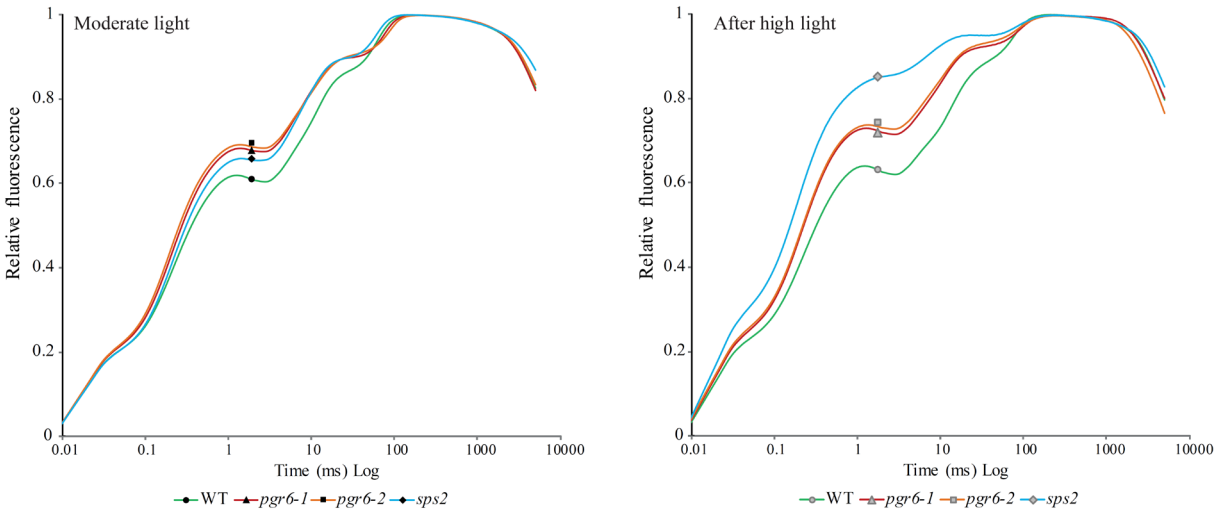

b

Moderate light				
	WT	*pgr6-1*	*pgr6-2*	*sps2*
ΦPo	0.97±0.00	0.97±0.00	0.97±0.00	0.97±0.00
ΦET2o	0.40±0.05	**0.35±0.06****	**0.33±0.07****	**0.34±0.05****
ΦRE1o	0.13±0.02	**0.11±0.03***	**0.11±0.01****	**0.10±0.01****

After high light				
	WT	*pgr6-1*	*pgr6-2*	*sps2*
ΦPo	0.97±0.00	0.96±0.00	0.96±0.02	0.96±0.00
ΦET2o	0.38±0.03	**0.28±0.04****	**0.28±0.07****	**0.15±0.05****
ΦRE1o	0.13±0.02	**0.08±0.02****	**0.07±0.03****	**0.05±0.02****

Supplementary figure 3.4. Analysis of electron flux impairment in *pgr6* mutants by rapid fluorescence induction. (a) Average traces of rapid chlorophyll *a* fluorescence induction in logarithmic scale from wild type (WT) (n=8), *pgr6-1* (n=6), *pgr6-2* (n=8), *sps2* (n=4) adult leaves harvested under moderate light (120 µmol m^{-2} s^{-1}) (left) and after 3 hours of high light (500 µmol m^{-2} s^{-1}) (right) using a Plant Efficiency Analyser (Handy-PEA Hansatech Instruments). **(b)** Calculated electron fluxes from the induction curve using the JIP-test as described in Strasser *et al.* (2010)[33] and Kalaji *et al.* (2014)[34]. ΦPo (maximum quantum yield of primary PSII photochemistry), ΦET2o (quantum yield of the electron transport from Q_A to Q_B) and ΦRE1o (quantum yield of the electron transport until the PSI electron acceptors). The mean and the standard deviation is reported, values statistically different from the WT are shown in bold (Student's t-test,** p<0.05; * p<0.10) (n=10 for WT, n=8 for *pgr6-1* and *pgr6-2*, n=4 for *sps2*).

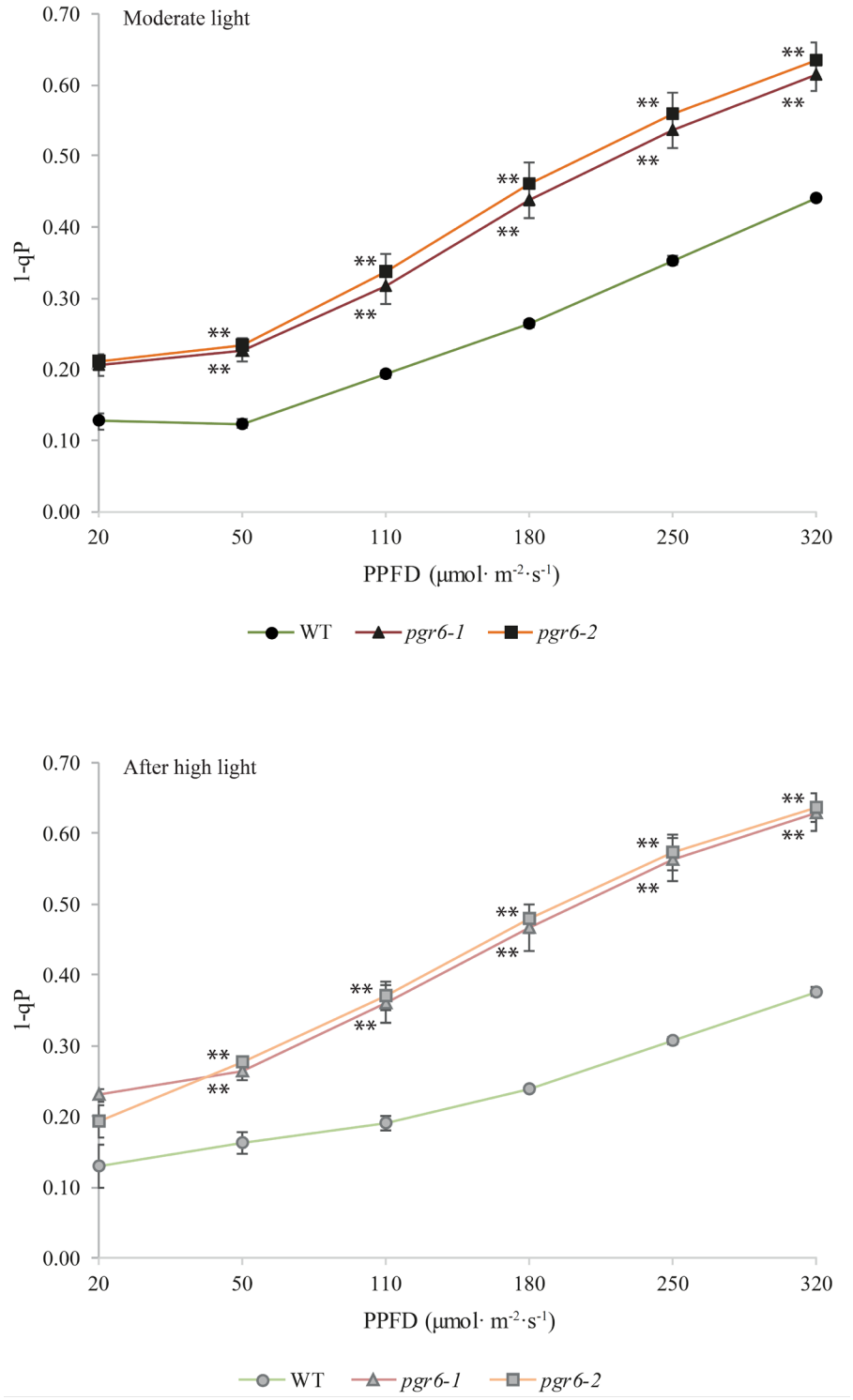

Supplementary figure 3.5. The fraction of "closed" PSII reaction centers increases in *pgr6* mutants. The fraction of closed Q_A sites, expressed as 1-qP, was calculated from room temperature chlorophyll fluorescence in wild type (WT), *pgr6-1* and *pgr6-2* adult plants exposed to moderate light (120 µmol m^{-2} s^{-1}) and after 3h of high light (500 µmol m^{-2} s^{-1}). Error bars indicate ±SD (n=3). (Student's t-test, ** : p<0.01). These measurements were performed with a Fluorcam (MF800 – PSI) with red light LEDs (660 nm).

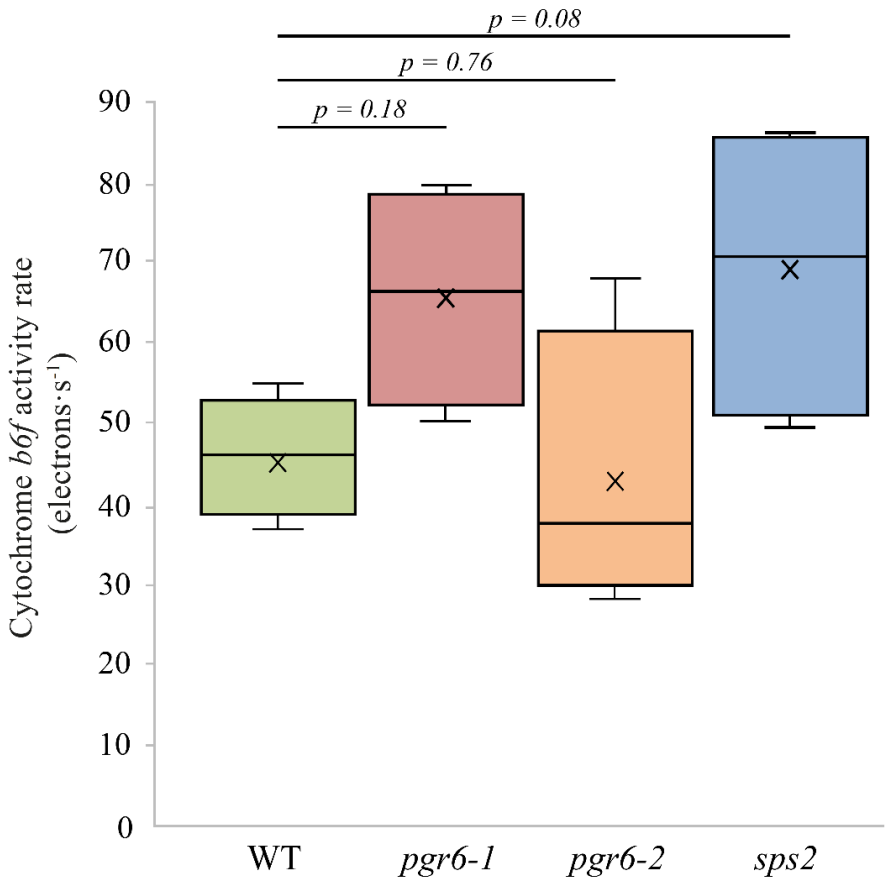

Supplementary figure 3.6. High light treatment does not perturb the cytochrome *b6f* turnover in *pgr6* mutant. Wild type (WT), *pgr6-1*, *pgr6-2* and *sps2* plants were grown under moderate light condition, fully expanded leaves were collected after 3h of high light (500 µmol m^{-2} s^{-1}). The turnover rate of the cytochrome *b6f* (expressed as electrons per second) was calculated by fitting the kinetics of the cytochrome *f* oxidation after a saturating pulse with an exponential curve. The measured signal was the absorption at 554 nm corresponding to the cytochrome *f* as described in Finazzi *et al.* (2002)[37]. Whiskers and box plot shows the minimum, first quartile, median, average, third quartile, and maximum of each data set (n=5). Mutant lines were compared to WT via a Student's t-test and corresponding p-values reported above each one.

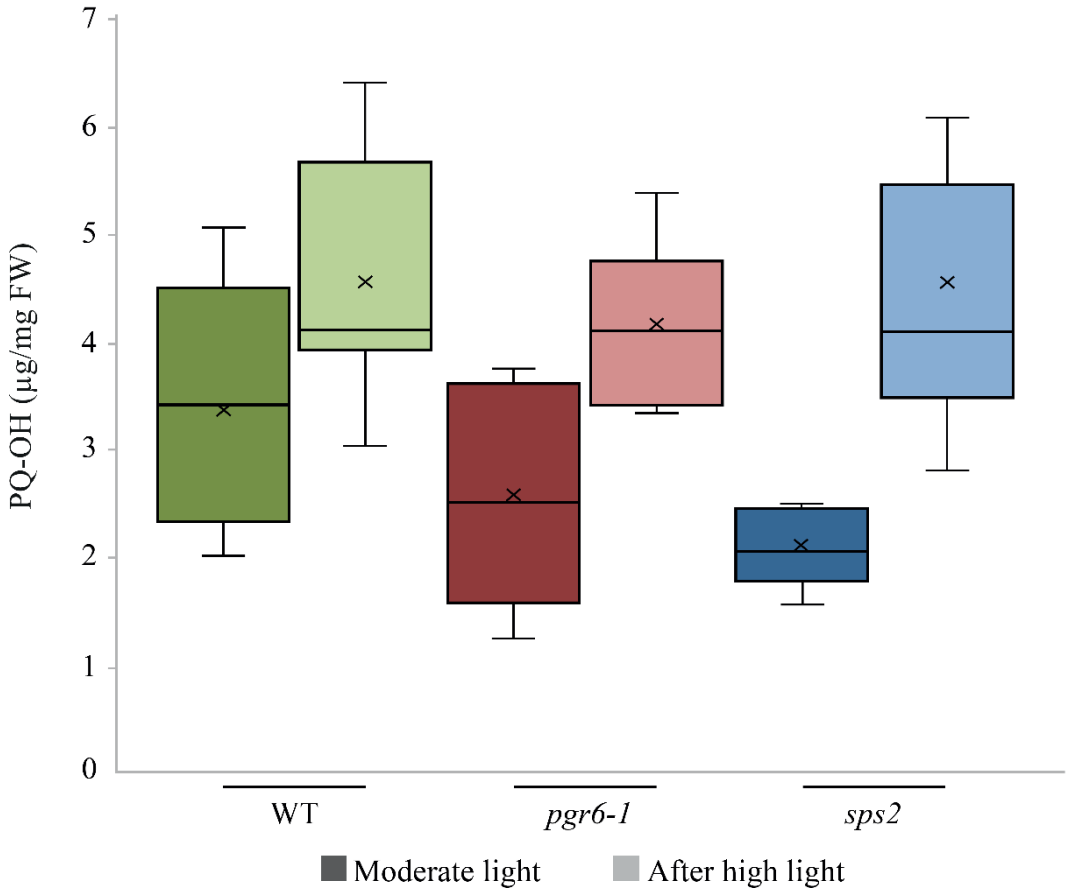

Supplementary figure 3.7. Hydroxyl-plastoquinone accumulation in leaves. Hydroxyl-plastoquinone (PQ-OH) accumulation in total leaves of wild type (WT), *pgr6-1* and *sps2* collected from plants exposed to moderate light (120 µmol m^{-2} s^{-1}) and after 3h of high light (500 µmol m^{-2} s^{-1}). Identification and quantification of this molecule performed as described in Eugeni-Piller *et al.* (2014)[45] and in Martinis *et al.* (2011)[46]. Whiskers and box plot shows the minimum, first quartile, median, average, third quartile, and maximum of each data set (n=4 biologically independent samples).

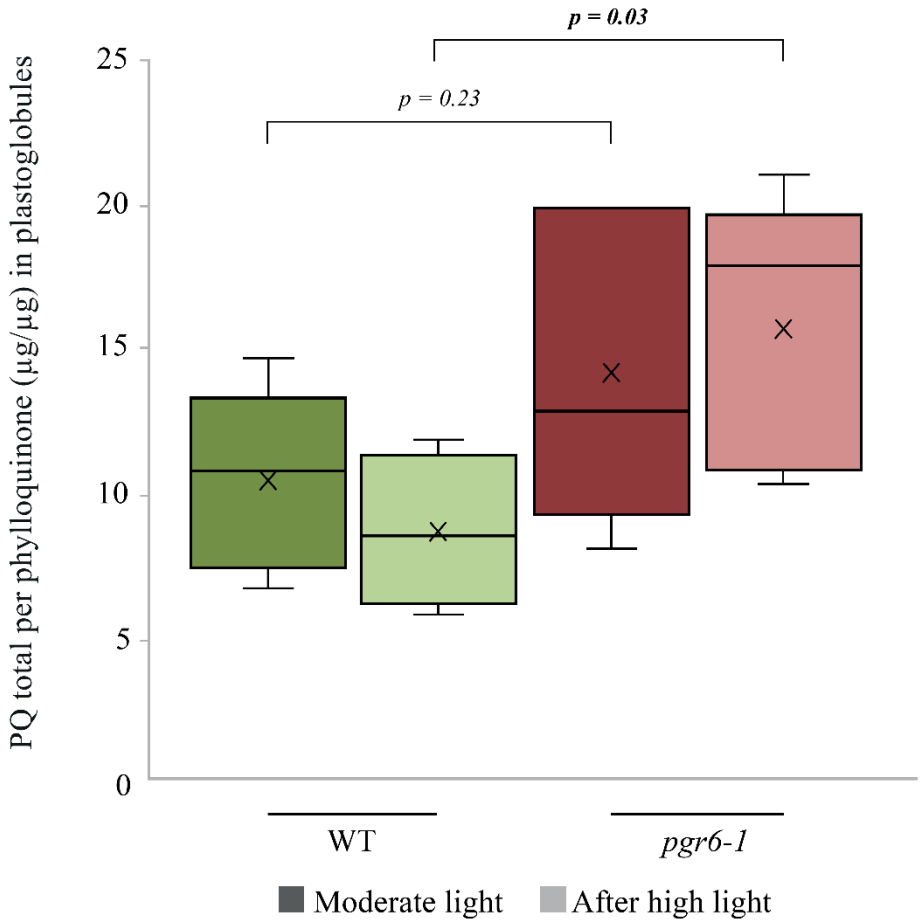

Supplementary figure 3.8. Plastoquinone accumulation in plastoglobules. Total plastoquinone (PQ) of wild type (WT) and *pgr6-1* plastoglobules fractions prepared from plants exposed to moderate light (120 µmol m^{-2} s^{-1}) and after 3h of high light (500 µmol m^{-2} s^{-1}). Plastoglobules were isolated by flotation on a sucrose gradient and prenyl lipids were analysed as described in Eugeni-Piller *et al.* (2014)[45] and in Martinis *et al.* (2011)[46]. Total plastoquinone content (oxidised + reduced PQ) was normalised on phylloquinone (µg/µg). Whiskers and box plot shows the minimum, first quartile, median, average, third quartile, and maximum of each data set (n=5 biologically independent samples). WT and *pgr6* were compared by Student's t-test; corresponding p-values are reported above each compared group.

Chapter IV

Mutation of the atypical kinase ABC1K3 alleviates the PROTON GRADIENT REGULATION 6 deficiency in *Arabidopsis thaliana*.

Pralon Thibaut, Collombat Joy, Pipitone Rosa, Ksas Brigitte, Shanmugabalaji Venkatasalam, Glauser Gaetan, Havaux Michel, Finazzi Giovanni, Longoni Paolo, Kessler Felix

Abstract

Photosynthesis is an essential pathway providing the chemical energy and reducing equivalents that sustain higher plant metabolism. It relies on natural light, but this is an inconstant source of energy that fluctuates in both intensity and spectrum. The fine and rapid tuning of the photosynthetic apparatus is essential to cope with changing light conditions and increase plant fitness. Recently PROTON GRADIENT REGULATION 6 (ABC1K1/PGR6), an atypical plastoglobule-associated kinase, was shown to regulate a newly discovered regulatory mechanism: homeostasis of photoactive plastoquinone (PQ). PQ is a crucial electron carrier existing as a free neutral lipid in the photosynthetic thylakoid membrane. Perturbed homeostasis of PQ impairs photosynthesis and plant acclimation to high light.

Here we show that a homologous kinase, ABC1K3, like PGR6 associated with plastoglobules, also contributes to the homeostasis of the photoactive PQ pool. Contrary to PGR6, it disfavours PQ availability for photosynthetic electron transport. In fact, in the *pgr6/abc1k3* double mutant the *pgr6* photosynthetic defect, observed under high light, is mitigated. However, the plastoquinone concentration in the photoactive pool of the complemented mutant is comparable to that of *pgr6* mutant. The mobility of the PQ, inferred from the kinetics of its oxidation in dark, showed that this process contributes to the photosynthetic defect of *pgr6* and is partially recovered in the double mutant. This is surprising and suggests that more than the absolute concentration of PQ, its mobility and exchange between storage and active pools are critical. The results also demonstrate that ABC1K3 contributes to the regulation of other mechanisms allowing the adaptation of the photosynthetic apparatus to changes in light quality and intensity such as the induction of thermal dissipation and state transitions.

4.1 Introduction

The photosynthetic conversion of light energy into chemical energy occurs via a series of redox reactions resulting in electron transport along the thylakoid membrane. The linear electron transport begins with water splitting at the level of photosystem II (PSII) and ends at photosystem I (PSI) with the reduction of $NADP^+$ by ferredoxin. Both PSII and PSI utilise photonic energy to fuel the redox reactions. Electrons are transferred from PSII to PSI via the cytochrome *b6f* complex (cyt *b6f*). At the Q_B site of PSII, a molecule of plastoquinone (PQ) is reduced twice and protonated to form plastoquinol (PQH_2). The PQH_2 can then diffuse within the thylakoid membrane to arrive at the Q_O site of cyt *b6f*. Oxidation of PQH_2 at cyt *b6f* occurs through the Q-cycle that releases protons into the thylakoid lumen contributing to the formation of the trans-thylakoid proton gradient. In addition, two electrons are released, one of which returns to PQ pool, while the other is transferred by plastocyanin to PSI. The proportion of PQ that participates in electron transport in thylakoid membrane is considered as the photoactive PQ pool; whereas the remaining proportion, which is approximately 60-70% of the total PQ, constitutes the non-photoactive pool and is largely stored inside thylakoid-associated lipid droplets known as plastoglobules (PG)[1-3].

In order to shuttle electrons, PQ has to rapidly navigate the thylakoid lipid bilayer[4]. However, the thylakoid membrane is crowded with integral proteins, up to 70% in the grana stacks, which drastically restrict PQ diffusion, especially at the long-range[5]. Thylakoid membranes are close to the percolation threshold, therefore it has been suggested that the organisation of the protein supercomplexes create lipid microdomains that facilitate PQ mobility and thus electron shuttling between PSII and cyt *b6f* [5-7]. On the other hand, long-range mobility of the PQ is also important, for instance during mobilization of reservoirs when damaged PQ molecules have to be replaced as it occurs during high light stress[3]. Therefore, the mobility of plastoquinone/ol molecules within the thylakoid lipid bilayer is a critical parameter to assure electron transport and maintain the photosynthetic electron transport chain (ETC).

Apart from the role of PQ as an electron carrier role, its redox state, is an important signal in the regulation of many physiological processes within the chloroplast such as state transitions, non-photochemical quenching (NPQ), gene expression, carotenoid biosynthesis and antioxidant activity[8-10]. A rapid readout of the PQ redox state allows photosynthetic adaptation to changing environmental conditions and therefore increases plant fitness in a natural environment. In fact, in natural environments, plants must cope with rapidly varying light intensities. Not surprisingly, adaptation to such varying light conditions is essential for plants to maintain the highest photosynthetic efficiency while avoiding photo-induced damage. To alleviate the negative effects of an imbalance between the

activity of the two photosystems, plants have developed a short-term adaptive mechanism: the state transitions. This process allows re-equilibrating the light energy input on a time scale of a few minutes by re-allocating mobile light-harvesting complexes II (LHCII) between the two photosystems[11-13]. Movement of the mobile part from PSII to PSI (state 2) involves LHCII phosphorylation by STN7 kinase, the activity of which is dependent on PQ redox state[14-16]. In contrary, dephosphorylation of LHCII operated by the PPH1/TAP38 phosphatase results in the migration of LHCII from PSI to PSII (state 1)[17-20]. Furthermore, to prevent harmful effects of excess light, plants can also dissipate this energy excess as heat by a set of regulated mechanisms summarily referred to as non-photochemical quenching (NPQ). Among the mechanisms allowing the dissipation there is a fast component based LHCII antenna rearrangement to a "quenched" state depending on the PsbS protein; the xanthophyll cycle in which zeaxanthin, a better quencher, is substituted for the violaxanthin associated to LHCII. The sum of all components create a system with differential kinetics activated within a few seconds to hours[21-26]. Nonetheless, upon continuous light stress, ROS can be produced at the PSII reaction center leading to protein damage and loss of the PSII activity, this partially regulated process is known as photoinhibition and contributes to the quenching of the excess light. To restore PSII activity after inhibition there is an efficient repair cycle. This mechanism is facilitated by the phosphorylation of the core proteins of the PSII reaction center by STN8 kinase. Damaged PSII has to migrate from grana to stroma lamellae where the damaged PsbA\D1 protein can be replaced by the *de novo* synthetized protein[27-31]. Photooxidative stress, also triggers other responses allowing the chloroplast to alleviate the damage. These responses involve regulation of gene expression[32,33], structural changes of the thylakoids[34] and synthesis of antioxidant molecules[1,3,35-41].

Another structure, within the chloroplast, that appears to be involved in the stress response is the plastoglobule (PG). PG are small protein-studded lipid droplets, attached to the outer lipid leaflet of the thylakoid membrane[42], which are delimited by a membrane lipid monolayer consisting mostly of galactolipids and coated with proteins. They are filled with several neutral lipids including prenylquinones, carotenoids, triacylglycerols, phytolesters[43-50]. In response to various stresses PG increase in size and number[39,43,51-53]. Physical connections between PG and thylakoid membranes suggest bidirectional lipid trafficking between these two compartments[42]. Besides being a lipid storage site, the PG proteome revealed the presence of specific proteins, several of which are involved in prenylquinone metabolism[54-56]. Fibrillins, the major protein family of PG[54], have presumed structural roles[57] but their predicted lipocalin domain hints to a function in lipid binding and/or trafficking; *e.g.* PG of *fbn4* knock-down apple leaves are not able to retain PQ, in contrast to wild type PG[58]. Some of the remaining PG proteins are enzymes with a characterized function. An example is the tocopherol cyclase VTE1, which is essential for chromanol ring formation in tocopherols and plastochromanol[55,59-

[61]; or the NAD(P)H dehydrogenase C1 (NDC1), which is involved in phylloquinone and plastochromanol accumulation[60,62], as well as in the tocopherol repair cycle[49,63].

The second most abundant protein family in PG is composed of members of the family of the ABC1 (Activity of BC1 complex) atypical kinases[54]. The ABC1 domain has been conserved through evolutionary process[64]. In microorganisms as well as in human cells, ABC1 proteins were shown to be essential in ubiquinone synthesis and in mitochondrial electron transport[65-68]. Six members of ABC1-like kinase family are found in PG and are likely to play regulatory roles. A member of this family, ABC1K1 (At4g31390), was identified as *PGR6* in a genetic screen to identify mutants affected in proton gradient formation (PGR)[69]. PGR mutants are characterized by high chlorophyll fluorescence and reduced NPQ under control conditions (50 µmol m^{-2} s^{-1}) and high light (300-500 µmol m^{-2} s^{-1})[39,69,70]. In fact, the electron transport rate as well as NPQ is constitutively limited in the *pgr6* mutant in a light fluency dependent manner when compared to the wild type. Under prolonged exposure to high light, *pgr6* adult plants exhibited almost complete photoinhibition during the early days of treatment and surprisingly, after several days PSII maximum efficiency recovered despite the plants still being under high light[39]. Nonetheless, the metabolic profile of *pgr6* was profoundly altered. In particular, plants displayed a decrease in tocopherol accumulation and a shift from starch production to soluble sugars[39]. Independently, PGR6 was identified as BDR1 (Bleached dwarf under red light)[71,72]. During early seedling development under continuous red light, the mutant is severely stunted and has white cotyledons. Since the bleaching phenotype was accompanied by a specific diminishment of the photosystem D1 (PsbA) protein but not that of other photosynthetic proteins tested (D2 (PsbD); PsbC; PsbB) it was attributed to photobleaching[71,72]. A repressor of the *bdr1* mutation, RBD1 (repressor of *bdr1*) was also identified as the PGR6 homolog ABC1K3. As the *rbd1/abc1k3* mutation repressed the *bdr*/*pgr6* phenotype, it led to the hypothesis that the two homologs have opposing functions[71]. Furthermore, *abc1k3* adult plants are not severely affected by prolonged high light, they showed reduction in plastochromanol accumulation[61]. However, double *pgr6/abc1k3* mutant adult plants were reported to have an additive, senescence-like phenotype characterized by conditional degreening, including the loss of chlorophyll and photosystem proteins, and recruitment of the jasmonate pathway to PG under prolonged high light treatment[46]. Furthermore, PGR6 and ABC1K3 may interact and form a complex that may be involved in the stabilization of plastoglobules proteins[46,61].

Recently, a molecular mechanism explaining the *pgr6* defect was proposed: in this model PGR6 is required for the homeostasis of photoactive PQ. Indeed, upon high light, the photoactive PQ pool in *pgr6* mutant becomes limiting and therefore the linear electron transport and NPQ are diminished, LHCII antenna are strongly dephosphorylated and state transitions are disturbed leading to an overall decrease in the photosynthetic efficiency[73].

In this study, we investigated if and how the mutation of ABC1K3 complements the *pgr6* photosynthetic defect and if a double mutant lacking both *PGR6* and *ABC1K3* is capable to acclimate to a short high light treatment (3h, 500 µmol m^{-2} s^{-1}).

Here, we show that the *abc1k3* mutant has no photosynthetic defect compared to the wild type under these conditions. However, by adding this mutation to the *pgr6* background we observed an alleviation of all the photosynthetic defects previously reported in this mutant[39,69,73]. Surprisingly, the phenotype complementation does not originate from an effect on the size of the photoactive PQ pool but rather from an effect on PQ mobility in the thylakoid membrane. The evidence suggests that there is a push-pull relationship of PGR6 and ABC1K3 with regard to the mobility of PQ, and that this regulated process is fundamental to ensure the photosynthetic efficiency under high light intensity.

4.2 Results

4.2.1 Isolation and selection of *pgr6/abc1k3* double mutants

To analyse potential interactions between PGR6 and ABC1K3 in the regulation of photosynthesis, two double mutant *pgr6/abc1k3* lines were obtained by crossing *pgr6.1* (Salk_068628) with *abc1k3.1* (Salk_128696) or with *abc1k3.2* (Sail_918_E10). Double *pgr6/abc1k3* mutant lines were selected and verified by PCR. The genotyping confirmed the presence of T-DNA insertions in both genes (Fig. 4.1).

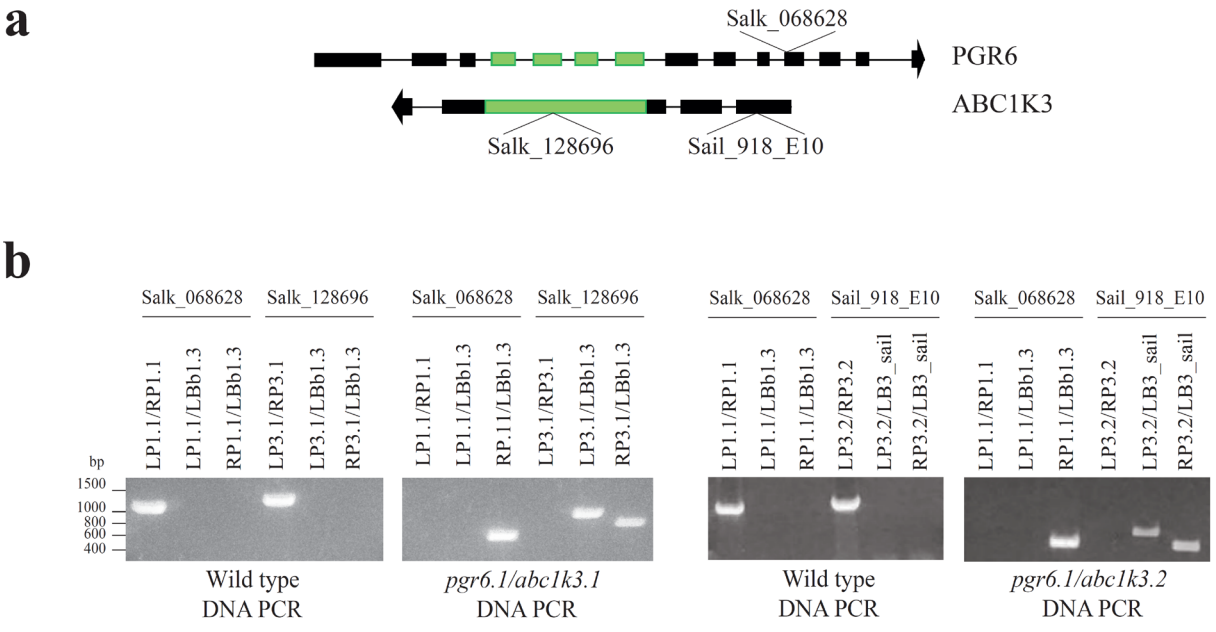

Figure 4.1. Selection and isolation of *pgr6/abc1k3* double mutant lines. (a) Schematic representation of the position of the T-DNA insertions in *PGR6* (At4g31390) and *ABC1K3* (At1g79600) gene sequences. **(b)** Electrophoresis of the amplification products obtained from genomic DNA extracted from wild type, *pgr6/abc1k3.1* and *pgr6/abc1k3.2* confirm the homozygous mutation of both loci. The double mutant *pgr6/abc1k3.1* was obtained from the crossing between *pgr6.1* (SALK_068628) and *abc1k3.1* (SALK_128696), while *pgr6/abc1k3.2* is the result of the crossing between *pgr6.1* (SALK_068628) and *abc1k3.2* (SAIL_918_E10). The primer used for the amplification are listed in Supplementary Materials and Methods Table 1.

4.2.2 Thermal dissipation and electron transport capacities are partially recovered in *pgr6/abc1k3*

Independent studies indicate that *pgr6* is impaired in non-photochemical quenching as well as electron transport[39,69,73], while the *abc1k3* mutant did not show defects in those parameters even after prolonged high light exposure[61]. To further characterize the *pgr6/abc1k3* double mutant lines, we measured photosynthetic parameters such as PSII maximum efficiency (ϕ_{MAX} = F_V/F_M), non-photochemical quenching (NPQ) as well as electron capacity of the ETC in 4-5 weeks old plants grown under moderate light (120µmol m^{-2} s^{-1}) (ML) and after 3h of high light (500µmol m^{-2} s^{-1}) (HL).

The maximum quantum yield of the PSII (ϕ_{MAX}) in wild type (WT), *pgr6*, *abc1k3* and *pgr6/abc1k3* slightly decreased after 3h of high light but without any significant difference between the lines (Fig. 4.2a). Therefore, after 3h of HL there was no detectable damage to PSII, and this allows to measure the impairments in the ETC avoiding potential bias caused by PSII photodamage.

a

Maximum PSII Quantum Yield (ΦMAX)							
	WT	***pgr6.1***	***pgr6.2***	***abc1k3.1***	***abc1k3.2***	***pgr6.1/abc1k3.1***	***pgr6.1/abc1k3.2***
ML	0.830 ± 0.010 [a]	0.817 ± 0.023 [a]	0.823 ± 0.006 [a]	0.830 ± 0.000 [a]	0.827 ± 0.015 [a]	0.817 ± 0.023 [a]	0.830 ± 0.000 [a]
HL 3h	0.773 ± 0.006 [b]	0.743 ± 0.031 [b]	0.723 ± 0.031 [b]	0.727 ± 0.012 [b]	0.763 ± 0.006 [b]	0.767 ± 0.017 [b]	0.740 ± 0.017 [b]

b

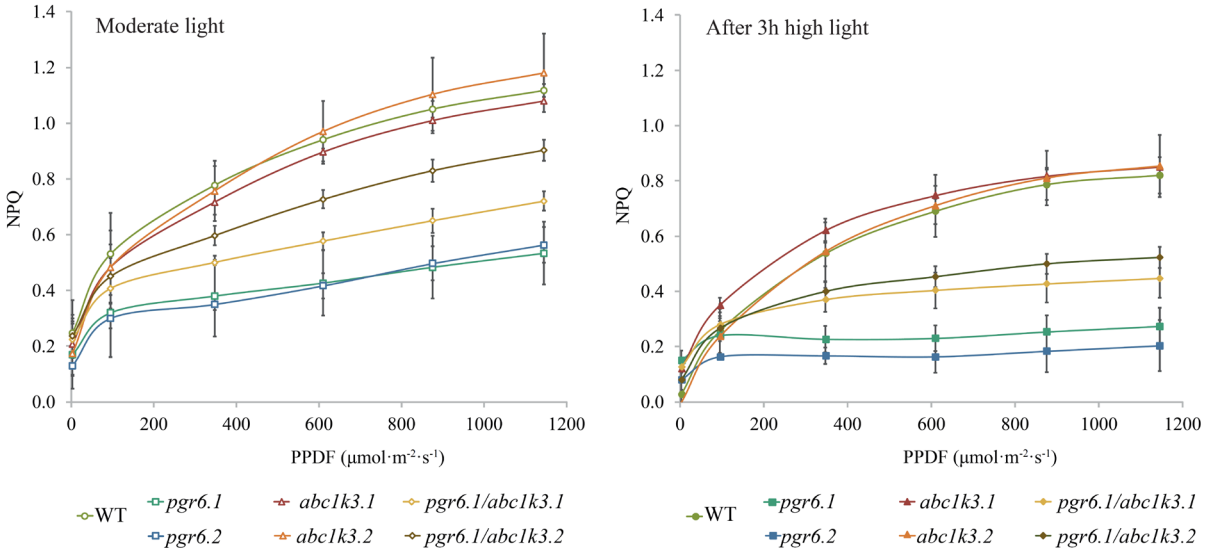

Figure 4.2. Non-photochemical quenching is partially recovered in *pgr6/abc1k3* lines compared to *pgr6*. (a) PSII maximum quantum efficiency (ΦPSII = (FM – FO)/FM) and **(b)** non-photochemical quenching (NPQ) of 4-5 weeks old plants of wild type (WT), *pgr6.1, -2, abc1k3.1, -2 and pgr6/abc1k3.1, -2* under moderate light and after 3h of high light. Plants were dark-adapted 10 min before measurement. Non-photochemical quenching (NPQ = FM -FM'/FM') was calculated from room the maximal fluorescence at room temperature recorded after one minute of exposure at increasing blue light intensities (470 nm). These measures were performed with a Fluorcam (MF800 – PSI). Each value represents the average of a pot containing 2-3 plants. Superscript letters are used to indicate statistically different groups ($p<0.05$) by paired Student's t-test. Error bars indicate ±SD between different pots (n=3).

Short-term high light treatment affects NPQ induction, which decreases in all the genotypes tested compared to moderate light conditions. Nonetheless, the NPQ in wild type and in *abc1k3* was always higher than the one measured in *pgr6* lines. Intriguingly, both under moderate light and after high light, the double mutants showed greater NPQ compared to *pgr6* lines but still lower than the wild type level (Fig. 4.2b), suggesting a partial rescue of the *pgr6* phenotype in the double mutant.

Using P_{700} oxidation kinetics[74] and the JIP-test[75-77], ETC capacity was measured from the PSI and PSII sides under moderate light and after exposure to high light to determine whether NPQ rescue in *pgr6/abc1k3* was related to an increase in the electron capacity in the ETC.

P_{700} oxidation kinetics were analysed after full reduction of the ETC by a saturating flash and its full oxidation by far-red illumination[73,74]. The maximum number of electrons (e^-) present in the electron transport chain per PSI was assessed from P_{700} oxidation kinetic curves: by dividing the lag time after a strong light pulse (time required to oxidize P_{700} when ETC is fully reduced) by the lag time after far-red exposure (oxidation time of a single electron present in P_{700} reaction center)[74]. Under moderate light, the *abc1k3.*2 single mutant had as many electrons per PSI (20±3) as wild type (20±4), whereas *pgr6.1* already contained fewer electrons in its ETC per PSI (8±1)[73] (Fig. 4.3). In *pgr6/abc1k3.2* the number of electrons measured per PSI (16±5) was intermediate between the *pgr6* mutant and the wild type. Upon high light exposure, the number of electrons present per PSI decreased to 13±3 in wild type. Similarly, in *pgr6.1* as well as *pgr6/abc1k3.2* the number of electrons per PSI dropped after high light treatment to 4±2 and 8±1 respectively. However, the measured electron transport capacity in *pgr6/abc1k3.2* always remained higher than in *pgr6.1*, indicating partial rescue of the ETC. Interestingly, *abc1k3.2* displayed only a very slight decrease in the number of electrons per PSI upon shifting to high light (18±4) (Fig. 4.3).

To confirm ETC recovery in double mutants, the number of electron carriers present in the photosynthetic electron transport chain per PSII was estimated using fast chlorophyll *a* fluorescence (JIP-test) by normalizing the area above JIP-curve over variable fluorescence ($Area/(F_M-F_O)$)[75-77]. The area surface correlates with the number of turnovers at the Q_A site of PSII before being fully closed which should correspond to the saturation of the ETC and reflects the number of electron acceptors in the ETC per PSII including the internal acceptors pheophytin and Q_A; the PQ molecules of the photoactive plastoquinone pool, the *b6f* complex and plastocyanin. Under moderate light the normalized area value was bigger in *abc1k3* (21±1; 21±1) than WT (17±2), while it was smaller in *pgr6* (15±1; 14±1)[73]. Interestingly, in *pgr6/abc1k3* lines the estimated electron capacity (18±2; 20±3) was comparable to WT (Fig. 4.4a). After 3h of high light, the number of electron acceptors in *pgr6/abc1k3* (19±2; 18±3) remained essentially unvaried and was similar to WT (19±2). The electron capacity in *pgr6*

mutants was diminished (13±1; 11±2) after high light treatment, consistently with previous report[73], whereas, surprisingly, *abc1k3* lines showed a tendency towards an increase in electron carriers (22±2; 24±3) (Fig.4.4a). These results are consistent with the recovery of the photosynthetic parameters observed in the double mutant.

To obtain an indication of the impact of the *pgr6/abc1k3* mutations on different components of the electron transport chain, we calculated the quantum yields of the electron transport flux from Q_A^- to PQ (ΦET2o) and down to the PSI electron acceptors (ΦRE1o) by analysing chlorophyll fluorescence inductions of JIP-curves at 3 ms (F_J) and 30 ms (F_I).

Already under moderate light *pgr6/abc1k3* (0.43±0.03; 0.43±0.02) as well as *pgr6* (0.42±0.03; 0.38±0.04) showed a lower ΦET2o when compared to WT (0.48±0.02) and *abc1k3* lines (0.48±0.01; 0.49±0.01). After 3h high light, ΦET2o dropped in all lines with the most severe decrease in *pgr6* (0.30±0.05; 0.26±0.06). However, this also led to a lower efficiency in *pgr6/abc1k3* (0.34±0.04; 0.34±0.04) in comparison to WT (0.42±0.04) and *abc1k3* mutants (0.40±0.03; 0.39±0.05) (Fig. 4.4b).

Interestingly, the quantum yield of electron transport to PSI final acceptors (ΦRE1o) was reduced in *pgr6* lines (0.11±0.02; 0.10±0.02) and higher in *abc1k3* mutants (0.18±0.01; 0.18±0.02), whereas ΦRE1o in *pgr6/abc1k3* (0.14±0.02; 0.13±0.03) was similar to wild type (0.14±0.03). After 3h of high light, *pgr6* ΦRE1o was diminished (0.07±0.01; 0.06±0.02), but it remained essentially unchanged in *pgr6/abc1k3* (0.11±0.02; 0.12±0.02) when compared to the moderate light value and was only slightly lower when compared to the wild type (0.15±0.02). Once again, the double mutation appears to alleviate the defects of the *pgr6* mutant. Interestingly, after high light, ΦRE1o in *abc1k3* (0.18±0.01; 0.18±0.02) did not change compared to moderate light and was higher than in the wild type (Fig. 4.4c).

To exclude that the recovery of photosynthetic parameters in *pgr6/abc1k3* as well as the higher photosynthetic capacities measured in *abc1k3* mutants, where due to an increased cytochrome *b6f* activity, this parameter was measured. The results demonstrate that its activity was similar among all lines (Supplementary figure 4.1).

Together, these results indicate that *abc1k3* mutants can cope with high light as well as the wild type, while photosynthetic parameters in *pgr6* mutants are confirmed to be severely affected. Interestingly, the *pgr6/abc1k3* double mutant has partially recovered NPQ and electron transport capacities when compared to *pgr6.*

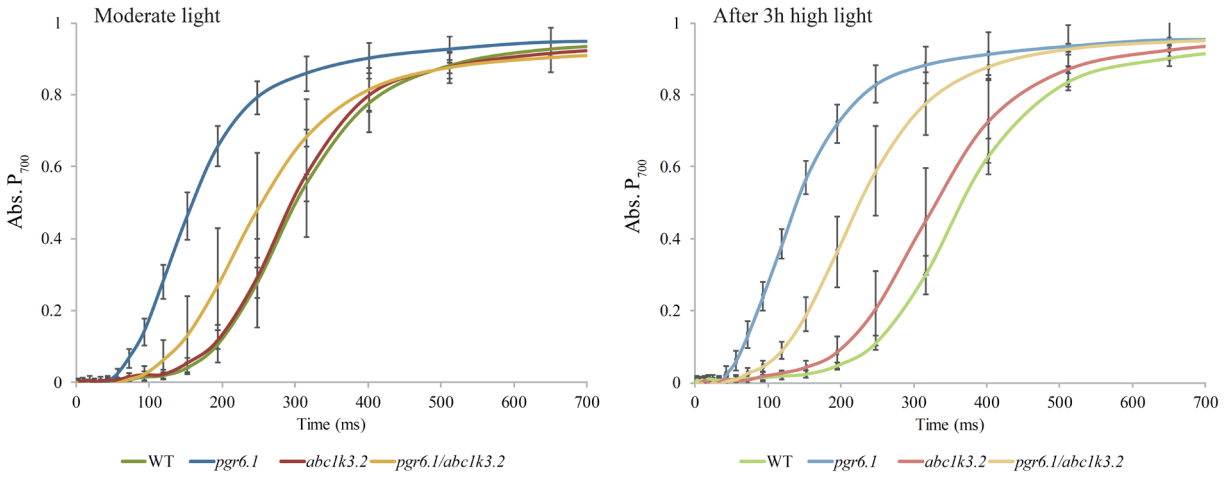

Moderate light				
	WT	***pgr6.1***	***abc1k3.2***	***pgr6.1/abc1k3.2***
Lag time after FAR (ms)	8.68	10.07	8.79	9.49
Lag time after pulse (ms)	173.68	75.22*	170.44	139.90*
Calculated pulse e^- number	20 ± 1	**8 ± 2***	20 ± 3	**16 ± 5***

After 3h high light				
	WT	***pgr6.1***	***abc1k3.2***	***pgr6.1/abc1k3.2***
Lag time after FAR (ms)	17.87	15.92	11.68	14.47
Lag time after pulse (ms)	215.14	49.85*	200.60	109.84*
Calculated pulse e^- number	13 ± 4	**4 ± 2***	18 ± 4	**8 ± 1***

Figure 4.3. The shortage of electron carriers per photosystem I of *pgr6* is partially recovered in *pgr6/abc1k3*. (a) Kinetics of P_{700} re-oxidation induced by far-red light were recorded after a saturating light pulse (Time 0 = far-red ON) in wild type, *pgr6.1, abc1k3.2* and *pgr6/abc1k3.2* kept under moderate light and after 3h of high light. The P_{700} oxidation status was measured by the increase in absorption at 810 nm on fully expanded leaves of each genotype. **(b)** Electron (e^-) carried by the electron transport chain per photosystem I calculated from the lag time of P_{700} oxidation after a saturating pulse divided by the lag time of the oxidation after dark. Asterisk are used to indicate statistically different groups by Student's t-test ($p<0.05$) (n=4 biologically independent samples).

a

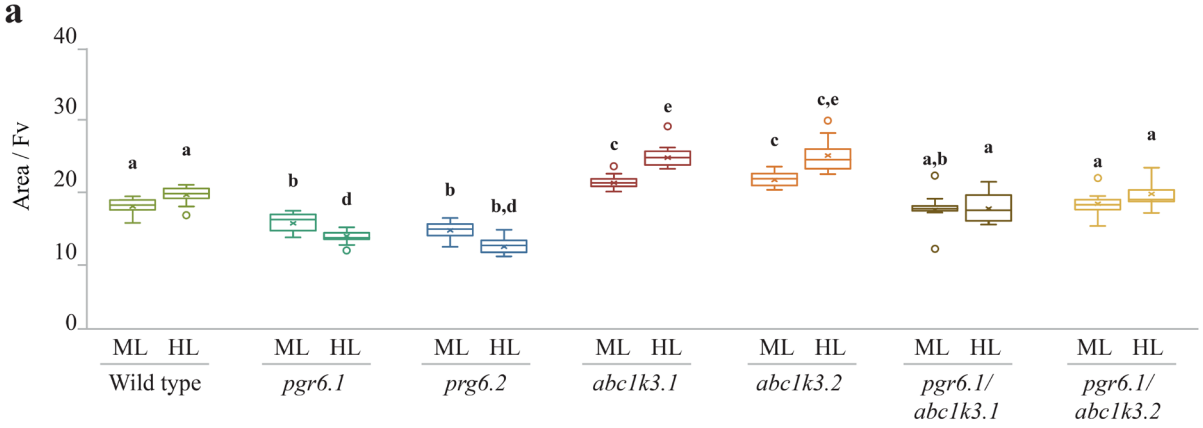

b

	φET2o						
	WT	***pgr6.1***	***pgr6.2***	***abc1k3.1***	***abc1k3.2***	***pgr6.1/abc1k3.1***	***pgr6.1/abc1k3.2***
ML	0.48 ± 0.02 [a]	**0.42 ± 0.03** [b]	**0.38 ± 0.04** [c]	0.48 ± 0.01 [a]	0.49 ± 0.01 [a]	**0.44 ± 0.02** [b]	**0.43 ± 0.03** [b]
HL 3h	0.42 ± 0.04 [b,c]	**0.31 ± 0.04** [d,e]	**0.26 ± 0.07** [e]	0.40 ± 0.03 [b,c]	0.40 ± 0.03 [b,c]	**0.32 ± 0.02** [d]	**0.33 ± 0.03** [d]

c

	φRE1o						
	WT	***pgr6.1***	***pgr6.2***	***abc1k3.1***	***abc1k3.2***	***pgr6.1/abc1k3.1***	***pgr6.1/abc1k3.2***
ML	0.14 ± 0.03 [a]	**0.11 ± 0.02** [b]	**0.10 ± 0.02** [b]	**0.18 ± 0.01** [c]	**0.18 ± 0.02** [c]	0.14 ± 0.02 [a]	0.13 ± 0.03 [a]
HL 3h	0.15 ± 0.02 [a]	**0.08 ± 0.01** [d]	**0.06 ± 0.02** [d]	**0.18 ± 0.02** [c]	**0.17 ± 0.02** [c]	0.11 ± 0.02 [a,b]	0.12 ± 0.02 [a,b]

Figure 4.4. High light as a moderate impact on photosynthetic electron transport fluxes in *pgr6/abc1k3*. Fully expanded leaves from Wild type (WT), *pgr6.1, -2, abc1k3.1, -2* and *pgr6/abc1k3.1, -2* plants were collected under moderate light conditions (120 µmol m^{-2} s^{-1}) (ML) and after 3h of high light (500 µmol m^{-2} s^{-1}) (HL). **(a)** Normalised area (Area/Fv) above the chlorophyll fluorescence induction curve measured after 15 minutes of dark incubation. This value estimates the number of available electron carriers per PSII reaction center. **(b)** Quantum electron transport yield from Q_A to PQ pool (ΦET2o), and **(c)** until the PSI electron acceptors (ΦRE1o). These measures were performed with Handy-PEA (Hansatech Instruments). Whiskers and box plot shows the minimum, first quartile, median, average, third quartile, and maximum of each data set (n=12 biologically independent samples). Superscript letters are used to indicate statistically different groups by paired Student's t-test ($p<0.05$).

4.2.3 The photoactive PQ pool size is not restored in *pgr6/abc1k3*

The level of NPQ and the electron acceptor capacity of the ETC may be related to the size of the photoactive PQ pool[1,73]. Therefore, we examined whether the partial rescue of the electron transport and NPQ capacities in *pgr6/abc1k3* compared to *pgr6* can be attributed to the size of the photoactive plastoquinone pool (*i.e.* the number of PQ molecules readily available per PSII). For this, we measured the total PQ (nmol cm^{-2}) and the relative photoactive PQ pool (in % of total PQ pool) in 4-5 weeks old plants under moderate light and after 3h of high light exposure. The photoactive PQ pool is defined as the fraction of total PQ that is rapidly reduced during a saturating light pulse and oxidized when the sample is exposed to far-red light. To determine this fraction, PQH_2 and PQ amounts were measured by HPLC-MS on leaves illuminated either with a strong light flash in order to completely reduce the photoactive PQ pool, or with far-red to obtain a complete oxidation[1-3,73]. The difference between the amount of reduced PQ after the saturating flash and that measured after far-red illumination determines the photoactive PQ pool.

Total plastoquinone levels (photoactive PQ pool + non-photoactive PQ pool) in *pgr6* and in *pgr6/abc1k3* lines were similar compared to wild type and only slightly decreased after 3h high light exposure[73]. Surprisingly, the total PQ level was lower in *abc1k3* compared to wild type (Fig. 4.5a).

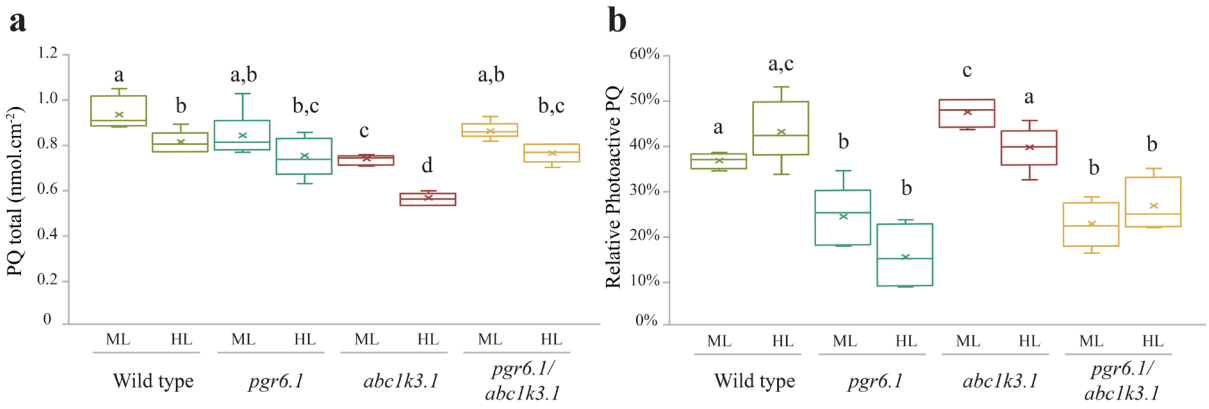

Figure 4.5. Photoactive PQ pool is smaller in all the lines containing the *pgr6* mutation. (a) Total plastoquinone content (nmol cm^{-2}) and **(b)** relative photoactive plastoquinone pool (as % of total PQ) were analysed from leaves of wild type, *pgr6.1*, *abc1k3.2* and *pgr6/abc1k3.2* under moderate light and after 3h high light. The photoactive plastoquinone pool was determined by the difference of the plastoquinol (PQH_2) amount measured when the PQ pool is maximally reduced by strong white light pulse (15 sec at 2'000 µmol m^{-2} s^{-1}), and the amount of PQH_2 measured when the PQ pool is fully oxidized after far-red illumination (2 min at 5.5 µmol m^{-2} s^{-1}). Whiskers and box plot shows the minimum, first quartile, median, average, third quartile, and maximum of each data set (n=4 biologically independent samples). Superscript letters are used to indicate statistically different groups by paired Student's t-test ($p<0.05$).

However, the relative photoactive PQ pool (photoactive PQ/total PQ) measured in *abc1k3* was identical to wild type even after high light (Fig. 4.5b), whereas in *pgr6* it was already low under

moderate light and was strongly diminished after high light, which is consistent with a previous report[73]. Intriguingly, although double mutants were not severely impaired in either ETC capacity or NPQ compared to *pgr6* (Fig. 4.2, 4.4), the relative photoactive PQ pool measured under moderate light in *pgr6/abc1k3* was unexpectedly small and similar to the one of *pgr6*. After high light, the photoactive PQ pool in double mutants remained very low compared to wild type or *abc1k3* mutants but did not show any further decrease compared to moderate light (Fig. 4.5b).

The analysis of the photoactive PQ pool suggests that the complementation of the *pgr6* photosynthetic phenotype induced by the *abc1k3* mutation does not simply arise from a change of the quantity of PQ readily available at PSII.

4.2.4 Mutation of PGR6 and ABC1K3 impact the kinetics of PQ re-oxidation in the dark

The redox state of the PQ under light is dependent on the activity of the PSII, which will reduce the photoactive pool, and that of the cytochrome *b6f*, which oxidises the PQ pool transferring electrons along the ETC towards PSI. However, in the dark the photosynthetic complexes are inactive and therefore the redox state of the PQ is mostly dependent on enzymatic reaction. In the transition from light to dark the photoactive PQ pool will tend to start in a reduced form and be re-oxidized. The principal actor of this re-oxidation is PTOX. This enzyme, in Arabidopsis, is mostly located in the stroma lamellae fraction of the thylakoid membrane[78-80]. Being PSII more abundant in the grana stacks, and considering the timescale of the mobility of the PQ[6], we may assume that a large portion of the photoactive PQ pool is located within the grana stack. Therefore, in order to be oxidised by PTOX the PQ has to migrate from the grana stack to the stroma lamellae and vice versa. Considering this, the kinetic of the oxidation of the photoactive PQ pool, represent a proxy of the mobility of the PQ across the different portions of the thylakoid membrane. To rapidly estimate the redox state of the photoactive PQ pool we used the rapid chlorophyll *a* fluorescence induction, we based the analysis on the relative fluorescence at 3 ms (V_J). It has been shown that the fluorescence recorded at this time interval correlates with the redox state of the photoactive PQ pool[75,76]. A high V_J value is recorded in samples where the photoactive PQ pool is mostly reduced, and it decreases with its oxidation[81]. The chlorophyll *a* fluorescence induction was measured at increasing time intervals of dark incubation after a saturating light pulse. The results show that the measured oxidation, which appears to be almost completely PTOX dependent, is faster in the *abc1k3* mutants, while severely impaired in *pgr6*. A limitation of total PQ, as in *sps2* mutant, results in a slower oxidation in the dark as well. The PQ oxidation in the double mutant *pgr6/abc1k3* progress more rapidly than in the single *pgr6* mutant (Fig.

4.6a). The dark re-oxidation of the photoactive PQ pool is independent on the activity of the ETC, in fact, all the tested mutant lines display the same kinetics when the PQ is oxidised activating the PSI with far red light (Fig. 4.6b). After 3h under high light, the dark re-oxidation of the photoactive PQ in the *pgr6* mutant is almost completely blocked, and it is overall slower in all the lines analysed. Once again, the defect is milder in the double *pgr6/abc1k3* mutant (Supplementary figure 4.2). It is worth noting that after 3h of high light also the oxidation kinetics with far red light are affected in *pgr6*, suggesting that 3h of high light exposure induce a perturbation of the ETC, consistently with the previous report[73].

This experiment shows that *pgr6* is impaired in the regulation of the photoactive PQ redox state independently of the activity of the ETC. Considering the specific localization of PTOX this supports the model of a limitation of the mobility of the PQ. Interestingly, said defect is partially complemented by *abc1k3* mutation.

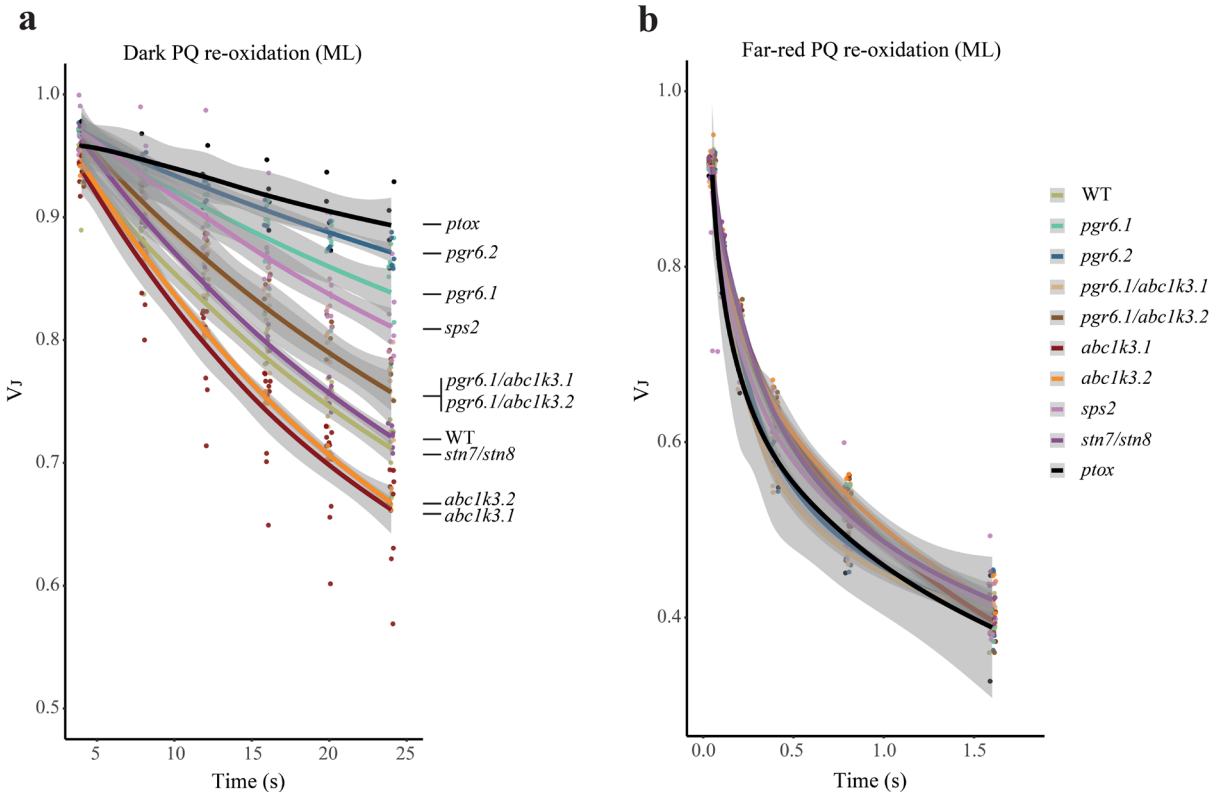

Figure 4.6. Mutations of PGR6 and ABC1K3 influence the dark re-oxidation kinetic of the photoactive plastoquinone. The relative fluorescence after 3 ms (VJ) is plotted over the time from the previous saturating pulse. The sample was incubated in dark (a) or with far-red light (b). Kinetics of the reoxidation are shown by interpolation of the data points with a logarithmic curve with the deviation of the model in grey (R-Studio) for wild type (WT) *pgr6.1, -2, abc1k3.1, -2* and *pgr6/abc1k3.1, -2, sps2, stn7/stn8, ptox* plants grown under moderate light (ML). These measures were performed with Handy-PEA (Hansatech Instruments) on detached leaves incubated for 10 minutes in dark.

4.2.5 Major thylakoid membrane protein phosphorylation and state transitions are maintained in *pgr6/abc1k3.*

A smaller photoactive PQ pool (Fig. 4.5b) should be prone to over-reduction or at least to "mimic" a condition of over-reduction as fewer PQ molecules are available (Fig. 4.4b). This would be expected to perturb state transitions[15,16,18,19,73,82]. Cytochrome *b6f* activity is dependent on the redox state of PQ and regulates the activation of STN7, the principal kinase involved in LHCII phosphorylation. Therefore, we evaluated the phosphorylation status of the major thylakoid membrane proteins as a proxy for the PQ redox state by western blot, and measured the re-allocation of mobile light harvesting complex II (LHCII) between the two photosystems by quenching of the room temperature chlorophyll fluorescence in *pgr6/abc1k3* during a state 1 to state 2 transition induced by changes in the light spectrum.

Anti-phosphothreonine immunoblotting was carried out on total protein extracts from leaves collected under moderate light and after 3h high light exposure. Under moderate light, the thylakoid phosphoprotein pattern was similar among all lines (Fig. 4.7a). After 3h high light exposure PSII core proteins D1 (PsbA) and D2 (PsbD) in *pgr6* were only slightly phosphorylated, while their phosphorylation was much more clearly visible in wild type, *abc1k3* as well as in *pgr6/abc1k3*. Furthermore, the light harvesting complex II proteins remained phosphorylated in *abc1k3* and wild type but the phosphorylation was clearly lower in *pgr6*. In comparison to *pgr6*, LHCII phosphorylation in *pgr6/abc1k3* was preserved even after 3h high light exposure (Fig. 4.7a). This suggests that, despite a shortage of photoactive PQ (Fig. 4.7a), in *pgr6/abc1k3* the STN7 kinase maintains its activity towards the LHCII even after exposure to high light. Furthermore, neither the change in total PQ nor in the photoactive fraction had an impact on the photosynthetic protein accumulation after 3h of high light (Fig. 4.7a).

To determine whether the restored phosphorylation observed in *pgr6/abc1k3* correlates with the ability to perform state transitions we followed and measured room temperature chlorophyll *a* fluorescence kinetics on dark-adapted plants by switching red light supplemented with far-red light (State 1) to red light only (State 2). The quenching (fluorescence decline) caused by state transitions (qT), was calculated as the difference between the maximal fluorescence (F_M) after "State 1" illumination (F_M_L1) and the one after "State 2" light (F_M_L2) normalized on maximal fluorescence (F_M) (qT = (F_M_L1 – F_M_L2)/ F_M), reflects the dissociation of antenna from PSII and its association to PSI.

Under moderate light, the qT in all genotypes was comparable to the wild type, indicating their ability to perform transition from State 1 to State 2 and only *pgr6* lines appeared to be slightly impaired (Fig.

4.7b). *stn7/stn8*, which is completely unable to perform state transitions, was used as a negative control (giving a negative qT value). After 3h high light exposure, *abc1k3* (qT: 2.4±1.4; 2.3±1.0) and WT (qT: 3.0±1.2) maintained their capacity for state transitions, while *pgr6* lines were defective in state transitions (qT: –2.1±2.4; –3.1±1.9). Interestingly, after 3h of high light, state transitions in *pgr6/abc1k3* lines exhibited a level of quenching (qT: 3.0±1.6; 1.7±2.6) comparable to WT and *abc1k3* (Fig. 4.7b). This shows that the phosphorylation and thus the activity of the STN7 kinase, which is maintained in *pgr6/abc1k3* mutants, allows to accomplish state transitions after high light.

a

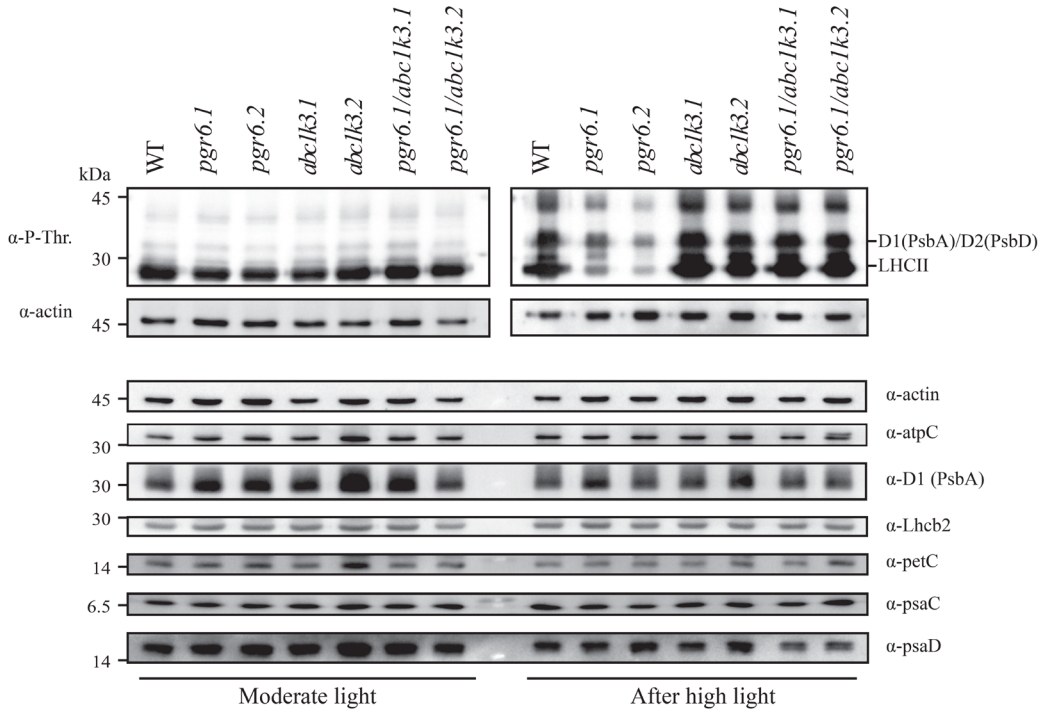

b

	State transition quenching (qT)							
	WT	***pgr6.1***	***pgr6.2***	***abc1k3.1***	***abc1k3.2***	***pgr6.1/abc1k3.1***	***pgr6.1/abc1k3.2***	***stn7/stn8***
ML	6,1 ± 1,2 [a]	3,8 ± 1,7 [b]	3,2 ± 2,4 [b]	6,1 ± 1,0 [a]	5,9 ± 1,3 [a]	6,0 ± 1,0 [a]	5,7 ± 0.9 [a]	**-3,8 ± 1,7** [c]
HL 3h	3,0 ± 1,2 [b]	**-2,1 ± 2,4** [c]	**-3,1 ± 1,9** [c]	2,4 ± 1,4 [b]	2,3 ± 1,0 [b]	3.0 ± 1.6 [a,b]	1.7 ± 2.6 [a,b,c]	**-11,0 ± 0,5** [d]

Figure 4.7. Double mutant maintains thylakoid protein phosphorylation and state transitions after high light. (a) Total protein extracts of wild type (WT), *pgr6.1, -2, abc1k3.1, -2* and *pgr6/abc1k3.1, -2* light-exposed leaves were separated by SDS-PAGE, transferred on nitrocellulose membrane and decorated with anti-phosphothreonine antibody. The main thylakoid phospho-proteins are indicated on the right according to their size. Core photosystem II proteins D1 (PsbA) and D2 (PsbD) are indicated together due their poor resolution. The accumulation of the principal photosynthetic complexes was assessed using antibodies against specific subunits of each complex: anti-Lhcb2 for the major LHCII, anti-D1 (PsbA) for PSII, anti-PetC for cytochrome *b6f*, anti-PsaD and anti-PsaC for PSI, and anti-AtpC for ATP synthase. Actin signal is shown as a loading control. **(b)** Fluorescence quenching related to the state transitions (qT) of wild type (WT), *pgr6.1, -2, abc1k3.1, -2* and *pgr6/abc1k3.1, -2* under moderate light (120 µmol m^{-2} s^{-1}) (ML) and after 3h of high light (500 µmol m^{-2} s^{-1}) (HL). qT was calculated from the maximal chlorophyll fluorescence measured after 10 minutes exposure to red light (660 nm) supplemented with far-red illumination (720 nm) "State 1" (FMST1) or to pure red light "State 2" (FMST2). Quenching related to state transition was calculated as qT = (FMST1 – FMST2) / FM. Each value represents the average of a pot containing 2-3 plants. Superscript letters are used to indicate statistically different groups ($p<0.05$) by paired Student's t-test.

4.3 Discussion

The photosynthetic apparatus has to adapt to photo-oxidative stress induced by excess light in order to prevent thylakoid membrane damage and maintain photosynthetic efficiency. Photo-protective strategies comprise adjustment of electron transport capacity (ETC)[83], equilibration of energy between photosystems (state transitions)[12] and induction of non-photochemical quenching (NPQ)[23,84]. All three mechanisms are directly or indirectly related to the activity of the plastoquinone as an electron carrier. Recently, it has been demonstrated that PGR6 is implicated in photosynthesis regulation by homeostasis of photoactive PQ under high light[73]. In this study, we describe the involvement of ABC1K3[46,61,71], a close homologue of PGR6, in this process.

We tested two *abc1k3* mutant lines for their ability to induce NPQ under increasing light intensities: contrary to *pgr6,* this mutation did not cause any perturbation in NPQ induction when compared with the wild type (Fig. 4.2). To address the role of *abc1k3* in the photosynthetic regulation we crossed this mutant with *pgr6* to obtain *pgr6/abc1k3* double mutant plants (Fig. 4.1). Intriguingly, the *abc1k3* mutation was capable to alleviate the NPQ defect observed in *pgr6*; while the NPQ level in *pgr6/abc1k3* was higher than in the single *pgr6* mutant, it remained lower than in the wild type (Fig. 4.2).

In order to confirm that the NPQ perturbation is derived from a lack of transport through the ETC we measured the number of electrons transported per PSI after a saturating light pulse by analysing the lag time of PSI oxidation. As expected from previous reports[39,69,73], *pgr6* transfers less electrons to PSI, and the difference compared to the wild type increases after exposure to 3h high light. On the contrary, *abc1k3* was not impaired and even appeared capable of increased electron transfer after 3h of high light when compared to the wild type (Fig. 4.3). In *pgr6/abc1k3*, the electron transport capacity was still lower than the wild type, however, more electrons were transferred per PSI compared to *pgr6* and the decrease after 3h of high light was comparable to the one observed in the wild type (Fig. 4.3). Suggesting that in *pgr6/abc1k3* the electron transport phenotype of *pgr6* was partially complemented presumably by maintaining the electron donors in the ETC. In a previous report the limitation of the electron transport capacity observed in *pgr6* was linked to a depletion of the photoactive PQ pool[73]. However, the decrease in the number of electrons transported to PSI appeared to be more severe than the measured decrease in the size of the photoactive pool. Therefore, it was hypothesized that the PQ mobility plays an additional role in limiting the electron transport capacity. To investigate this hypothesis the energy fluxes along the ETC were analysed by rapid fluorescence induction curves. The estimation of the number of electrons present in the ETC before saturation, expressed as the Area/Fv (Fig. 4.4a), was consistent with the P_{700} oxidation analysis (Fig. 4.3). In fact, the area was smaller in the *pgr6* mutant and bigger in *abc1k3*, in the latter it was even bigger than in wild type, consistent with

pgr6 having limited electron transport and *abc1k3* being even more efficient than wild type. Interestingly, *pgr6/abc1k3* had a value in between those of the two mutants, suggesting once again, a partial recover of photosynthetic efficiency. Upon exposure to high light only *pgr6* worsened while all the other lines had a tendency to increase the area value indicating a better, or at least unchanged, electron transport capacity (Fig. 4.4a). By analysing the induction curve's principal steps, we can obtain hints regarding the different components that may be affected in the ETC. The first step, at 3 ms from the start of the saturating flash, was reported to be dependent of the Q_B redox state at the PSII and therefore linked to the redox state of the photoactive PQ pool which is also affected by the size of the photoactive PQ pool[73]. From the fluorescence value at 3 ms (F_J) it is therefore possible to calculate the ΦET2o, the efficiency of the electron transport between Q_A and Q_B (which depends on the status of the photoactive PQ pool)[75-77]. We observed that this efficiency is lower both in *pgr6* and in *pgr6/abc1k3*, suggesting a similar defect in the photoactive PQ pool. The defect appears to be somewhat milder in the double mutant compared to *pgr6* (Fig. 4.4b). The second step in the fluorescence rise is at 30 ms (F_I), and the level of the fluorescence recorded as this step was linked with the electron transport up to the PSI final acceptors in the OJIP model[75-77], from this value it is also possible to calculate the electron transport efficiency, defined as ΦRE1o. Comparison of this efficiency revealed that *pgr6* has a lower efficiency but that is not the case for *pgr6/abc1k3*. In the latter the ΦRE1o was the same as in the wild type, and was less affected upon the exposure to 3h high light compared to the *pgr6* (Fig. 4.4c). Simple mutation of *abc1k3* did not create any measurable defect in electron transport; on the contrary, the efficiency of the transport to PSI acceptors appeared to be even higher than in the wild type, both under normal light and after exposure to high light (Fig. 4.4c). This would suggest that mutation of the *ABC1K3* gene leads to an increased efficiency in the electron mobility between PSII and PSI.

To support the fluorescence induction results, we biochemically measured the size of the photoactive pool in the mutants exposed to moderate light and to high light. Consistent with the biophysical observations, the photoactive PQ pool was smaller in both *pgr6* and *pgr6/abc1k3* (Fig. 4.5b). Exposure to 3h high light had a limited effect on the size of the photoactive PQ pool in wild type (Fig. 4.5a). while we detected a slight depletion of the photoactive PQ pool in *pgr6* that was previously reported [73], however a similar depletion was observed in *abc1k3* even though the relative photoactive PQ pool size was still larger than in *pgr6* (Fig. 4.5a, 4.5b). On the contrary, the double mutant *pgr6/abc1k3* has constitutively a small photoactive PQ pool that is not further depleted by the exposure to high light. This leads to the conclusion that the photoactive PQ pool size *per se* has a limited influence on photosynthetic efficiency, and that the photosynthetic defect becomes symptomatic only when PQ limitation is associated with an additional impairment in its mobility (Fig. 4.6a).

After 3h of high light we observed a decrease in the amount of the total PQ in *abc1k3*. This may be explained by an impairment between degradation/consumption and PQ synthesis. This can be an indirect effect of the increased photosynthetic electron transport observed in *abc1k3* compared to WT or caused by a lack of a signal promoting the PQ synthesis. If the latter is the case, it would create a link between the ETC and PQ biosynthesis, which would be important to ensure the photosynthetic electron transport under changing environmental conditions. It is necessary to point out that this condition is transitory and that, if the light intensity is permissive, this mutant is capable of restoring PQ levels as it has been shown in *abc1k3* plants analysed after several days of exposure to 500 µmol m^{-2} s^{-1} [61].

Another feature linked to the *pgr6* mutation was the loss of thylakoid protein phosphorylation. These phosphorylation events are mostly dependent on the STN7 and STN8 kinases the activity of which depends on the redox status of the PQ pool[20,85-87]. Interestingly the mutation of *abc1k3* in the *pgr6* background was sufficient to re-establish the phosphorylation of the thylakoid proteins. This observation has an interesting implication in understanding the factors regulating the redox state of the photoactive PQ pool. In fact, the PQ pool redox state appears to be dependent also on the exchanges between the photoactive pool and storage (*i.e.* PQ mobility) and not only on the size of the photoactive pool and the activity of the ETC. We cannot exclude that protein phosphorylation has a positive feedback loop effect; in fact, the phosphorylation of the thylakoid proteins may favour their mobility in the membrane and by doing so increase also the mobility of the PQ[5,6,88]. We also cannot exclude the involvement of the phosphorylation of others, less evident targets, such as CURT1, the phosphorylation of which is also dependent on STN kinases. This set of protein may change the conformation of the thylakoid membrane and, by this, also the mobility and exchange of the PQ, and other lipids, between the photoactive pool and the reservoir[89]. Moreover, PGR6 and ABC1K3 are also predicted to function as kinases; therefore, they may phosphorylate yet unknown target proteins leading to the regulation of the photosynthetic activity and potentially influencing membrane fluidity and/or thylakoid protein organisation[90].

The results lead us to propose the following model for the action of PGR6 and ABC1K3, being two kinases located at the plastoglobule[39,54,55,61]. The role of PGR6 would be to promote the release, or the exchange of the PQ between the storage and the photoactive pool, while ABC1K3 would act in limiting such a diffusion blocking all the PQ fluxes between the different pools. This model would explain the slightly bigger size of the photoactive pool in *abc1k3* and also the difference between *pgr6* and *pgr6/abc1k3* the latter having a better photosynthetic performance since is missing the ABC1K3 protein that would otherwise act as a "brake" to the PQ exchanges between the pool. To fully explain the observed results, we also have to assume that, without the activity of PGR6, the PQ tends to over-

accumulate in the non-photoactive pool thus leading to a depletion of the photoactive pool. In this regard, the role of PGR6 is crucial to maintaining the photosynthetic efficiency by promoting the movement and accumulation of the PQ against its "passive" distribution. In contrast ABC1K3, acting as a brake to said mobilisation, may have a more important role in other processes and phases of plant development when lipids need to be efficiently accumulated in the reserve compartments (*e.g.* senescence, fruit maturation). It has to be underlined that the condition of the double mutant *pgr6/abc1k3* is still not optimal and that the absence of ABC1K3 alleviates the photosynthetic phenotype without fully complementing it, it is therefore not surprising that a double mutant, lacking both kinases will display a phenotype under prolonged stress conditions[46].

In conclusion, we show that *abc1k3* mutation allows a partial recovery of the *pgr6* phenotype. Consequently, PGR6 and ABC1K3 act in an opposite manner in order to cope with short-term high light. Therefore, we suggest that the system of the atypical kinases PGR6 and ABC1K3 allows a dynamic regulation of the PQ pool mobility and availability, creating a double regulation, which is fundamental for the plant to cope with variations in environmental conditions and potentially to allow the plastids' plasticity that is essential for the different developmental stages of the plant life.

References

1 Block, A., Fristedt, R., Rogers, S., Kumar, J., Barnes, B., Barnes, J., Elowsky, C. G., Wamboldt, Y., Mackenzie, S. A., Redding, K., Merchant, S. S. & Basset, G. J. Functional modeling identifies paralogous solanesyl-diphosphate synthases that assemble the side chain of plastoquinone-9 in plastids. *J Biol Chem* **288**, 27594-27606 (2013).

2 Kruk, J. & Karpinski, S. An HPLC-based method of estimation of the total redox state of plastoquinone in chloroplasts, the size of the photochemically active plastoquinone-pool and its redox state in thylakoids of *Arabidopsis*. *Biochim Biophys Acta* **1757**, 1669-1675 (2006).

3 Ksas, B., Legeret, B., Ferretti, U., Chevalier, A., Pospisil, P., Alric, J. & Havaux, M. The plastoquinone pool outside the thylakoid membrane serves in plant photoprotection as a reservoir of singlet oxygen scavengers. *Plant Cell Environ* **41**, 2277-2287 (2018).

4 Blackwell, M., Gibas, C., Gygax, S., Roman, D. & Wagner, B. The plastoquinone diffusion coefficient in chloroplasts and its mechanistic implications. *Biochim Biophys Acta Bioenerg* **1183**, 533-543 (1994).

5 Kirchhoff, H., Horstmann, S. & Weis, E. Control of the photosynthetic electron transport by PQ diffusion microdomains in thylakoids of higher plants. *Biochim Biophys Acta Bioenerg* **1459**, 148-168 (2000).

6 Kirchhoff, H. Diffusion of molecules and macromolecules in thylakoid membranes. *Biochim Biophys Acta Bioenerg* **1837**, 495-502 (2014).

7 Lavergne, J. & Joliot, P. Restricted diffusion in photosynthetic membranes. *Trends Biochem Sci* **16**, 129-134 (1991).

8 Karpinski, S., Reynolds, H., Karpinska, B., Wingsle, G., Creissen, G. & Mullineaux, P. Systemic signaling and acclimation in response to excess excitation energy in *Arabidopsis*. *Science* **284**, 654-657 (1999).

9 Li, Z., Wakao, S., Fischer, B. B. & Niyogi, K. K. Sensing and responding to excess light. *Annu Rev Plant Biol* **60**, 239-260 (2009).

10 Suzuki, N., Koussevitzky, S., Mittler, R. & Miller, G. ROS and redox signalling in the response of plants to abiotic stress. *Plant Cell Environ* **35**, 259-270 (2012).

11 Allen, J. F., Bennett, J., Steinback, K. E. & Arntzen, C. J. Chloroplast protein phosphorylation couples plastoquinone redox state to distribution of excitation energy between photosystems. *Nature* **291**, 25-29 (1981).

12 Rochaix, J. D. Role of thylakoid protein kinases in photosynthetic acclimation. *FEBS Lett* **581**, 2768-2775 (2007).

13 Rochaix, J. D. Redox regulation of thylakoid protein kinases and photosynthetic gene expression. *Antioxid Redox Signal* **18**, 2184-2201 (2013).

14 Dumas, L., Zito, F., Blangy, S., Auroy, P., Johnson, X., Peltier, G. & Alric, J. A stromal region of cytochrome *b6f* subunit IV is involved in the activation of the Stt7 kinase in *Chlamydomonas*. *Proc Natl Acad Sci U S A* **114**, 12063-12068 (2017).

15 Shapiguzov, A., Chai, X., Fucile, G., Longoni, P., Zhang, L. & Rochaix, J. D. Activation of the Stt7/STN7 kinase through dynamic interactions with the cytochrome *b6f* complex. *Plant Physiol* **171**, 82-92 (2016).

16 Bellafiore, S., Barneche, F., Peltier, G. & Rochaix, J. D. State transitions and light adaptation require chloroplast thylakoid protein kinase STN7. *Nature* **433**, 892-895 (2005).

17 Pesaresi, P., Pribil, M., Wunder, T. & Leister, D. Dynamics of reversible protein phosphorylation in thylakoids of flowering plants: the roles of STN7, STN8 and TAP38. *Biochim Biophys Acta* **1807**, 887-896 (2011).

18 Shapiguzov, A., Ingelsson, B., Samol, I., Andres, C., Kessler, F., Rochaix, J. D., Vener, A. V. & Goldschmidt-Clermont, M. The PPH1 phosphatase is specifically involved in LHCII dephosphorylation and state transitions in *Arabidopsis*. *Proc Natl Acad Sci U S A* **107**, 4782-4787 (2010).

19 Trotta, A., Suorsa, M., Rantala, M., Lundin, B. & Aro, E. M. Serine and threonine residues of plant STN7 kinase are differentially phosphorylated upon changing light conditions and specifically influence the activity and stability of the kinase. *Plant J* **87**, 484-494, (2016).

20 Pesaresi, P., Hertle, A., Pribil, M., Schneider, A., Kleine, T. & Leister, D. Optimizing photosynthesis under fluctuating light. *Plant Signal Behav* **5**, 21-25 (2010).

21 Dall'Osto, L., Caffarri, S. & Bassi, R. A mechanism of nonphotochemical energy dissipation, independent from PsbS, revealed by a conformational change in the antenna protein CP26. *Plant Cell* **17**, 1217-1232 (2005).

22 Nilkens, M., Kress, E., Lambrev, P., Miloslavina, Y., Müller, M., Holzwarth, A. R. & Jahns, P. Identification of a slowly inducible zeaxanthin-dependent component of non-photochemical quenching of chlorophyll fluorescence generated under steady-state conditions in *Arabidopsis*. *Biochim Biophys Acta Bioenerg* **1797**, 466-475 (2010).

23 Ruban, A. V. Nonphotochemical chlorophyll fluorescence quenching: mechanism and effectiveness in protecting plants from photodamage. *Plant Physiol* **170**, 1903-1916 (2016).

24 Ruban, A. V. Light harvesting control in plants. *FEBS Lett* **592**, 3030-3039 (2018).

25 Sylak-Glassman, E. J., Malnoe, A., De Re, E., Brooks, M. D., Fischer, A. L., Niyogi, K. K. & Fleming, G. R. Distinct roles of the photosystem II protein PsbS and zeaxanthin in the regulation of light

harvesting in plants revealed by fluorescence lifetime snapshots. *Proc Natl Acad Sci U S A* **111**, 17498-17503 (2014).

26 Joliot, P. & Finazzi, G. Proton equilibration in the chloroplast modulates multiphasic kinetics of nonphotochemical quenching of fluorescence in plants. *Proc Natl Acad Sci U S A* **107**, 12728-12733 (2010).

27 Aro, E. M., Virgin, I. & Andersson, B. Photoinhibition of photosystem II. Inactivation, protein damage and turnover. *Biochim Biophys Acta* **1143**, 113-134 (1993).

28 Bonardi, V., Pesaresi, P., Becker, T., Schleiff, E., Wagner, R., Pfannschmidt, T., Jahns, P. & Leister, D. Photosystem II core phosphorylation and photosynthetic acclimation require two different protein kinases. *Nature* **437**, 1179-1182 (2005).

29 Li, L., Aro, E. M. & Millar, A. H. Mechanisms of photodamage and protein turnover in photoinhibition. *Trends Plant Sci* **23**, 667-676 (2018).

30 Theis, J. & Schroda, M. Revisiting the photosystem II repair cycle. *Plant Signal Behav* **11**, e1218587 (2016).

31 Tikkanen, M., Nurmi, M., Kangasjarvi, S. & Aro, E. M. Core protein phosphorylation facilitates the repair of photodamaged photosystem II at high light. *Biochim Biophys Acta* **1777**, 1432-1437 (2008).

32 Pfannschmidt, T. Chloroplast redox signals: how photosynthesis controls its own genes. *Trends Plant Sci* **8**, 33-41 (2003).

33 Pfannschmidt, T., Nilsson, A. & Allen, J. F. Photosynthetic control of chloroplast gene expression. *Nature* **397**, 625 (1999).

34 Moejes, F. W., Matuszynska, A., Adhikari, K., Bassi, R., Cariti, F., Cogne, G., Dikaios, I., Falciatore, A., Finazzi, G., Flori, S., Goldschmidt-Clermont, M., Magni, S., Maguire, J., Le Monnier, A., Muller, K., Poolman, M., Singh, D., Spelberg, S., Stella, G. R., Succurro, A., Taddei, L., Urbain, B., Villanova, V., Zabke, C. & Ebenhoh, O. A systems-wide understanding of photosynthetic acclimation in algae and higher plants. *J Exp Bot* **68**, 2667-2681 (2017).

35 Ferretti, U., Ciura, J., Ksas, B., Rac, M., Sedlarova, M., Kruk, J., Havaux, M. & Pospisil, P. Chemical quenching of singlet oxygen by plastoquinols and their oxidation products in *Arabidopsis*. *Plant J* **95**, 848-861(2018).

36 Gruszka, J., Pawlak, A. & Kruk, J. Tocochromanols, plastoquinol, and other biological prenyllipids as singlet oxygen quenchers-determination of singlet oxygen quenching rate constants and oxidation products. *Free Radic Biol Med* **45**, 920-928 (2008).

37 Kanwischer, M., Porfirova, S., Bergmüller, E. & Dörmann, P. Alterations in tocopherol cyclase activity in transgenic and mutant plants of *Arabidopsis* affect tocopherol content, tocopherol composition, and oxidative stress. *Plant Physiol* **137**, 713-723 (2005).

38 Ksas, B., Becuwe, N., Chevalier, A. & Havaux, M. Plant tolerance to excess light energy and photooxidative damage relies on plastoquinone biosynthesis. *Sci Rep* **5**, 10919 (2015).

39 Martinis, J., Glauser, G., Valimareanu, S., Stettler, M., Zeeman, S. C., Yamamoto, H., Shikanai, T. & Kessler, F. ABC1K1/PGR6 kinase: a regulatory link between photosynthetic activity and chloroplast metabolism. *Plant J* **77**, 269-283 (2014).

40 Munné-Bosch, S. & Alegre, L. Plant aging increases oxidative stress in chloroplasts. *Planta* **214**, 608-615 (2002).

41 Nowicka, B. & Kruk, J. Plastoquinol is more active than α-tocopherol in singlet oxygen scavenging during high light stress of *Chlamydomonas reinhardtii*. *Biochim Biophys Acta* **1817**, 389-394 (2012).

42 Austin, J. R., 2nd, Frost, E., Vidi, P. A., Kessler, F. & Staehelin, L. A. Plastoglobules are lipoprotein subcompartments of the chloroplast that are permanently coupled to thylakoid membranes and contain biosynthetic enzymes. *Plant Cell* **18**, 1693-1703 (2006).

43 Gaude, N., Bréhélin, C., Tischendorf, G., Kessler, F. & Dormann, P. Nitrogen deficiency in *Arabidopsis* affects galactolipid composition and gene expression and results in accumulation of fatty acid phytyl esters. *Plant J* **49**, 729-739 (2007).

44 Lichtenthaler, H. K. & Peveling, E. Plastoglobuli in different types of plastids from *Allium cepa* L. *Planta* **72**, 1-13 (1966).

45 Lippold, F., vom Dorp, K., Abraham, M., Holzl, G., Wewer, V., Yilmaz, J. L., Lager, I., Montandon, C., Besagni, C., Kessler, F., Stymne, S. & Dormann, P. Fatty acid phytyl ester synthesis in chloroplasts of *Arabidopsis*. *Plant Cell* **24**, 2001-2014 (2012).

46 Lundquist, P. K., Poliakov, A., Giacomelli, L., Friso, G., Appel, M., McQuinn, R. P., Krasnoff, S. B., Rowland, E., Ponnala, L., Sun, Q. & van Wijk, K. J. Loss of plastoglobule kinases ABC1K1 and ABC1K3 causes conditional degreening, modified prenyl-lipids, and recruitment of the jasmonic acid pathway. *Plant Cell* **25**, 1818-1839 (2013).

47 Rottet, S., Devillers, J., Glauser, G., Douet, V., Besagni, C. & Kessler, F. Identification of plastoglobules as a site of carotenoid cleavage. *Front Plant Sci* **7**, 1855 (2016).

48 Steinmuller, D. & Tevini, M. Composition and function of plastoglobuli 1. Isolation and purification from chloroplasts and chromoplasts. *Planta* **163**, 201-207 (1985).

49 van Wijk, K. J. & Kessler, F. Plastoglobuli: Plastid Microcompartments with integrated functions in metabolism, plastid developmental transitions, and environmental adaptation. *Annu Rev Plant Biol* **68**, 253-289 (2017).

50 Zbierzak, A. M., Kanwischer, M., Wille, C., Vidi, P. A., Giavalisco, P., Lohmann, A., Briesen, I., Porfirova, S., Brehelin, C., Kessler, F. & Dormann, P. Intersection of the tocopherol and plastoquinol metabolic pathways at the plastoglobule. *Biochem J* **425**, 389-399 (2010).

51 Hall, J. D., Barr, R., Al-Abbas, A. H. & Crane, F. L. The ultrastructure of chloroplasts in mineral-deficient maize leaves. *Plant Physiol* **50**, 404-409 (1972).

52 Taylor, A. O. & Craig, A. S. Plants under climatic stress: II. Low temperature, high light effects on chloroplast ultrastructure. *Plant Physiol* **47**, 719-725 (1971).

53 Zechmann, B. Ultrastructure of plastids serves as reliable abiotic and biotic stress marker. *PLoS One* **14**, e0214811 (2019).

54 Lundquist, P. K., Poliakov, A., Bhuiyan, N. H., Zybailov, B., Sun, Q. & van Wijk, K. J. The functional network of the *Arabidopsis* plastoglobule proteome based on quantitative proteomics and genome-wide coexpression analysis. *Plant Physiol* **158**, 1172-1192 (2012).

55 Vidi, P. A., Kanwischer, M., Baginsky, S., Austin, J. R., Csucs, G., Dormann, P., Kessler, F. & Brehelin, C. Tocopherol cyclase (VTE1) localization and vitamin E accumulation in chloroplast plastoglobule lipoprotein particles. *J Biol Chem* **281**, 11225-11234 (2006).

56 Ytterberg, A. J., Peltier, J. B. & van Wijk, K. J. Protein profiling of plastoglobules in chloroplasts and chromoplasts. A surprising site for differential accumulation of metabolic enzymes. *Plant Physiol* **140**, 984-997 (2006).

57 Singh, D. K., Maximova, S. N., Jensen, P. J., Lehman, B. L., Ngugi, H. K. & McNellis, T. W. *FIBRILLIN4* is required for plastoglobule development and stress resistance in apple and *Arabidopsis*. *Plant Physiol* **154**, 1281-1293 (2010).

58 Singh, D. K., Laremore, T. N., Smith, P. B., Maximova, S. N. & McNellis, T. W. Knockdown of *FIBRILLIN4* gene expression in apple decreases plastoglobule plastoquinone content. *PLoS One* **7**, e47547 (2012).

59 Eugeni Piller, L., Abraham, M., Dormann, P., Kessler, F. & Besagni, C. Plastid lipid droplets at the crossroads of prenylquinone metabolism. *J Exp Bot* **63**, 1609-1618 (2012).

60 Eugeni Piller, L., Besagni, C., Ksas, B., Rumeau, D., Brehelin, C., Glauser, G., Kessler, F. & Havaux, M. Chloroplast lipid droplet type II NAD(P)H quinone oxidoreductase is essential for prenylquinone metabolism and vitamin K_1 accumulation. *Proc Natl Acad Sci U S A* **108**, 14354-14359 (2011).

61 Martinis, J., Glauser, G., Valimareanu, S. & Kessler, F. A chloroplast ABC1-like kinase regulates vitamin E metabolism in *Arabidopsis*. *Plant Physiol* **162**, 652-662 (2013).

62 Fatihi, A., Latimer, S., Schmollinger, S., Block, A., Dussault, P. H., Vermaas, W. F. J., Merchant, S. S. & Basset, G. J. A dedicated type II NADPH dehydrogenase performs the penultimate step in the biosynthesis of vitamin K_1 in *Synechocystis* and *Arabidopsis*. *Plant Cell* **27**, 1730-1741 (2015).

63 Eugeni-Piller, L., Glauser, G., Kessler, F. & Besagni, C. Role of plastoglobules in metabolite repair in the tocopherol redox cycle. *Front Plant Sci* **5**, 298 (2014).

64 Lohscheider, J. N. & Rio Bartulos, C. Plastoglobules in algae: A comprehensive comparative study of the presence of major structural and functional components in complex plastids. *Mar Genomics* **28**, 127-136 (2016).

65 Bousquet, I., Dujardin, G. & Slonimski, P. P. *ABC1*, a novel yeast nuclear gene has a dual function in mitochondria: it suppresses a cytochrome *b* mRNA translation defect and is essential for the electron transfer in the *bc1* complex. *EMBO J* **10**, 2023-2031 (1991).

66 Brasseur, G., Tron, P., Dujardin, G., Slonimski, P. P. & Brivet-Chevillotte, P. The nuclear *ABC1* gene is essential for the correct conformation and functioning of the cytochrome *bc1* complex and the neighbouring complexes II and IV in the mitochondrial respiratory chain. *Eur J Biochem* **246**, 103-111 (1997).

67 Mollet, J., Delahodde, A., Serre, V., Chretien, D., Schlemmer, D., Lombes, A., Boddaert, N., Desguerre, I., de Lonlay, P., de Baulny, H. O., Munnich, A. & Rotig, A. *CABC1* gene mutations cause ubiquinone deficiency with cerebellar ataxia and seizures. *Am J Hum Genet* **82**, 623-630 (2008).

68 Poon, W. W., Davis, D. E., Ha, H. T., Jonassen, T., Rather, P. N. & Clarke, C. F. Identification of *Escherichia coli ubiB*, a gene required for the first monooxygenase step in ubiquinone biosynthesis. *J Bacteriol* **182**, 5139-5146 (2000).

69 Shikanai, T., Munekage, Y., Shimizu, K., Endo, T. & Hashimoto, T. Identification and characterization of *Arabidopsis* mutants with reduced quenching of chlorophyll fluorescence. *Plant Cell Physiol* **40**, 1134-1142 (1999).

70 Yamori, W. & Shikanai, T. Physiological Functions of cyclic electron transport around photosystem I in sustaining photosynthesis and plant growth. *Annu Rev Plant Biol* **67**, 81-106 (2016).

71 Huang, H., Yang, M., Su, Y., Qu, L. & Deng, X. W. *Arabidopsis* atypical kinases ABC1K1 and ABC1K3 act oppositely to cope with photodamage under red light. *Mol Plant* **8**, 1122-1124 (2015).

72 Yang, M., Huang, H., Zhang, C., Wang, Z., Su, Y., Zhu, P., Guo, Y. & Deng, X. W. *Arabidopsis* atypical kinase ABC1K1 is involved in red light-mediated development. *Plant Cell Rep* **35**, 1213-1220 (2016).

73 Pralon, T., Shanmugabalaji, V., Longoni, P., Glauser, G., Ksas, B., Collombat, J., Desmeules, S., Havaux, M., Finazzi, G. & Kessler, F. Plastoquinone homoeostasis by *Arabidopsis* proton gradient regulation 6 is essential for photosynthetic efficiency. *Commun Biol* **2**, 220 (2019).

74 Joliot, P. & Joliot, A. Cyclic electron flow in C3 plants. *Biochim Biophys Acta* **1757**, 362-368 (2006).

75 Kalaji, H. M., Oukarroum, A., Alexandrov, V., Kouzmanova, M., Brestic, M., Zivcak, M., Samborska, I. A., Cetner, M. D., Allakhverdiev, S. I. & Goltsev, V. Identification of nutrient deficiency in maize and tomato plants by *in vivo* chlorophyll *a* fluorescence measurements. *Plant Physiol Biochem* **81**, 16-25 (2014).

76 Strasser, R. J., Tsimilli-Michael, M., Qiang, S. & Goltsev, V. Simultaneous *in vivo* recording of prompt and delayed fluorescence and 820-nm reflection changes during drying and after rehydration of the resurrection plant *Haberlea rhodopensis*. *Biochim Biophys Acta* **1797**, 1313-1326 (2010).

77 Kalaji, H. M., Schansker, G., Ladle, R. J., Goltsev, V., Bosa, K., Allakhverdiev, S. I., Brestic, M., Bussotti, F., Calatayud, A., Dąbrowski, P., Elsheery, N. I., Ferroni, L., Guidi, L., Hogewoning, S. W., Jajoo, A., Misra, A. N., Nebauer, S. G., Pancaldi, S., Penella, C., Poli, D., Pollastrini, M., Romanowska-Duda, Z. B., Rutkowska, B., Serôdio, J., Suresh, K., Szulc, W., Tambussi, E., Yanniccari, M. & Zivcak, M. Frequently asked questions about *in vivo* chlorophyll fluorescence: practical issues. *Photosynth Res* **122**, 121-158 (2014).

78 Lennon, A. M., Prommeenate, P. & Nixon, P. J. Location, expression and orientation of the putative chlororespiratory enzymes, Ndh and IMMUTANS, in higher-plant plastids. *Planta* **218**, 254-260 (2003).

79 Houyoux, P.-A., Ghysels, B., Lecler, R. & Franck, F. Interplay between non-photochemical plastoquinone reduction and re-oxidation in pre-illuminated *Chlamydomonas reinhardtii*: a chlorophyll fluorescence study. *Photosynth Res* **110**, 13 (2011).

80 Joet, T., Genty, B., Josse, E. M., Kuntz, M., Cournac, L. & Peltier, G. Involvement of a plastid terminal oxidase in plastoquinone oxidation as evidenced by expression of the *Arabidopsis thaliana* enzyme in tobacco. *J Biol Chem* **277**, 31623-31630 (2002).

81 Tóth, S. Z., Schansker, G. & Strasser, R. J. A non-invasive assay of the plastoquinone pool redox state based on the OJIP-transient. *Photosynth Res* **93**, 193 (2007).

82 Tikkanen, M., Gollan, P. J., Suorsa, M., Kangasjarvi, S. & Aro, E. M. STN7 operates in retrograde signaling through controlling redox balance in the electron transfer chain. *Front Plant Sci* **3**, 277 (2012).

83 Rochaix, J. D. Regulation of photosynthetic electron transport. *Biochim Biophys Acta* **1807**, 375-383 (2011).

84 Müller, P., Li, X. P. & Niyogi, K. K. Non-photochemical quenching. A response to excess light energy. *Plant Physiol* **125**, 1558-1566 (2001).

85 Puthiyaveetil, S. A mechanism for regulation of chloroplast LHC II kinase by plastoquinol and thioredoxin. *FEBS Lett* **585**, 1717-1721 (2011).

86 Puthiyaveetil, S., Ibrahim, I. M. & Allen, J. F. Oxidation-reduction signalling components in regulatory pathways of state transitions and photosystem stoichiometry adjustment in chloroplasts. *Plant Cell Environ* **35**, 347-359 (2012).

87 Aro, E. M. & Ohad, I. Redox regulation of thylakoid protein phosphorylation. *Antioxid Redox Signal* **5**, 55-67 (2003).

88 Fristedt, R., Willig, A., Granath, P., Crèvecoeur, M., Rochaix, J. D. & Vener, A. V. Phosphorylation of photosystem II controls functional macroscopic folding of photosynthetic membranes in *Arabidopsis*. *Plant Cell* **21**, 3950-3964 (2009).

89 Armbruster, U., Labs, M., Pribil, M., Viola, S., Xu, W., Scharfenberg, M., Hertle, A. P., Rojahn, U., Jensen, P. E., Rappaport, F., Joliot, P., Dormann, P., Wanner, G. & Leister, D. *Arabidopsis* CURVATURE THYLAKOID1 proteins modify thylakoid architecture by inducing membrane curvature. *Plant Cell* **25**, 2661-2678 (2013).

90 Yokoyama, R., Yamamoto, H., Kondo, M., Takeda, S., Ifuku, K., Fukao, Y., Kamei, Y., Nishimura, M. & Shikanai, T. Grana-localized proteins, RIQ1 and RIQ2, affect the organization of light-harvesting complex II and grana stacking in *Arabidopsis*. *Plant Cell* **28**, 2261-2275 (2016).

Supplementary figures

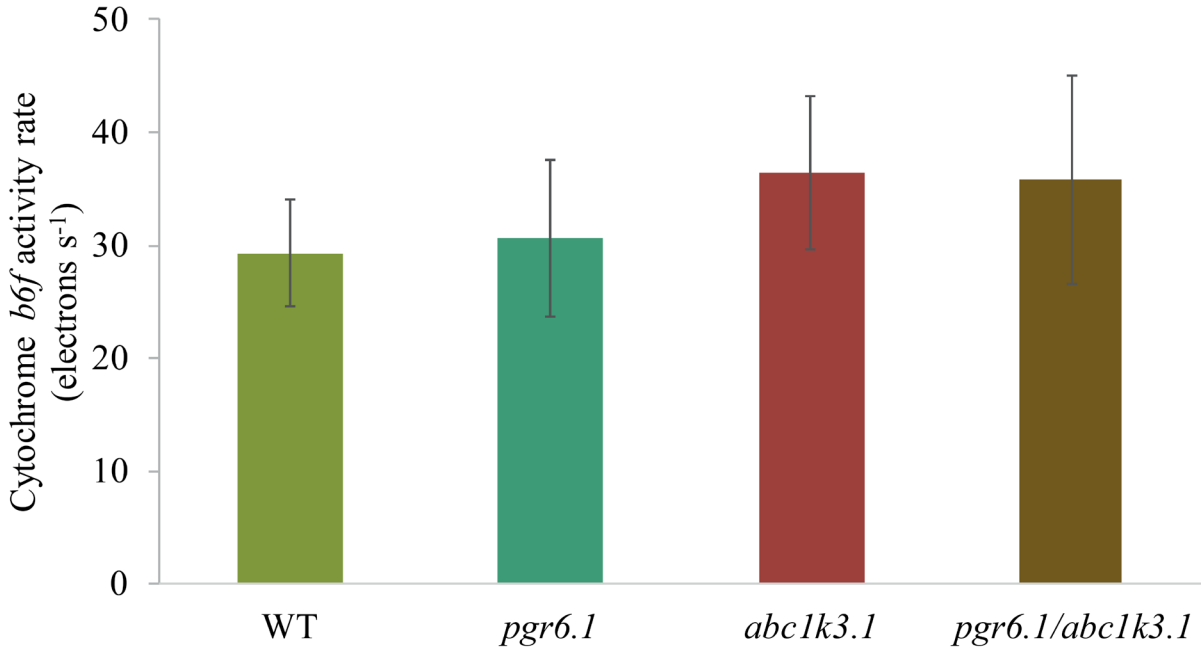

Supplementary figure 4.1. Cytochrome *b6f* activity rate is not affected by *pgr6* and/or *abc1k3* mutation. Turnover rate of cytochrome *b6f*, expressed as number of electrons per second, calculated from the kinetics of the cytochrome *f* oxidation after a saturating pulse fitted with an exponential curve. The kinetics were obtained from the changes in the cytochrome *f* absorption at 554 nm as described in Finazzi *et al.* (2002). The error bars show the standard deviation of the points (n=4).

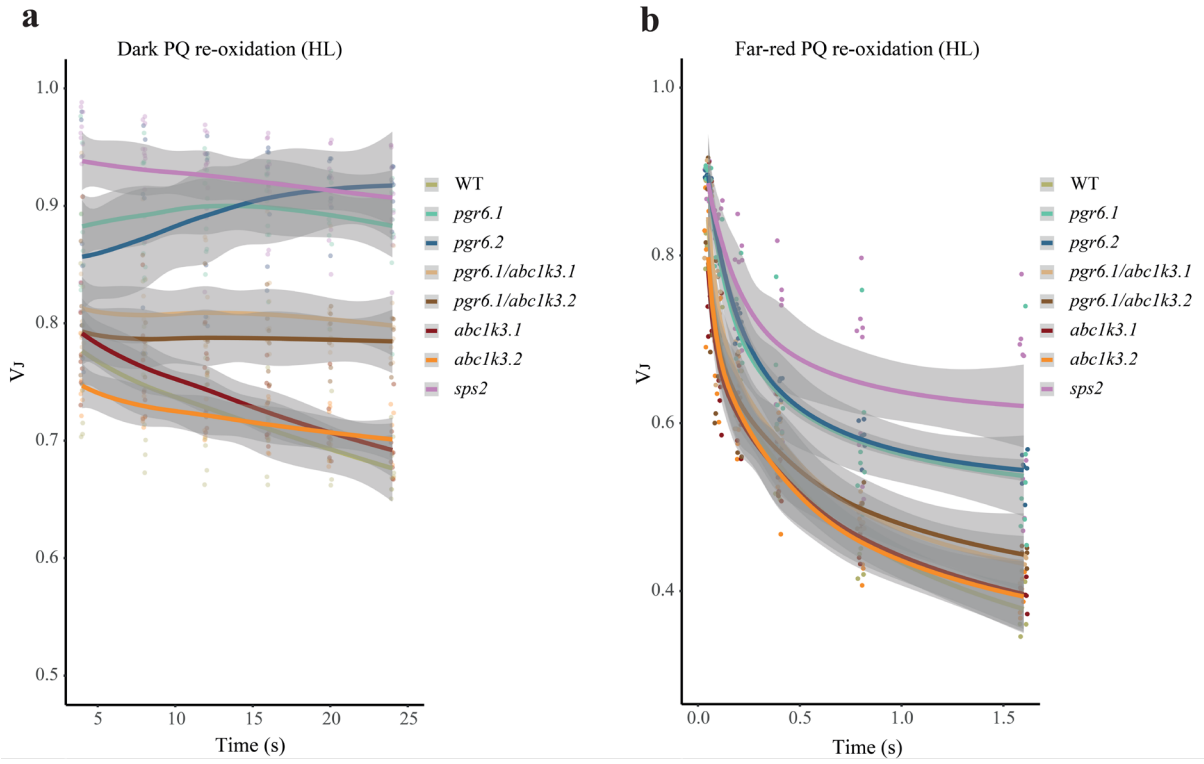

Supplementary figure 4.2. Enzymatic dark re-oxidation PQ after high light. Time course of fluorescence quenching kinetics during incubation in dark **(a)** or after exposure to increasing time with far-red **(b)** of wild type (WT) *pgr6.1, -2, abc1k3.1, -2* and *pgr6/abc1k3.1, -2, sps2, stn7/stn8, ptox* plants. Before leaf collection the plants were exposed for 3h under high light (500 µmol m^{-2} s^{-1}) (HL). The values of the V_J were plotted over the time after the previous saturating flash and interpolated with a logarithmic curve (R-Studio). The measures were performed with Handy-PEA (Hansatech Instruments).

Materials and Methods

Plants material and treatments

Arabidopsis thaliana wild type plant refers to var. Columbia-0 (Col-0). *pgr6-1* T-DNA insertion line (Salk_068628), *pgr6-2* T-DNA insertion line (Salk_130499C), *abc1k3-1* (Salk_128696) and *abc1k3-2* (Sail_918_E10) were purchased at Nottingham Arabidopsis Stock Centre (NASC, http://arabidopsis.info). Breeding crossing between *pgr6-1* and *abc1k3-1* or *abc1k3-2* mutants give rise to double mutant *pgr6/abc1k3-1* and *-2* lines, which were selected and verified by PCR. *stn7/stn8* and *sps2* were gifts from Profs Goldschmidt-Clermont and Basset, respectively.

Seedlings were grown for 14 days in 0.5x MS plates under continuous light condition (80 µmol m^{-2} s^{-1} for control and 500 µmol m^{-2} s^{-1} for the high light). Plants were grown on soil with solbac (Andermatt) under moderate light conditions (120 µmol m^{-2} s^{-1}, 20-22°C, 8h light /16h dark) in a controlled environment room. For high light treatment, 4-5 weeks old plants were exposed to 500 µmol m^{-2} s^{-1}, 20-22°C, for 3h.

Samples were collected under light, directly frozen in liquid nitrogen, and store at -20°C.

Photosynthetic parameters

Maximum quantum yield of photosystem II (Φ_{MAX}), quantum yield of photosystem II (Φ_{PSII}) and Non-Photochemical Quenching (NPQ) were determined using Fluorcam (Photon System Instrument, Czech Republic, http://www.psi.cz) with blue light LED (470 nm). Plants were dark-adapted for 10 minutes before measurements. $\Phi_{MAX} = (Fv/FM)$; $\Phi_{PSII} = (FM' - FS)/ FM'$; $NPQ = (FM - FM')/ FM'$; where FM, maximum fluorescence; FO, minimum fluorescence; Fv the variable fluorescence (FM – FO) in dark-adapted state; FM', maximum fluorescence; FS, steady-state chlorophyll fluorescence in the light[1]. The employed PPFD, (photosynthetic photon flux density), measured by LI-189 photometer (LI-COR), are 2.5 – 95 – 347 – 610 – 876 – 1145 µmol m^{-2} s^{-1}. State transitions were measured with the same instrument. After measurement of the FO and FM, plants were exposed to 10 minutes red light (50 µmol m^{-2} s^{-1} 660 nm peak measured as PPFD) supplemented with far-red (17 µmol m^{-2} s^{-1} calculated from the 733 nm peak area considering values between 500 and 800 nm). At the end of this phase the FM' (FMST1) was measured, and then the far-red light was turned off. The transition from State 1 to State 2 was followed during 10 minutes then again the FM' (FMST2) was measured. Quenching related to state transitions (qT) was calculated as $qT = (FMST1 - FMST2) / FM$.

Chlorophyll *a* fluorescence curve kinetics (OJIP, JIP-test)

Fast chlorophyll *a* fluorescence induction (OJIP, JIP-test) kinetics were measured at room temperature using a Plant Efficiency Analyser (Handy-PEA; Hansatech Ltd., King's Lynn, Norfolk, England), following manufacturer instructions. Plants were dark-adapted for 10 minutes before measurements. Measured data were extracted with the WinPEA software (Hansatech) and analysed with JIP-test according to Strasser *et al.* (2010)[2] and Kalaji *et al.* (2014)[3]. In detail, ΦPo (maximum quantum yield of primary PSII photochemistry) was calculated as $1 - F_O/F_M$. ΦET2o (quantum yield of the electron transport from Q_A to Q_B) as $((F_M-F_O)/F_M)$ $(1-(F_{3ms}-F_O)/(F_M-F_O))$. ΦRE1o (quantum yield of the electron transport until the PSI electron acceptors) as $((F_M-F_O)/F_M)$ $(1-(F_{30ms}-F_O)/(F_M-F_O))$. Where F_M is the maximum fluorescence, F_O the minimal fluorescence calculated by the Handy-PEA, F_{3ms} and F_{30ms} are the fluorescence levels measured at 3 and 30 ms respectively.

P_{700} oxidation

The kinetics of photosystem I photoxidation were measured on detached leaves using a JTS-10 LED spectrometer (BioLogic Science Instruments) in absorbance mode.

P_{700} oxidation was assessed by increase in absorption at 810 nm (after deconvolution of plastocyanin absorption as described in Joliot and Joliot (2006)[4]). Far-red (FAR) illumination was provided by a LED peaking at 735nm, filtered through three Wratten filters 55 that block wavelengths shorter than 700 nm. When needed, the maximum extent of P_{700}^+ was estimated by imposing a white light saturating flash on top of the FAR. A red LED provided actinic light peaking at 640 nm [5]. In order to measure the number of electrons present in the electron transport chain (ETC) per PSI the plants were incubated 2 minutes under strong white light (500 µmol m^{-2} s^{-1}) in order to reduce the contribution of the cyclic electron flow by activating CO_2 assimilation in the leaves[4]. Reactivation of cyclic flow only occurs after a long period of dark[4,5]. Therefore, after a short dark adaptation, electrons available to P_{700}^+ are only reflecting the reduction level of the PSI donors including the PQ pool. We exposed the leaf to FAR for 2 minutes to oxidise the ETC and, after 2 seconds of dark adaptation to allow P_{700} reduction, we followed its re-oxidation induced by FAR either in the presence or in the absence of a short saturating flash of actinic light (1000 µmol m^{-2} s^{-1} for 100 µs) to fully reduce the ETC. The time interval between the beginning of FAR illumination and the beginning of P_{700} oxidation was measured after a saturating pulse (PSI electron donors reduced) and after dark incubation (PSI electron donors oxidised). The ratio between these two values is used as a proxy for the number of available electrons per PSI.

Immunoblot analysis

Total proteins were extracted from *Arabidopsis* light-exposed leaves and homogenized in 400 µL of lysis buffer (100 mM Tris-HCl pH 8.5, 2% SDS, 10 mM NaF, 0.05% of protease inhibitor cocktail for plant (Sigma)) with a micro-pestle in a 1.5 mL microtube. Proteins were denatured at 37°C for 30 minutes, then centrifuge for 5 minutes at 16'000g at room temperature. 200 µL of supernatant were precipitated by chloroform-methanol, then resuspended in sample buffer (50 mM Tris-HCl pH 6.8, 100 mM Dithiothreitol, 2% SDS, 0.1% Bromophenol Blue, 10% Glycerol) at 0.5 µg chlorophyll per µL; and denatured at 65°C for 10 minutes. 5-10 µL of supernatant was mixed with 1 mL of 80% acetone, and chlorophylls concentration was determined according to Arnon (1949)[6]. An amount of thylakoids equivalent to two µg of chlorophyll were loaded. Proteins were separated by 12% SDS-PAGE and transferred onto a nitrocellulose membrane for western blotting.

For Phostag™-pendant acrylamide gels we followed the protocol for the antenna proteins previously described in Longoni *et al.* (2015)[7]. For the detection of PSII core subunits and STN7 phosphorylation the protocol was modified as follows: a Phostag™ gradient (0 to 25 µM) and $Zn(NO_3)_2$ (0 to 50 µM) was introduced in the upper half of the resolving 7% Acrylamide in 0.35 M Bis-Tris pH 6.8 gel. The stacking gel (4% Acrylamide, 0.35 M Bis-Tris pH 6.8) was cast above the resolving gel. The gels were incubated at room temperature for at least 3h before loading. Samples were prepared as previously described in Longoni *et al.* (2015)[7]. Briefly, total leaf protein was ground in liquid nitrogen and resuspended in lysis buffer (100 mM Tris HCl pH 7.8, 2% SDS, 10mM NaF, 1x complete™, EDTA-free Protease Inhibitor Cocktail (Roche)). Following incubation at 37°C for 30 min under agitation (1000 rpm Eppendorf thermomixer) protein content was measured with the Bicinchoninic Acid Protein Assay Kit (Sigma-Aldrich) and samples were diluted to equal protein concentration (0.5 µg/µL). Samples were further diluted in 2x lithium dodecyl sulfate (LDS) loading buffer (10% glycerol, 244 mM Tris HCl pH 8.5, 2% LDS, 0.33 mM Coomassie Brilliant Blue G-250, 100 mM dithiothreitol) and heated for 5 min at 70°C before loading.

Immunodetections were performed using anti-Actin (Sigma, A 0480) at 1/3000 dilution in 5% fat free milk/PBS, anti-Lhcb1 (Agrisera, AS09 522), anti-Lhcb2 (Agrisera, AS01 003), anti-D1 (PsbA) (Agrisera, AS05 084), anti-PsbO (Agrisera, AS14 2825), anti-PetC (Agrisera, AS08 330); anti-PsaD (Agrisera, AS09 461), anti-PsaC (Agrisera, AS04 042P), anti-AtpC (Agrisera, AS08 312); anti-STN7 (Agrisera, AS16 4098), anti-PsbD (Agrisera, AS06 146) at 1/5000 dilution in 5% fat free milk/TBS, and anti-Phosphothreonine (Cell Signaling Technology, #9381) at 1/10'000 in 3% BSA/TBS Tween20 0.1%. Secondary antibodies anti-rabbit (Merck, AP132P) or anti-mouse (Sigma, A5278) at 1/3000) conjugated with HRP allowed the detection of proteins of interest with 1 mL of enhanced chemiluminescence and 3.3 µL of H_2O_2 3% using an chemiluminescence imager (Amersham Imager 600, Amersham Biosciences, Inc.).

Plastoquinone analysis

Small leaf discs (0.8 cm diameter) were taken from 5 weeks old plants. Total lipids were extracted after 15 seconds of saturating white light (2000 µmol m^{-2} s^{-1}) using a fiber optic system allowing a maximal reduction of the PQ pool. Samples were directly flash frozen in liquid nitrogen at the end of the light treatment while still illuminated. A second disc from the same leaf was treated with far-red light (735 nm, 5.5 µmol m^{-2} s^{-1}) for 2 minutes allowing a maximal oxidation of the PQ pool. For prenyl lipid determination, samples were grinded immediately in the frozen state and extracted with cold ethyl acetate. This step as well as the analyses were performed as described in Kruk and Karpinski (2006)[8] and Ksas *et al.* (2015, 2018)[9,10]. The photoactive PQ pool was determined from the difference between the reduced PQ after 2 minutes of far-red light, upon which all the photoactive pool is oxidised, and the reduced PQ after a high irradiance light flash, upon which all the photoactive pool is reduced.

Plastoglobule isolation from chloroplasts and prenyl lipid analysis were performed according to Martinis *et al.* (2011)[11] and Eugeni-Piller *et al.* (2014)[12]. Intact chloroplasts were extracted from whole leaves by grinding in HB buffer (Sorbitol 450 mM, Tricine-KOH pH 8.4 20 mM, EDTA pH 8.4 10 mM, $NaHCO_3$ 10 mM, $MnCl_2$ 1 mM, Na-ascorbate 5 mM, PMSF 1 mM). The chloroplast suspension was filtered through 2 layers of Miracloth (Merck Millipore) and collected by centrifugation (5' 600g). The chloroplasts were lysed by osmotic shock in TED buffer (Tricine pH 7.5 50 mM, EDTA-Na_2 2 mM, dithiothreitol 2 mM) supplemented with 0.6 M Sucrose. Chloroplasts were diluted to a concentration of 2 mg/ml of chlorophyll and incubated for 10 min on ice to allow complete lysis and further incubated for 2h at -80°C. The samples were diluted four times in TED buffer. The sample was homogenised with 20 strokes of a Dounce homogenizer (PTFE Tissue grinder 50 cm^3, VWR®). The membranes and plastoglobules were separated from the stroma by ultracentrifugation (60 min 100'000g at 4°C). The pellet was dissolved in TED Buffer supplemented with 45% Sucrose to a concentration of 2-3 mg/ml of chlorophyll. Further homogenization of the sample was performed with a Dounce homogenizer (20 strokes). This solution was used as a lower phase of a discontinuous sucrose gradient. The gradient was assembled in TED buffer with the following sucrose concentrations: 15 ml of sample in 45% sucrose, 6 mL of 38% sucrose, 6 mL of 20% sucrose, 4 mL of 15% sucrose and 8 mL of 5% sucrose. The gradient was centrifuged to allow the fractionation by flotation (16h, 100'000g at 4°C). 1 ml fractions were collected from the top of the gradient. The lipids from each fraction were extracted with Ethyl-Acetate (0.75 volumes, 2 times), the Ethyl-Acetate phase was recovered upon centrifugation (1 min 10000g) and dried in a speedvac. The dried pellet was dissolved in a Tetrahydrofuran-Methanol (1:1) solution and used for UHPLC-APCI-MS-QTOF analysis.

Statistics and Reproducibility

The sample size was determined empirically for each experiment (minimum of three independent organisms and two experimental replicates), on the basis of experience with similar assays and from sample sizes generally used by other investigators. No data were excluded from the analysis. The experiment were replicated at least two times, the results were reproducible when the plants were not stressed before the experiment. When testing light conditions, the position of individuals of different genotypes was changed randomly in order to reduce any possible position effects. The data were compared for statistical difference by a two-tailed, heteroscedastic Student's t-test (Excel 2016).

References

1 Maxwell, K. & Johnson, G. N. Chlorophyll fluorescence - a practical guide. *J Exp Bot* **51**, 659-668 (2000).

2 Strasser, R. J., Tsimilli-Michael, M., Qiang, S. & Goltsev, V. Simultaneous *in vivo* recording of prompt and delayed fluorescence and 820-nm reflection changes during drying and after rehydration of the resurrection plant *Haberlea rhodopensis*. *Biochim Biophys Acta* **1797**, 1313-1326 (2010).

3 Kalaji, H. M., Oukarroum, A., Alexandrov, V., Kouzmanova, M., Brestic, M., Zivcak, M., Samborska, I. A., Cetner, M. D., Allakhverdiev, S. I. & Goltsev, V. Identification of nutrient deficiency in maize and tomato plants by *in vivo* chlorophyll *a* fluorescence measurements. *Plant Physiol Biochem* **81**, 16-25 (2014).

4 Joliot, P. & Joliot, A. Cyclic electron flow in C3 plants. *Biochim Biophys Acta* **1757**, 362-368 (2006).

5 Trouillard, M., Shahbazi, M., Moyet, L., Rappaport, F., Joliot, P., Kuntz, M. & Finazzi, G. Kinetic properties and physiological role of the plastoquinone terminal oxidase (PTOX) in a vascular plant. *Biochim Biophys Acta* **1817**, 2140-2148 (2012).

6 Arnon, D. I. Copper Enzymes in Isolated Chloroplasts. Polyphenoloxidase in *Beta Vulgaris*. *Plant Physiol* **24**, 1-15 (1949).

7 Longoni, P., Douchi, D., Cariti, F., Fucile, G. & Goldschmidt-Clermont, M. Phosphorylation of the Light-Harvesting Complex II Isoform Lhcb2 Is Central to State Transitions. *Plant Physiol* **169**, 2874-2883 (2015).

8 Kruk, J. & Karpinski, S. An HPLC-based method of estimation of the total redox state of plastoquinone in chloroplasts, the size of the photochemically active plastoquinone-pool and its redox state in thylakoids of *Arabidopsis*. *Biochim Biophys Acta* **1757**, 1669-1675 (2006).

9 Ksas, B., Becuwe, N., Chevalier, A. & Havaux, M. Plant tolerance to excess light energy and photooxidative damage relies on plastoquinone biosynthesis. *Sci Rep* **5**, 10919 (2015).

10 Ksas, B., Legeret, B., Ferretti, U., Chevalier, A., Pospisil, P., Alric, J. & Havaux, M. The plastoquinone pool outside the thylakoid membrane serves in plant photoprotection as a reservoir of singlet oxygen scavengers. *Plant Cell Environ* **41**, 2277-2287 (2018).

11 Martinis, J., Kessler, F. & Glauser, G. A novel method for prenylquinone profiling in plant tissues by ultra-high pressure liquid chromatography-mass spectrometry. *Plant Methods* **7**, 23 (2011).

12 Eugeni-Piller, L., Glauser, G., Kessler, F. & Besagni, C. Role of plastoglobules in metabolite repair in the tocopherol redox cycle. *Front Plant Sci* **5**, 298 (2014).

Supplementary Materials and Methods

Genes	Primer Names	Sequences
pgr6.1	LP1.1	AGC TGA TTC ATC ATC TGT CGG
	RP1.1	TCC CTT CCC ACA CTA AAA GT
abc1k3.1	LP3.1	TGT TGC TGT CAA AGT TCA ACG
	RP3.1	CAA GCG TAC TTT GAA GTT CCG
abc1k3.2	LP3.2	GGG AGG AGG TAG TGA CAA AGG
	RP3.2	AAG GTA ATC GGG TGG ACA GAG
Salk TDNA	LBb1.3	ATT TTG CCG ATT TCG GAA C
Sail TDNA	LB3_Sail	TAG CAT CTG AAT TTC ATA ACC AAT CTC GAT ACA C

Supplementary Table 1. List of primers

General conclusion

Photosynthesis, by converting sunlight energy into chemical energy and organic molecules, provides the primary building blocks for life on Earth. In order to maintain efficient photosynthesis and to cope with environmental conditions changes, plants have developed a panoply of strategies.

This PhD thesis highlights a novel strategy, which implicates plastoglobules and in particular two atypical kinases, ABC1K1/PGR6 and ABC1K3 in the regulation of photosynthetic electron flow.

Plastoglobules, small lipid droplets attached to the thylakoid membrane, are filled with lipids essential for photosynthetic activities and include electron carriers and lipid antioxidants. Plastoglobules were initially considered only as passive lipid storage particles. It was not until the early 2000s and the discovery of the plastoglobule proteome that the role of plastoglobules in lipid metabolism emerged. Today, plastoglobules are viewed as an essential compartment in chloroplast lipid metabolism. In addition to this, my thesis provides strong indications that plastoglobules also have regulatory functions and contribute to fast photosynthesis control.

A plastoglobule-located atypical kinase, ABC1K1/PGR6, was earlier shown to be implicated in photosynthesis, due to the *prg6* (*proton gradient regulation 6*) mutant phenotype, that is characterized by defects in electron transport and in non-photochemical quenching. However, up to now, the causes of these defects remained unknown.

Several lines of evidence in my PhD thesis suggest the likely causes for the *proton gradient regulation 6 (pgr6)* phenotype. In the first experimental part of this thesis, it was shown that deregulation of LHCII phosphorylation and detailed analysis of photosynthetic parameters point to diminished availability and possibly mobility of photoactive plastoquinone in thylakoid electron transport chain. Fractionation experiments suggest that plastoquinone is retained in plastoglobules in the *abc1k1/prg6* mutant and prevented from accessing the photosynthetic machinery in the thylakoids. Such a role for ABC1K1/PGR6 clearly would be central for photosynthetic electron transport and is in agreement with the characteristics of the mutant phenotype: The lack of plastoquinone in the electron transport chain and the failure to generate a sufficient proton gradient under high light provides a plausible explanation for the inhibition of non-photochemical quenching. In addition, the effects on the redox state of the photoactive PQ pool in *abc1k1/prg6* is expected to affect STN7 activity and, indeed, a decrease of LHCII phosphorylation and perturbed state transitions was observed. The findings underline the important role of plastoquinone in photosynthesis besides electron transport, and shows the importance of regulating its availability. Thus, this thesis identifies the key role of ABC1K1/PGR6 in

the control of availability of plastoquinone and its distribution between plastoglobules and the thylakoid membrane.

In a second experimental part, my thesis confirms that mutation of ABC1K3 alone does not negatively impact photosynthesis and even enhances some properties of photosynthetic electron transport. Importantly, this work also confirms that mutation of both proteins, ABC1K1/PGR6 and ABC1K3, does not lead to additive defects. On the contrary, certain photosynthetic parameters of the *pgr6* phenotype recovered at least partially in the double mutant, and this despite a small photoactive PQ pool. Therefore, I suggest that ABC1K1/PGR6 and ABC1K3 may act on PQ diffusion between plastoglobules and thylakoids, by promoting or slowing its movement. However, I do not exclude that, being predicted kinases, they may phosphorylate unidentified proteins and thereby control and modify thylakoid membrane fluidity which in turn would affect photosynthetic activity.

In conclusion, this PhD thesis provides unprecedented evidence for the role of two atypical kinases of plastoglobules, ABC1K1/PGR6 and ABC1K3, on the fast adaptation of photosynthesis under high light and doing so by regulating the availability and the mobility of the electron carrier molecule, plastoquinone. Therefore, this thesis points out a new role of PG in photosynthesis regulation.

Nevertheless, future research needs to clarify the molecular mechanisms. How do ABC1K1/PGR6 and ABC1K3 exactly act on plastoquinone availability? Are other players (proteins, lipid and other small molecules) involved in this process? Is there kinase-network signalling at work? How exactly does plastoquinone move in the thylakoid membrane? How is plastoquinone distribution and trafficking between thylakoid and plastoglobules achieved? This just to mention some interesting questions that could be explored in the future and were beyond the scope of my PhD thesis.

Acknowledgements

First of all, I would like to thank my thesis director Professor Dr. Felix KESSLER for giving me the opportunity to carry out my PhD thesis in his laboratory. I am so grateful for his support, encouragement, constructive criticism and especially his enthusiasm.

I am grateful to Dr. Paolo LONGONI and Dr. Shamungabalaji VENTAKASALAM, without whom this would not have been possible. Many thanks for your help, your good idea, your numerous corrections and your fruitful discussions.

I would like to thank Dr. Giovanni FINAZZI (CEA, Grenoble, France) as well as Dr. Michel HAVAUX and Dr. Brigitte KSAS (CEA, Cadarache, France) for their precious collaboration for biophysics analysis as well as for PQ photoactive pool measurements.

I especially thank my friend and PhD colleague Rosa PIPITONE for her inestimable friendship, her helpful discussions, her strong motivation and her infectious joie de vivre.

I am also grateful to Saskia DESMEULES for her lab bench help, without whom I would still be at the paillasse.

I would like also to thanks Professor. Dr. Stephan HÖRTENSTEINER from University of Zurich, Dr. Laurent MÈNE- É from University of Fribourg and Dr. Gaetan GLAUSER from Neuchâtel Platform of Analytical Chemistry of University de Neuchâtel for accepting to be members of my thesis committee.

I would like to thank the University of Neuchâtel Faculty Science and the Swiss National Funding (SNF) for providing funding, materials and space to work in the best conditions.

I also thanks my colleagues: Céline BESAGNI, Sonia ACCOSSATO, Emilie DEMARSY, Lucia EUGENI PILLER, Sarah ROTTET, Livia SPICHER, Sophie SCHEUNER, Julie DEVILLERS, Miwa BAUMANN, Joy COLLOMBAT, Véronique DOUET, Jane MARY, Bruno CABETE, Cyrille MONTANDON, David BORNAND, Axel MEYRAT, Adrien BOTTARELLI, Wayne ZITA, Gautier PIZZOLON, Hamed SATTARI VAYGHAN and Mounaïm KHAYI.

Finally, the last but not least thanks are for my lovely family and all my friends.

Thank you all.